東海大学大学院平成３０年度博士論文

Geochemical Mapping of the Mineralized Lower Lom Basin, Eastern Cameroon, Using Stream Water and Stream Sediments: Implication for Environmental Studies
（カメルーン東部の鉱化体が分布する Lower-Lom 盆地における河川水および河川堆積物分析に基づいた地球化学図：環境研究に対する意義）

指導　大場　武　教授

東海大学大学院総合理工学研究科

総合理工学専攻

Mumbfu Ernestine Mimba

Geochemical Mapping of the Mineralized Lower Lom Basin, Eastern Cameroon, Using Stream Water and Stream Sediments: Implication for Environmental Studies

A Thesis Submitted to the Graduate School of Science and Technology, Tokai University in Partial Fulfilment of the Requirements for the Degree of Doctor of Philosophy (PhD)

By:

Mumbfu Ernestine Mimba

2018

DEDICATION

To my uncle, the late Mimba Jato Alfred, and my sister, Vera Mimba who contributed tremendously to make me the scholar that I am today. Both of you are my great cheerleaders.

PREFACE

The work documented in the thesis (**Geochemical mapping of the mineralized lower Lom Basin, Eastern Cameroon, using stream water and stream sediments: Implication for environmental studies**) was done at Tokai University, Japan through the support of the Japanese Government MONBUKAGAKUSHO Scholarship Programme from October 2015 to September 2018. This thesis involved two field geochemical surveys to Cameroon for six weeks each. The thesis, supervised by Prof Takeshi Ohba, is arranged in six chapters. Chapter 1 outlines the study background and defines the objectives of the study. Chapter 2 documents the outcome of relevant literature and identifies knowledge gaps. Chapters 3 and 4 describe the study area, stream water sampling and the laboratory analyses of the samples. These chapters also present results from these investigations in the lower Lom Basin published in accredited journals. Chapter 5 focuses on the mineralogical composition and trace metal levels in stream sediments from the basin. Chapter 6 summarizes the major conclusions based on the results from Chapters 3 to 5 and gives recommendation for future research in the study area. Finally, following the list of references, full suite analytical results and data analysis techniques are provided as relevant supporting data in a few appendices.

ACKNOWLEDGEMENTS

I would like to express sincere gratitude to the Japanese Government for awarding the prestigious MONBUKAGAKUSHO Scholarship to me, which covered the tuition and living expenses in Japan. This work would not have been possible without the financial support of the Japan Agency of Science and Technology (JST). I thank the Institute of Geological and Mining Research (IRGM) for providing transportation facilities during the field campaigns.

Sincere appreciation is extended to my primary research supervisor Prof. Ohba Takeshi for his professional guidance and valuable support during the planning and development of this work. I wish to acknowledge my co-supervisor Prof. Aka Festus for his inspiring suggestions and enthusiastic encouragement throughout this research. The advice given by Dr. Wirmvem, M.J. and Dr. Nforba, M.T. has been a great help in keeping my progress on schedule. Moreover, special thanks to Prof. Suh, C.E., Dr. Asobo, N.E., Dr. Chako, B., Dr. Vishiti, A. and Dr. Mbunwe, E. for their useful and constructive recommendations on this project.

Special thanks go to all the technicians of the Laboratory of Inorganic Chemistry and Material Science at Tokai University for performing the mineralogical analysis. Assistance with chemical analyses by Mr. Numanami and Dr. Nishino is greatly appreciated. The author is also grateful to Nguemhe Fils for his help in producing the geochemical maps. Ivo Sumbele is truly thanked for his constant support during the field work.

Last but not the least, I would like to extend my heartfelt gratitude to my parents (Edward Mimba, Angelica Mimba, Ma Mimba) siblings (Vera, Kelly, Franklin, Bertrand, Roland, Elvis) relatives and friends (Oliver Tamfu, Rev. Ngwani Joseph, Adeline Mbinkar, Glory Nyugap, Bafon Godlove, Hans Mimba, Emos Sange, Adie Unimke, Bama Cyprian, Christian Nwankpa, Ajah Friday, Pastor Nkosi, Mensah George and David Darko) whose love and prayers kept me going in the pursuit of this project. I am particularly indebted to my husband, Fils Salomon and our two daughters, Esperanza and Esha, who had to put up with my absence for several months. I really could not have made it without your sacrifices.

Finally, I am forever thankful to God Almighty whose grace, strength and mercy sustained me.

PUBLICATIONS IN REFERRED JOURNALS

Mimba, M.E., Ohba, T., Nguemhe Fils, S.C., Wirmvem, M.J, Bate Tibang, E.E., Nforba, M.T., Aka, F.T. (2017). Regional hydrogeochemical mapping for environmental studies in the mineralized Lom Basin, East Cameroon: a pre-industrial mining survey. **Hydrology**. 5(2), 15–31. https://doi.org/10.11648/j.hyd.20170502.11. **June 2017.**

Mimba, M.E., Ohba, T., Nguemhe Fils, S.C., Wirmvem, M.J., Numanami, N., Aka, F.T. (2017). Seasonal hydrological inputs of major ions and trace metal composition of streams draining the mineralized Lom Basin, East Cameroon: Basis for environmental studies. **Earth Systems and Environment.** 1:22. https://doi.org/10.1007/s41748-017-0026-6. **November 2017**.

Mimba, M.E., Ohba, T., Nguemhe Fils, S.C., Nforba, M.T., Numanami, N., Aka, F.T., Suh, C.E. (2018). Regional geochemical baseline concentration of potentially toxic trace metal in the mineralized Lom Basin, East Cameroon: A tool for contamination assessment. **Geochemical Transactions.** 19:11, 1–17. https://doi.org/10.1186/s12932-018-0056-5. **May 2018.**

CONFERENCE PROCEEDINGS

Mimba, M.E., Ohba, T., Aka, F.T., Nguemhe Fils, S.C. Geochemical mapping using surface water and stream sediments of the mineralized Lom Basin, East Cameroon. *Japan Geoscience Union Meeting*, **May 20-25, 2016**. Makuhari, Japan.

Mimba, M.E., Ohba, T., Nguemhe Fils, S.C., Wirmvem, M.J. Geochemical composition of surface water in the mineralized Lom Basin, East Cameroon: Natural and anthropogenic sources. *American Geoscience Union*, **December 10-16, 2016**. San Francisco, USA.

Mimba, M.E., Ohba, T., Nguemhe Fils, Nforba, M.T., Numanami, N., Bafon, T.G., Aka, F.T., Suh, C.E. Baseline concentrations of trace metals in stream sediments of the lower Lom Basin, East Cameroon: implications for environmental studies. *European Geoscience Union General Assembly,* **April 8-13, 2018**. Vienna, Austria.

Mimba, M.E., Ohba, T., Nguemhe Fils, S.C., Wirmvem, M.J., Numanami, N., Aka, F.T. Trace metal concentrations in stream water draining the lower Lom mining area, eastern Cameroon. *Japan Geoscience Union Meeting*, **May 20-24, 2018**. Makuhari, Japan.

ACRONYMS AND ABBREVIATIONS

Acronym/abbreviation	Meaning
AAS	Atomic Absorption Spectrometry
ASM	Artisanal and Small-Scale Mining
AYD	Adamawa-Yadé Domain
CAFB	Central African Fold Belt
CC	Congo Craton
CCSZ	Central Cameroon Shear Zone
Cr	Chromium
Cu	Copper
EC	Electrical Conductivity
FOREGS	Forum of European Geological Surveys
GB	Garoua Boulai-Bétaré Oya
GIS	Geographical Information System
IC	Ion Chromatography
ICP-MS	Inductively Coupled Plasma Mass Spectrometry
IDW	Inverse Distance Weight
LOD	Limit of Detection
MAD	Median Absolute Deviation
PCA	Principal Component Analysis
TDS	Total Dissolved Solids
UNICEF	United Nations Children's Fund
WHO	World Health Organization

ABSTRACT

In the heavily mineralized Lom Basin in East Cameroon, environmental studies have focused mainly on soil and water quality. This study is the first appraisal of regional geochemical mapping using stream water and stream sediment for environmental assessment of the lower part of the basin. The aim of this work is to investigate the major ion and trace metal compositions in stream water, determine the response of major ions to seasonal variations and to examine stream sediment quality. Accordingly, 52 water samples were collected during the dry season and 29 samples during the rainy season. These were analyzed for major cations Ca^{2+}, Mg^{2+}, Na^{+}, K^{+} by AAS and major anions HCO_3^-, F^-, Cl^-, NO_2^-, NO_3^-, Br^-, PO_4^{3-}, SO_4^{2-} using ion chromatography. Trace metal concentrations of stream water and 55 sediment samples were determined by a combination of AAS and ICP-MS. The major ion levels in stream water were within the WHO safe limits for drinking water and also indicated a fresh water source. From the major ion geochemistry, Ca^{2+}, Mg^{2+}, Na^{+}, $K^{+}$and HCO_3^- were derived from silicate weathering, SO_4^{2-} from the partial dissolution of sulphide minerals under neutral pH while NO_3^- and Cl^- distributions indicated pollution from domestic activities within the area. The seasonal regime of stream water chemistry is controlled by groundwater supply of major cations and HCO_3^- from chemical weathering, leaching of cations from surface soil layers during precipitation and dilution of nitrate by surface runoff during the wet season. Except for Fe and Mn, water samples had very low concentrations (<1 µg/l) of V, Cr, Co, Cu Zn, Cd and Pb while concentrations of Fe and Mn exceeded the WHO threshold values for drinking water. Similarly, trace metal levels in sediments were low (e.g As = 99.40 µg/kg, Zn= 573.24 µg/kg, V= 963.14 µg/kg and Cr= 763.93 µg/kg). Iron and Mn had significant average concentrations of 28.325 and 442 mg/kg, respectively. Background and threshold values of the trace metals were computed statistically to determine geochemical anomalies of geologic or anthropogenic origin, particularly mining activity. Factor analysis, applied on normalized data, identified three associations: Ni–Cr–V–Co–As–Se–pH, Cu–Zn–Hg–Pb–Cd–Sc and Fe–Mn. The first association is controlled by source geology and the neutral pH, the second by sulphide mineralization and the last by chemical weathering of ferromagnesian minerals. Spatial analysis revealed that Co, Cr, V, Ni were slightly enriched in the east of the study area underlain by granitic rocks. Relatively high As levels corresponded to some reported gold indications in the area. The background distribution

patterns for Cu, Zn and Pb are indicative of sulphide mineralization while Fe and Mn distribution are consistent with their source from ferromagnesian rocks. Based on the low levels of trace metals, the stream water and sediment have not been impacted by mining activities. However, the water should be treated for Fe and Mn. Furthermore, the continuous use of Hg in refining gold should be monitored. The data generated in this study provide the geochemical baseline data crucial for the sustainable development of the basin ecosystems and serve as guidelines for studies in other mineralized areas in the country.

TABLE OF CONTENTS

CHAPTER 1. GENERAL INTRODUCTION

1.1 Background

Regional and national geochemical mapping surveys have been conducted in different parts of the world (Laszlo, 1997; Rapant et al., 1999; Chiprés et al., 2008; Garrett et al., 2008; Caritat et al., 2008b; Smith and Reimann, 2008; Birke et al., 2015; Caritat and Cooper, 2016; Reimann et al., 2017). Although such mapping programmes were developed primarily for geochemical prospecting (Webb et al., 1978; Rose et al., 1979), the same principles and techniques have been expanded to encompass environmental–related issues such as land use planning, agricultural development, environmental monitoring and medical geology (Howarth and Thornton, 1983; Forstner et al., 1991; Kim and Chon, 2001; Likuku et al., 2013; Boboye and Abumere, 2014). The geochemical maps resulting from such surveys show the distribution (background) of the elements analyzed. The term geochemical background was first used in exploration geochemistry (Hawkes and Webb, 1962) and a precise definition is still debatable (Salminen and Gregorauskiene, 2000; Reimann and Garrett, 2005; Gałuszka, 2007). Commonly, background is used interchangeably with baseline or threshold value and may refer to element concentrations in real sample collectives due to natural processes in pristine areas or describe anthropogenic conditions (Matschullat et al., 2000; Guillen et al., 2011). Considering its spatial and temporal variability, geochemical background represents the natural concentration range of an element in a given environmental medium (Gałuszka and Migaszewski, 2011). Geochemical surveys often target diverse sampling media including rock, soil, sediment, surface water, groundwater, rain, plant and animals, with the aim of providing basic information for policymakers and industry purposes.

Hydrogeochemical mapping is an integral part of most regional and local mapping surveys (Ibe and Akaolisa, 2010; Gray et al., 2016) and is particularly useful in mapping a drainage basin that includes a proposed mine site (Kelepertzis et al., 2012). The dissolved ion contents can be of natural or anthropogenic origin and have been routinely used to evaluate the surface water quality (Jorquera et al., 2015). Likewise, stream sediments have been extensively used as a reliable medium in geochemical mapping investigations because they provide the composite sample of the catchment area upstream of the sampling point (Ohta et al., 2004, 2011; Dinelli et al., 2005; Lapworth et al., 2012; Zhizhong et al., 2014; Zuluaga et

al., 2017). Accordingly, their geochemical composition is considered to be a representative of the drainage basin geology (Chandrajith et al., 2001). Nevertheless, the spatial distribution pattern of elemental levels in sediments is characterized by a high degree of diversity. Such spatial heterogeneity is due to myriad factors including the lithology and size of the basin, weathering processes, hydrological features and land use (Plant and Raiswell 1983). The natural weathering of mineral deposits, as well as human activities such as small–scale mining (ASM), can result in high concentrations of trace metals in stream water and stream sediments (Hook, 2005; Ako et al., 2014; Kpan et al., 2014; Agyarko et al., 2014; Taiwo and Awomeso, 2017).

The Lom Basin in East Cameroon is heavily mineralized, especially in gold, endemic to its regional geological setting. This has led to ASM dating back to the 1940s. Presently, this region is a target for industrialized mining. While small–scale gold mining is a major source of income for the miners and their dependents, and an economic booster for the countries involved (Bansah et al., 2016), these operations are a potential menace to the surrounding ecosystem (plants, animals, microorganisms, soil, rocks, minerals, water sources and the local atmosphere) (Cobbina et al., 2013; Kpan et al., 2014). Because of the economic benefits of ASM, the sector has helped in springing rural–urban migration in the region.

Investigations on the impacts of the past and ongoing mining activities in the area have been limited to water quality in the Mari sub–basin (Rakotondrabe et al., 2017), soils and mine tailings (Tehna et al., 2015; Manga et al., 2017). No studies involving the combined investigation of water and sediment samples of streams draining the lower Lom Basin have been performed. In the light of planned mining developments and the growing concerns about associated environmental problems with artisanal mining, this work provides valuable geochemical information that can be used in future comparisons. From a broader point of view, this work represents a pre–industrial mining baseline geochemical study that can be used as a reference for other mineralized areas in the region.

1.2 Aims and Objectives

The overall aim of this study is to generate the baseline concentrations of major ions and trace metals in stream water and stream sediments, prior to any new type of mining activities in the mineralized lower Lom Basin.

Major objectives to address the aim of this study are as follows:

(1) To determine the physical and chemical characteristics of stream water and assess its suitability for drinking, distinguish between natural and anthropogenic sources of dissolved ions, and produce geochemical maps of dissolved ions through a systematic sampling of stream water draining the catchment (Chapter 3).

(2) To assess the variation in major ion distribution patterns of stream water throughout a hydrological year; examine the source, geochemical behavior of some trace metals in stream water and evaluate its suitability for drinking and domestic purposes (Chapter 4).

(3) To characterize the mineralogical composition of stream sediments, assess the level of trace metal contamination in stream sediments and evaluate the spatial relationships among metal concentrations, geology, reported mineralization and mining activities (Chapter 5).

CHAPTER 2. GEOLOGY, GOLD MINERALIZATION AND MINING ACTIVITY

This chapter reviews the geology, gold mineralization as well as the past and active mining practices in the study area. It also explores the current understanding of the impacts of such practices in order to identify knowledge gaps relevant to the framework of this research.

2.1 Regional geological setting

The Lom Basin constitutes part of the Precambrian basement of Cameroon which is divided into two significant litho–structural units; the Congo craton (CC) and the Central African Fold Belt (CAFB) (De Wit and Linol, 2015). These rock units are separated by a major N–dipping thrust structure (Fig. 2.1).

The CC outcrops in the southern part of Cameroon and consists of mainly Archean rocks (Ntem Complex) and the Palaeoproterozoic Nyong Series, marking the earliest formed crust in Cameroon (Toteu et al., 1994; Basseka et al., 2011). Detailed information on the geology, geochronology, tectonism and geochemistry of the CC has been documented (Nédélec et al., 1990; Feybesse et al., 1998; Tchameni et al., 2001; Penaye et al., 2004; Shang et al., 2004, 2007; Lérouge et al., 2006; Van Schmus et al., 2008; Kankeu et al., 2017).

The CAFB (~600+700Ma) also known as the Pan–African belt of central Africa lies between the CC to the south and the Western Nigerian Shield to the north, and is described as the southernmost part of the Pan–Africano–Braziliano belt (Poidevin, 1983; Nzenti et al., 1988). This domain underlies Chad, Cameroon, Central African Republic and continues to parts of Uganda and Sudan (Toteu et al., 2004; Van Schmus et al., 2008). According to Castaing et al., (1994), the evolution of this belt is due to the convergence and collision between the São Francisco–Congo cratons and the West African Craton, and a Pan–African mobile belt. In Cameroon, the present structure of the Pan–African belt can be attributed to the collision between the West Africa and Congo cratons (Toteu et al., 2004). The authors outlined three possible phases of evolution of the CAFB: a) The pre–collision emplacement of calc–alkaline granitoids (670–660 Ma); b) Proceeding crustal thickening, high–grade metamorphism and syntectonic emplacement of calc–alkaline and S–type granitic rocks (640–610); c) Finally, the development of a post–tectonic nappe, semi–alkaline to alkaline magmatism and molasses basin deposition (600–545 Ma).

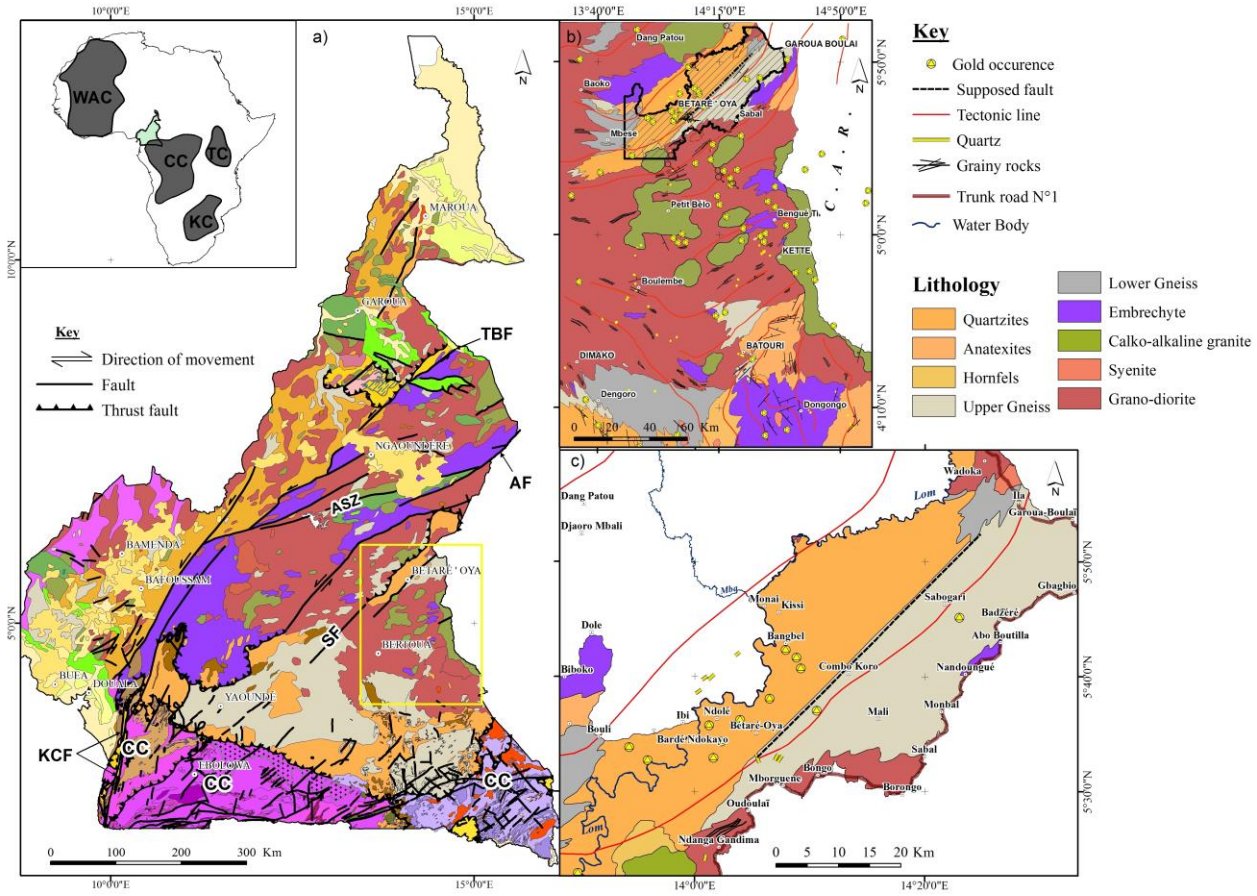

Figure 2.1. Geology of Cameroon. **a)** Geological map of Cameroon (modified from Toteu et al. (2008)) **Faults:** Tcholliré-Banyo Fault (TBF), Adamawa Fault (AF), Sanaga Fault (SF), and Kribi-Campo Fault (KCF); **Cratons and mobile belts:** West African Craton (WAC), Tanzanian Craton (TC), Kalahari Craton (KC), Congo Craton (CC), Adamaoua Shear Zone (ASZ) **b)** Regional geological map of eastern Cameroon showing reported gold indications. **c)** Geology of the lower Lom Basin.

Structurally, the CAFB is dominated by the Yaoundé Domain, Adamawa–Yadé Domain (AYD), and the Northwestern Cameroon Domain (Toteu et al., 2004; Ngako et al., 2008; Van Schmus et al., 2008). The AYD is the largest litho–structural unit of the CAFB in Cameroon (Fig. 2.1) extending eastwards into the Central African Republic where it is known as the Yadé Massifs. This domain is confined to the north by Tcholliré Banyo faults and to the south by the Yaoundé Domain (Fig. 2.1). The following lithological groups have been identified in the AYD: relics of Palaeoproterozoic metasediments and orthogneisses with inputs from the Archean crust, metavolcanic rocks of the Lom Basin, the Yadé Massifs in western Central African Republic and the extensive 640–610 Ma syn–to late–tectonic granitoids of transitional composition and crustal origin (Toteu et al., 2001, 2004). The syn–to late–collisional calc–alkaline granitoids are ubiquitous within this domain. These rocks intrude orthogneisses representing the Paleoproterozoic basement which underwent extension and was probably dismembered during the Pan–African event.

Pan–African tectonism in Cameroon resulted in the formation of extensional basins including the Lom Basin (Ngako et al., 2003; Toteu et al., 2006). The Lom basin is a post–collisional basin and consists mainly of metasedimentary rocks. These rocks are grouped into two main structural and metamorphic units: a monocyclic unit which comprises volcanoclastic schists, upper gneisses, quartzites and conglomerates metamorphosed under greenschist facies and associated with grabens. Staurolite mica schists, lower gneisses and mylonites comprise the polycyclic unit (Soba et al., 1991; Toteu et al., 2001, Ngako et al., 2003). The widespread S–type granitic plutons intrude the low–grade metamorphic schists units interpolated with quartzites and metaconglomerates (Fig. 2.1). U–Pb dating on zircons of the Lom Group yielded constrained ages of 612–600 Ma. This suggested that the Lom basin sedimentation occurred after 612 Ma followed by a rapid deformation and low–pressure metamorphism (Toteu et al., 2004). Recent U–Pb dating of zircon grains from the gold–bearing granitic body in Bétaré-Oya suggests that the granitic pluton was emplaced at 635–620Ma, marking an early mineralization event (Ateh et al., 2017). Structures in the Lom Group include trending NE–SW, NNE–SSW and ENE–WSW faults associated with the Central Cameroon Shear Zone (CCSZ, Toteu et al., 2001; Ngako et al., 2003, Kankeu et al., 2009, 2012). The evolution of this pull-apart basin is characterized by the reworking and remobilization of an Archean to Paleoproterozoic basement (Toteu et al., 2004). This accounts for the economic potential (especially gold) of the Lom Basin.

2.2 Reconnaissance gold investigation and gold mining

Gold mineralization in the study area is associated with quartz veins and veinlets, weathering profiles and wall rock alterations (Fon et al., 2012; Vishiti et al., 2017). Here, gold is commonly disseminated in quartz veins associated with sulphides (pyrite, chalcopyrite, galena, arsenopyrite) and hematite, hence As, Fe and Cu are considered as gold pathfinders (Mboudou et al., 2017). In most places, the gold ore is concentrated in conglomerate beds which are the target of current mining. The gold deposit is a placer type formed by the reworking of the primary mineralized rocks; and it is lithologically controlled (Toteu et al., 2004; Vishiti et al., 2017). Accordingly, alluvial gold is won from the weathered sedimentary sequences and active stream sediments from the Lom River and its tributaries. Artisanal and small–scale gold mining (ASM) started over six decades. Gold production in Cameroon reached a maximum of 717 kg in 1942 and plummeted to 4–5 kg in 1956 (Laplaine, 1969). Alluvial mining represents 90 % of the economic activity in the area. In addition, a stream sediment survey in the upper Lom Basin reported Au concentrations of up to 450 ppm (Omang et al., 2014).

During the last four decades, there has been a mining boom (exploration and exploitation) in the East Region of Cameroon, particularly in the districts of Bétaré-Oya, Batouri, Garoua-Boulai, Colomines and Kette (Bakia, 2014; Weng et al., 2015). Since 2000, semi–mechanized gold mining which is known to pose considerable risk to the environment was introduced. Gold extraction methods in the area involve open pit mining of the weathered primary (quartz veins) gold deposits or from alluvial sediments using primitive methods. Semi–mechanized exploitation often involves the use of heavy machinery (Kouankap Nono et al., 2017). The negative impacts of such practices on both the local population and environment include loss of biodiversity due to deforestation, land degradation as result of abandoned pits without rehabilitation and untreated waste, and water pollution (Awudu, 2002). Besides these, the use of harmful chemicals like cyanide and mercury by some companies to refine gold is a major concern in the protection of the environment.

2.3 Water and soil quality

There has been growing concerns about environmental contamination by toxic metals released from ASM. In this regard, studies by Rakotondrabe et al. (2017) reported high concentrations of As, Pb, Cr and Cd in surface water of the Mari sub–basin in the Lom catchment, with the Lom River being the most deteriorated. Surface water quality in the

downstream of the Mari River has also been affected by artisanal mining activities. Trace metals in this sub–basin originate from chemical weathering and ASM. Following the recommendations of the WHO, the surface water is not suitable for consumption. Meanwhile, other investigations showed that the mine tailings soils in Bétaré-Oya have been polluted by a range of metals including As, Ag, Cr, Cd, Cu, Pb and Zn (Tehna et al., 2015; Manga et al., 2017). In this area, the mining residues were dumped in the immediate environment without prior treatment. The concentrations of the trace metals Cr (210 mg/kg), Zn (136 mg/kg), As (34 mg/kg), Cu (30 mg/kg), Pb (25 mg/kg) and Cd (0.5mg/kg) were higher compared to the local soil background values and the upper continental crust (Tehna et al., 2015). Concentrations of Cu (6–58 ppm), Zn (26–11 ppm), As (5–43 ppm), W (1–13 ppm), Mo (1–5 ppm) and Ag (2–18 ppm) have been greatly affected by mining and identified as potential pollutants following the computation of pollution indices (Manga et al., 2017). Among these, As was considered the most threatening. Briefly, ASM in this area is hazardous to the aquatic environment and human health. Based on the comparisons above, it is now obligatory to develop a geochemical baseline prior to the onset of any new type of mining in the lower Lom Basin.

CHAPTER 3. REGIONAL HYDROGEOCHEMICAL MAPPING FOR ENVIRONMENTAL STUDIES IN THE MINERALIZED LOM BASIN, EAST CAMEROON: A PRE-INDUSTRIAL MINING SURVEY[1]

3.1 Introduction

Hydrogeochemical mapping is an inherent concept of most geochemical mapping surveys (Ibe and Akaolisa, 2010; Gray et al., 2016) and is especially useful in mapping a mineralized drainage basin (Kelepertzis et al., 2012). Undoubtedly, water is the principal transport pathway for elements derived from the chemical weathering of mineralized rocks and the dissolved ion contents are routinely used to evaluate the surface water quality (Jorquera et al., 2015). The quality of water depends largely on the desired use of water. Hence, the chemistry of water is vital for evaluating its suitability for various purposes. Communities in the lower Lom Basin like those in other semi–urban areas in Cameroon lack access to adequate infrastructural facilities for drinking water. The absence of such good water supply has compelled the estimated 229,000 inhabitants to rely on water from streams, wells, springs and boreholes of unknown quality for drinking and domestic purposes. Moreover, this basin is endowed with mineral resources especially gold, owing to its regional geological setting. It also has a long ASM history and is currently a target for industrialized mining. Accordingly, research reporting the rock type, age, and the formation history or the reconnaissance gold investigations in this region are numerous (e.g Toteu et al., 2001; Ngako et al., 2003; Kankeu et al., 2009; Omang et al., 2014). Despite this extensive coverage, there is limited available data on the chemical composition of stream water required to establish quality criteria for water in the area.

The chemical composition of streams draining the Lom basin is fundamental for preparing regional geochemical baseline maps. Here, baseline refers to the present elemental concentrations in the stream water (Salminen and Gregorauskiene, 2000). These background levels in surface water can be of natural or anthropogenic origin and distinguishing their sources can be quite challenging. Multivariate statistical procedures such as Correlation

---

[1] *This chapter is an edited version of the article:*
***Mimba, M.E.**, Ohba, T., Nguemhe Fils, S.C., Wirmvem, M.J., Edith Etakah, B.T., Nforba, M.T., Aka, F.T. (**2017a**.). Regional Hydrogeochemical Mapping for Environmental Studies in the Mineralized Lom Basin, East Cameroon: A Pre-industrial Mining Survey.* Hydrology, 5(2), 15–31.

matrix and Principal Component Analysis have often been used to discriminate between patterns of natural and anthropogenic origin (Reimann and Garrett, 2005). Hence, it is imperative to take into account the origin of the occurrence and concentrations of the dissolved elements for environmental legislation and regulation (Plant et al., 2001). In addition, Geographical Information System (GIS) is an effective tool for preparing spatial distribution maps of water quality parameters. This allows for rapid transfer of information to water resources managers and environmental professionals for taking quick policy decisions (Srivastava et al., 2011; Singh et al., 2013).

This study, therefore, presents a regional hydrogeochemical baseline prior to industrial mining in the Lom Basin. Other goals are (i) to determine the physical and chemical characteristics of stream water and evaluate its potability (ii) to distinguish between natural and anthropogenic sources of dissolved ions through a systematic sampling of stream water draining the catchment and (iii) to produce geochemical maps of dissolved ions in the area. These data provide information necessary for setting guidelines and legal standards in the region. Moreover, this study forms a reference for hydrogeochemical mapping in other mineralized areas in Cameroon.

3.2 Study Area

3.2.1 Geographical setting

The study area comprises three sub–basins, Mari, Mbigala and Bedobo with a surface area of 2574.67 km^2. These catchments are located in the Lom Basin which is the largest and most important basin in Cameroon in terms of water and mineral resources. The study area is found in the Lom–and–Djerem Division, East Region of Cameroon which forms part of the Equatorial Rainforest Belt. It lies between latitudes 5^o 24' 40" and 5^o 55' 40" North, and 13^o 55' 20" and 14^o 26' 20" East. This basin encompasses the Garoua-Boulai and Bétaré-Oya gold districts with a total population of about 229,000. Monotonous, gently undulating hills of altitude ranging from 600 to 1000 m above sea level extend throughout the area. This characteristic landform has led to the development of a dendritic drainage pattern (Fig. 3.1). Hydrologically, the basin is drained by the Lom River and its tributaries. Streams within the study area rise from the hills, flow in a general south–west direction and discharge into the Lom River which eventually empties into the Atlantic Ocean. Some of the lower order streams

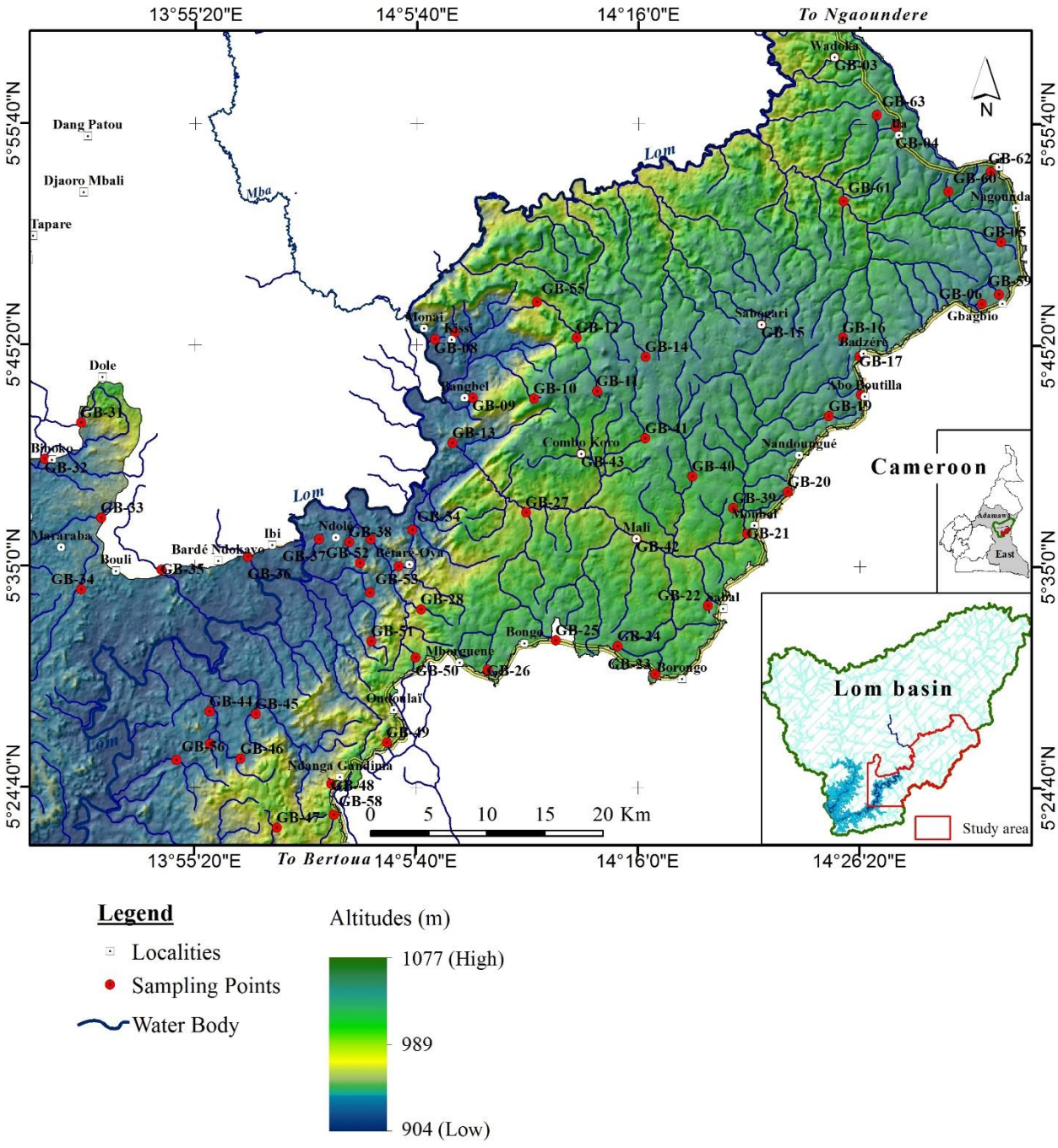

Figure 3.1. Drainage map of study area showing sampling locations.

have no water flow during the dry season. Water recharge in this area is controlled mainly by precipitation. In 2015–2016, the lowest monthly flow rate of 56 m^3/s was recorded in February while the maximum flow rate of 328 m^3/s was observed in October (Rakotondrabe et al. 2017). The study area is covered mostly by shrubs and herbaceous savanna in the north and an evergreen forest in the south. High temperatures (average, 24.58 ^oC), rainfall (mean annual rainfall, 1440 mm) and humidity support the luxuriant vegetation cover and enhance deep weathering of rocks and the formation of iron–rich, red ferallitic soils. There is a lack of traditional seasons but instead a long dry season from December to May, a light wet season from May to June, a short dry season from July to August and a heavy wet season from September to November.

In the East Region of Cameroon, subsistence agriculture is a major form of livelihood. The low population density, poorly developed farm to market roads, the absence of lucrative markets for the farm products and a luxuriant and impassable evergreen forest hinder agricultural production in the area. As a consequence, most people choose ASM as a source of income. Besides mining, the inhabitants also practice fishing and logging.

3.3 General methodology

3.3.1 Stream water sampling

Systematic sampling of stream water was carried out in 2016, in the southeastern portion of the Lom basin (Fig. 3.1). During this survey, abandoned and active mine sites were greatly avoided. Field observations such as potential sources of contamination, land use and upstream lithology were documented.

Two sampling campaigns (February to March and September to October 2016) were conducted, covering a hydrological year. During these field surveys, a total of 81 water samples were collected from lower order streams: 52 samples were collected during base–flow conditions and 29 samples during periods of high flow, for feasibility studies. Field sampling was done in accordance with the FOREGS (Forum of European Geological Surveys) Geochemical field mapping manual (Salminen et al., 1998). A sampling density of 1 sample every 5 to 10 km was used based on the accessibility and availability of streams. The geographical parameters of each sampling site were obtained using a Garmin etrex GPS. A plastic bucket used to collect water, and all the bottles for storing samples were rinsed severally with the water to be sampled. Water was manually collected below the surface in

the center of streams, preferably where the flow velocity was high. This allows for homogenization of the solid particles and dissolved ions (Ndam Ngoupayou et al., 2016). During sampling, field measurements were conducted for the physico–chemical parameters including pH, electrical conductivity (EC), total dissolved solids (TDS) and temperature using the HI 9811–5 Portable pH/EC/TDS/T meter which was calibrated before and during the campaign. The electrodes were rinsed before each measurement with the same water that was sampled and after with distilled water. Alkalinity was conducted using a Hach field titration kit (HACH Digital Titrator model 16900) within 8 hours of sample collection whereby a volume of 0.16 N H_2SO_4 was added dropwise to the sample while continuously stirring with a pH meter to reach the end–point titration (pH 4.5). Two sets of the water sample were collected at each site. One set was filtered through 0.45 µm Millipore membrane filters using 50 ml syringes and stored in previously washed new, narrow–mouth, transparent 50 ml polyethylene bottles. On the same day, 1 ml of 20 wt. % pure concentrated HNO_3 was added to the samples to prevent precipitation and loss of ions to the container walls. These were used to determine major cations and trace elements. A second sample set was collected but not acidified and was utilized for the analysis of major anions.

3.3.2 Analytical methods

Laboratory analyses were performed at the Laboratory of Geochemistry and Volcanology in Tokai University, Japan within two weeks of sample collection. Stream water samples were analyzed for the major cations Calcium (Ca^{2+}), Magnesium (Mg^{2+}), Sodium (Na^{+}) and Potassium (K^{+}) by Flame Atomic Absorption Spectrometer (AAS, ContrrAA700). The major anions Fluoride (F^{-}), Chloride (Cl^{-}), Nitrite (NO_2^{-}), Nitrate (NO_3^{-}), Bromide (Br^{-}), Phosphate (PO_4^{3-}) and Sulphate (SO_4^{2-}) were measured using Ion Chromatography (Dionex ICS–900). Laboratory standard solutions of these ions were prepared to calibrate the system. Also, two replicates were run per sample to check for accuracy. The cation–anion ionic balance error (IBE) proposed by Appelo and Postma, (1999), was used to assess the quality of the chemical analyses. An ionic balance error less than ±10 % (Appendix I) and an overall precision better than 4 % Relative Standard Deviation were considered in further analysis and discussion of the geochemical dataset. Total dissolved solids (TDS) were estimated by summing the major ionic species (Ca^{2+}, Mg^{2+}, Na^{+}, K^{+}, F^{-}, Cl^{-}, NO_2^{-}, NO_3^{-}, Br^{-}, PO_4^{3-} and SO_4^{2-}). The software "DIAGRAMMES" was used to produce the graphical representation of the hydrochemical parameters.

Silica (Si) and trace element (Fe, Mn, V, Cr, Co, Ni, Cu, Zn, As, Cd, Pb, Hg) concentrations were determined by Inductively Coupled Plasma Mass Spectrometry (ICP–MS) (ThermoScientific). Certified reference materials JA–3, JB–3, JG–3 (Geological Survey of Japan) and blanks were simultaneously analyzed to check for analytical precision and accuracy.

3.3.3 Statistical analyses and map production

Statistical analyses were performed using Microsoft Excel and SPSS 20.0 for Windows. The geochemical dataset was subjected to multivariate statistical analyses (correlation matrix and principal component analysis) to explore and investigate the data structure and identify the likely origins of dissolved ions in the water samples.

The Geographic Information System (GIS) software package ESRI ArcMap 10.2 was employed to produce the hydrogeochemical baseline maps of the study area. Inverse Distance Weighted (IDW) technique was chosen to prepare the colored maps. This approach of interpolation is based on the assumption that the influence of the mapped variable diminishes with distance from a sampled location. IDW estimates the value for an unknown location by averaging the measured values surrounding the prediction location. In the IDW interpolation method, the significance of known points can be controlled by using weighting coefficient or power. The higher the power, the greater the influence of the nearest points, and the resulting surface will be less smooth. As the power increases, the value of the unknown location approaches the immediate surrounding data points. In addition, specifying a lower power will give more influence to distant data points, resulting in a smoother surface (http://webhelp.esri.com/arcgisdesktop/9.2/index.cfm?TopicName=Implementing_Inverse_Distance_Weighted_ (IDW). In this study, a power of two was defined and a variable search radius was used for each interpolated cell. Other information such as catchment geology and land use were used in interpreting element distributions within the basin.

3.4 Results and Discussions

3.4.1 Physico–chemical characteristics of surface water and water quality

The variations in physico–chemical parameters for all 52 samples from the lower Lom Basin are given in Table 3.1 and a summary of the statistics for the stream water data is presented in Table 3.2. Most streams of the Lom Basin were predominantly neutral to mildly acidic in

Table 3.1. Physico–chemical parameters of surface water (N = 52) in the lower Lom Basin.

Sample ID	Temp	pH	TDS	EC	Na^+	K^+	Ca^{2+}	Si	Mg^{2+}	SO_4^{2-}	F^-	Cl^-	NO_2^-	Br^-	NO_3^-	PO_4^{2-}	HCO_3^-
	oC		mg/l	µS/cm	mg/l	mg/l	mg/l	mg/l	mg/l	mg/l	mg/l	mg/l	mg/l	mg/l	mg/l	mg/l	mg/l
GB-01	20.4	7.3	33.2	51	2.85	2.69	3.57	7.87	2.11	0.25	0.09	0.20	0.03	bdl	0.35	bdl	28.9
GB-02	18.4	7.2	27.3	42	3.66	2.14	3.05	8.40	1.14	bdl	0.05	0.11	0.01	0.02	bdl	0.06	25
GB-03	17.3	6.2	17.6	27	1.93	1.78	1.75	6.87	0.68	bdl	0.11	0.10	0.06	bdl	0.02	0.02	14.9
GB-04	22.4	6.4	7.8	12	0.56	1.34	0.57	4.44	0.15	bdl	0.06	0.11	0.11	bdl	0.04	0.02	6.02
GB-05	20.7	6.3	12.4	19	1.36	1.31	0.84	5.45	0.13	0.01	0.02	0.29	0.06	bdl	0.87	bdl	7.01
GB-06	19.7	6	7.15	11	0.69	0.69	0.80	3.63	0.13	bdl	0.05	0.13	0.05	bdl	bdl	bdl	6.11
GB-07	23.7	6.8	71.5	110	6.18	2.97	9.48	12.70	4.74	0.02	0.21	0.09	0.06	bdl	0.02	bdl	60.9
GB-08	18.1	7.1	72.8	112	6.47	3.71	9.19	16.1	4.35	bdl	0.21	0.21	bdl	bdl	0.02	0.08	62.7
GB-09	21.1	6.1	12.4	19	0.79	1.81	1.11	5.82	0.49	0.01	0.06	0.16	0.05	0.04	0.09	0.02	11.2
GB-10	21.4	6.2	5.85	9	0.06	0.81	0.55	4.09	0.16	0.21	0.03	0.12	0.02	bdl	bdl	bdl	3.23
GB-11	21	6	10.4	16	0.71	0.42	0.80	4.42	0.90	0.27	0.04	0.1	0.04	0.04	bdl	0.02	9.55
GB-12	24.2	6.5	10.4	16	0.19	1.08	1.12	3.63	0.37	bdl	0.04	0.11	0.05	bdl	0.02	bdl	7.27
GB-13	20.5	6.4	69.6	107	8.96	2.41	5.97	10.8	4.59	0.01	0.19	0.78	0.09	bdl	0.37	bdl	54.1
GB-14	22.3	6.2	15.6	24	1.25	1.01	1.13	3.21	0.80	0.57	0.04	0.47	0.06	0.10	bdl	bdl	10.5
GB-15	23.1	6.4	6.5	10	0.43	0.40	0.79	2.52	0.34	0.05	0.03	0.08	0.04	bdl	bdl	0.06	5.45
GB-16	21.2	5.8	10.4	16	1.25	0.78	0.93	3.57	0.34	bdl	0.03	0.76	0.06	bdl	0.01	bdl	8.11
GB-17	24.1	5.5	15.6	24	4.21	0.99	0.79	1.83	0.24	bdl	0.06	1.28	0.05	0.05	20	bdl	3.02
GB-18	21	5.6	9.1	14	1.21	0.99	0.81	4.64	0.09	0.01	0.04	0.40	0.05	0.02	bdl	0.02	7.04
GB-19	21.3	6.2	9.1	14	0.85	1.13	0.82	4.63	0.21	bdl	0.04	0.10	0.08	bdl	bdl	bdl	7.63
GB-20	24	5	8.45	13	0.37	0.73	0.39	3.34	0.16	bdl	0.03	0.25	0.06	0.04	bdl	bdl	3.45
GB-21	20.8	6.5	10.4	16	0.71	1.11	1.24	3.46	0.38	0.01	0.05	0.39	0.05	bdl	1.80	0.03	6.55
GB-22	21.9	5.6	9.75	15	0.59	0.96	0.85	3.66	0.33	0.02	0.03	0.29	0.13	0.02	bdl	bdl	6.52
GB-23	26.2	5.7	9.75	15	0.64	0.89	0.95	2.92	0.13	bdl	0.03	0.32	0.02	bdl	bdl	bdl	6.02
GB-24	20.4	5.6	10.4	16	0.70	0.63	1.50	3.28	0.20	0.26	0.01	0.08	0.05	bdl	bdl	0.02	8.00
GB-25	24.2	5.5	7.15	11	0.31	0.40	0.51	2.25	0.03	bdl	0.03	0.11	0.02	0.02	0.01	0.04	2.73
GB-26	22.6	5.8	7.8	12	0.50	0.93	0.81	3.94	0.15	0.01	0.03	0.07	0.02	bdl	bdl	bdl	5.43
GB-27	22.6	6.5	9.1	14	0.88	1.22	0.95	4.45	0.25	0.02	0.03	0.13	0.01	bdl	0.03	bdl	7.50
GB-28	22.9	6.1	10.4	16	1.43	2.13	0.20	6.03	0.00	0.01	0.03	0.34	bdl	bdl	0.95	0.11	5.63
GB-29	22.4	6.4	40.9	63	5.44	1.80	3.03	11	2.51	0.03	0.09	0.35	bdl	bdl	bdl	0.02	36.1
GB-30	21.1	6.3	61.75	95	6.79	1.91	5.62	11.5	4.10	bdl	0.14	0.09	0.01	bdl	0.03	bdl	52.8
GB-31	21.2	7.1	37.7	58	4.01	2.55	3.92	11.7	1.51	0.34	0.08	0.15	0.02	bdl	0.07	0.04	33.2
GB-32	21.9	6.9	52	80	5.26	3.44	5.48	11.7	2.46	0.21	0.10	0.18	0.00	bdl	0.36	bdl	43.6
GB-33	23.1	6.8	35.1	54	4.95	2.14	3.83	10.4	1.58	0.13	0.13	0.09	0.03	0.03	0.01	0.08	31.8
GB-34	22	6.1	13.7	21	1.51	0.72	1.45	5.09	0.59	bdl	0.04	0.07	0.01	bdl	0.04	bdl	12.1
GB-35	21.8	6.7	55.3	85	5.14	2.84	6.50	11.4	2.84	0.09	0.10	0.18	0.01	0.06	0.79	0.00	46.1
GB-36	29	6.8	52.7	81	3.38	1.25	6.61	6.40	3.66	0.15	0.10	0.32	0.08	0.02	0.02	0.10	44.7
GB-37	23.5	6.7	59.2	91	4.84	1.42	8.52	12.3	3.38	0.11	0.10	0.22	0.02	bdl	0.24	0.02	51.2
GB-38	26.2	6.5	48.1	74	4.51	1.78	5.04	9.69	3.20	0.03	0.11	0.11	0.01	0.06	0.13	bdl	42.1
GB-39	19	5.8	7.8	12	0.87	0.74	0.87	3.81	0.13	0.01	0.06	0.15	0.02	bdl	0.04	0.10	5.81

Sample ID	Temp	pH	TDS	EC	Na^+	K^+	Ca^{2+}	Si	Mg^{2+}	SO_4^{2-}	F^-	Cl^-	NO_2^-	Br^-	NO_3^-	PO_4^{2-}	HCO_3^-
GB-40	20.4	6.1	13	20	0.71	1.06	1.57	3.63	0.55	0.18	0.03	0.09	0.05	0.06	0.04	bdl	9.89
GB-41	20.2	6.1	15.6	24	1.56	2.33	1.33	6.69	0.45	0.15	0.04	0.07	0.04	bdl	0.01	0.23	12.5
GB-42	20.7	6.2	10.4	16	0.93	1.18	1.17	3.83	0.35	0.01	0.03	0.14	0.02	0.03	0.16	0.17	8.79
GB-43	27.2	6.6	10.4	16	0.84	1.35	1.30	4.16	0.53	0.07	0.05	0.12	0.01	0.05	0.04	bdl	10.6
GB-44	20	6.5	21.5	33	1.90	1.22	2.00	5.93	1.47	0.08	0.07	0.17	0.01	0.05	0.38	bdl	18.9
GB-45	21.3	6.4	25.4	39	2.47	1.75	2.33	7.61	1.50	0.02	0.06	0.31	0.04	0.02	0.42	bdl	21.9
GB-46	22.3	6.3	18.9	29	1.14	1.49	2.12	5.27	1.16	0.54	0.05	0.27	bdl	0.02	0.43	bdl	16.3
GB-47	24.7	6.4	27.9	43	3.32	2.53	2.46	7.99	1.11	0.26	0.12	0.33	bdl	0.05	0.19	0.10	22.7
GB-48	22.8	5.8	18.2	28	1.72	1.50	1.01	6.17	1.48	0.49	0.07	0.36	0.02	0.02	0.20	bdl	15.4
GB-49	22.2	6	13.7	21	1.01	1.17	1.08	5.51	0.84	0.04	0.04	0.17	0.02	0.03	0.22	0.06	11.21
GB-50	21	5.8	9.1	14	1.19	1.13	0.55	5.06	0.08	0.02	0.03	0.07	bdl	0.02	0.01	bdl	7.03
GB-51	21.2	6.4	26.7	41	2.88	2.60	1.87	7.55	1.39	0.15	0.07	0.16	bdl	bdl	0.02	0.04	21.8
GB-52	25.5	6.4	48.8	75	5.42	2.48	3.84	11.5	3.57	0.01	0.13	0.08	0.01	bdl	0.04	0.03	42.5

TDS, total dissolved solids; EC, electrical conductivity; Temp, surface water temperature; bdl, below detection limit; GB, Garoua-Boulai–Bétaré-Oya; N, number of samples

Table 3.2. Descriptive statistics of physico–chemical parameters of surface water in the lower Lom Basin. Dissolved ion levels are compared to WHO proposed levels.

Parameters	Units	Minimum	Maximum	Average	SD	WHO standard (2011)
Temp	^{o}C	17.3	29	22.1	2.23	–
pH	–	5	7.3	6.26	0.47	6.5-8.5
EC	µS/cm	9	112	36.4	30.3	–
TDS	mg/l	4	87	27.9	23.5	500
Na^{+}	mg/l	0.06	8.96	2.34	2.13	50
K^{+}	mg/l	0.4	3.71	1.54	0.8	100
Ca^{2+}	mg/l	0.2	9.48	2.4	2.37	75
Mg^{2+}	mg/l	0.01	4.74	1.23	1.37	30
HCO_3^{-}	mg/l	2.73	62.7	19.4	17.3	200
Si	mg/l	1.83	16.1	6.43	3.36	–
NO_3^{-}	mg/l	0.01	20	0.75	3.23	50
Cl^{-}	mg/l	0.07	1.28	0.23	0.21	250
SO_4^{2-}	mg/l	0.01	0.57	0.13	0.15	200
F^{-}	mg/l	0.01	0.21	0.07	0.05	1
NO_2^{-}	mg/l	bdl	0.13	0.04	0.03	–
Br^{-}	mg/l	0.02	0.1	0.04	0.02	–
PO_4^{2-}	mg/l	bdl	0.23	0.06	0.05	–

TDS, total dissolved solids; EC, electrical conductivity; Temp, surface water temperature; SD, standard deviation; bdl, below detection limit; (–), not available

nature with pH values between 5.0 and 7.3. The water temperature varied from 17.3 to 29 °C with a mean value of 22.1 °C. This is close to the atmospheric temperature (26 °C) implying recharge under present climatic conditions. Electrical conductivity varied from 9 to 112 µS/cm indicating less mineralized water. This is typical of most waters in the forest zones of southern Cameroon, which flow on the metamorphic bedrock (Beoglin et al., 2003; Braun et al., 2005). Like EC, TDS values were relatively low and ranged from 4 to 87 mg/l, with an average value of 27.98 mg/l. EC and TDS had high standard deviation values of 30.31 and 23.45, respectively; which implies diverse hydrochemical processes characterize water composition within the catchment. In agreement with Freeze and Cherry (1979) classification, all stream water samples in the study area were categorized as fresh (TDS < 1000 mg/l).

Given that no standard guideline for drinking water exists in Cameroon, the quality of surface water was assessed by comparing the hydrochemical parameters of surface water in the basin with the safe limits set by the World Health Organization (WHO, 2011). Besides pH, all the investigated samples had concentrations lower than the threshold values for the various parameters.

3.4.2 Major ion geochemistry and hydrogeochemical facies of surface water

Major ion chemistry showed that Ca^{2+} and Na^{+} were the dominant cations followed by K^{+} and Mg^{2+} (Fig 3.2a). The concentration of Ca^{2+} varied from 0.2 to 9.48 mg/l and accounted for 32 % of the total cations. Concentrations of Na^{+} were higher than those of Ca^{2+} in 40 % of the samples. In addition, Na^{+} and K^{+} contributed 52 % of the total cations. HCO_3^{-}, like Ca^{2+} and N^{a+}, was the dominant anion with a secondary contribution from NO_3^{-}. The order of abundance was $HCO_3^{-} > NO_3^{-} > Cl^{-} > SO_4^{2-} > F^{-} > NO_2^{-} > Br^{-} > PO_4^{3-}$ (Fig 3.2a). The dominance of HCO_3^{-} suggests chemical weathering process occurs within the catchment. Natural processes such as the weathering of alumino–silicate minerals by dissolved CO_2 produced from the decay of organic matter or root respiration is the likely source of Ca^{2+}, Na^{+} and HCO_3^{-} in the water. (Njitchoua and Ngounou, 1997; Rose, 2002). The levels of NO_3^{-} in the samples were generally low (<2 mg/l). The only exception was sample GB–17 (NO_3^{-} = 20.01 mg/l) collected from a stream flowing close to an established refugee camp in Gado Badzéré suggesting an anthropogenic source. Common sources of dissolved NO_3^{-} in water include

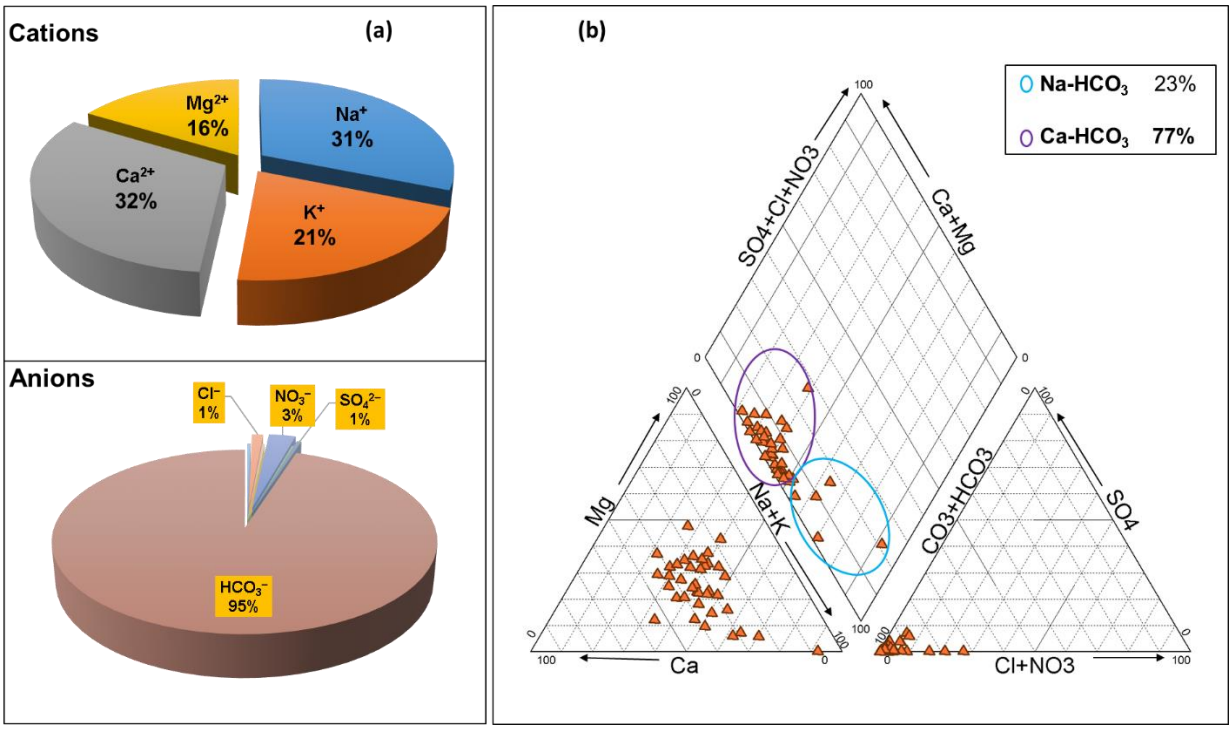

Figure 3.2. Pie chart of mean concentrations of major ions (mg/l) (**a**) and Piper trilinear diagram (**b**) showing alkali metals (Na + K) slightly exceed the alkaline earth metals (Ca + Mg) and the dominance of weak acids (CO_3 + HCO_3). Stream water is classified as Ca–HCO_3 and Na–HCO_3 water types.

atmospheric precipitation, domestic sewage, agriculture fertilizers, human and animal excrement (Appelo and Postma, 1996). Sulphate concentrations (0.01–0.57 mg/l) were lower than concentrations (2–80 mg/l) in natural water (Tiwari and Singh, 2014) and reflect the low sulphide dissolution in the area.

The relationship between different dissolved constituents and the chemical patterns of the stream water were elucidated by plotting the major ions on a trilinear diagram described by Piper (1944). The hydrochemical classification is presented in Fig. 3.2b. All water samples were chemically dominated by alkali metals (Na and K) and the weak acid (HCO_3). Two distinctive water types were produced based on their ionic concentrations; 77 % of samples plotted as Ca–HCO_3 and 23 % as Na–HCO_3. These water species are typical of surface water draining igneous/metamorphic rocks in hot and humid equatorial climate, resulting in the discordant dissolution of primary silicate minerals such as Na–feldspars, plagioclases, pyroxene and hornblende (Srinivasamoorthy et al., 2014; Tame-Mélendez et al., 2016). Also, the water facies indicate short residence time thus low water–rock interaction (Ahialey et al., 2015), ion exchange and active recharge from freshwater (Ako et al., 2012; Edjah and Akiti, 2015).

3.5 Geochemical processes controlling stream water chemistry

3.5.1 Compositional relations among dissolved ions

Weathering of silicate and carbonate minerals is a primary source of alkalinity in natural water. Also, the stoichiometric relationships between dissolved species have been used to unravel the origin of solutes and the processes that influence the observed water chemistry. To investigate the role of mineral weathering, Kim et al. (2005) suggested the plot of total cations against alkalinity. Based on this method, a 1:1 relation between the sum of cations and alkalinity is an indication that mineral weathering is the primary process controlling the water chemistry. In this study, all samples plot on or near the 1:1 dissolution line in Fig. 3.3a indicating that silicate weathering is the main hydrogeochemical process affecting the surface water chemistry. These common rock–forming minerals are altered by the mildly acidic stream water through hydrolysis to form metal cations in solution as expressed in the following generalized equation:

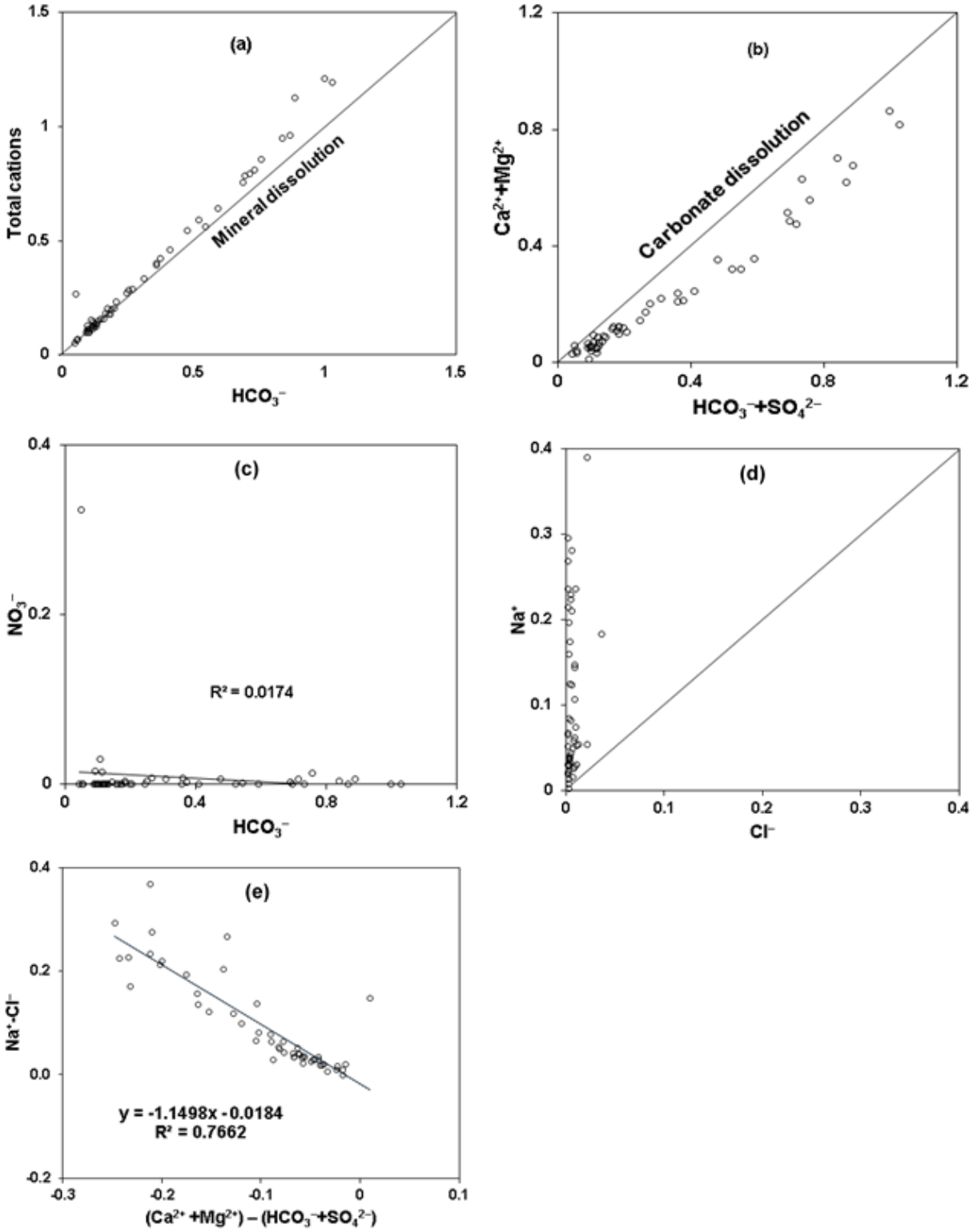

Figure 3.3. Relations among dissolved species in surface water of the lower Lom Basin. (**a**) Total cations (TZ*) vs HCO_3^-; (**b**) $Ca^{2+} + Mg^{2+}$ vs $HCO_3^- + SO_4^{2-}$; (**c**) NO_3^- vs HCO_3^-; (**d**) Na^+ vs Cl^-; (**e**) $Na^+ - Cl^-$) vs $(Ca^{2+} + Mg^{2+}) - (HCO_3^- + SO_4^{2-})$; concentrations of ions are in meq/l.

$$Rocks + H_2CO_3 \rightarrow cations + H_2SiO_4 + HCO_3^- + Al(silicates) \quad (3.1)$$

From the computed equivalent ionic ratios of the samples in Table 3.3, (Ca^{2+} + Mg^{2+})/total ions (TZ*) ratios ranged from 0.08 to 0.78 with 76 % of the values above 0.5, suggesting a high contribution of alkaline metals in TZ*. The equivalent (Na^+ + K^+)/TZ* ratios varied from 0.22 to 0.92 with 79 % of values less than 0.5 indicating that the major cations are released through silicate weathering (Srinivasamoorthy et al., 2008). Moreover, (Fisher and Mullican, 1997) proposed that the plot of Ca^{2+} + Mg^{2+} against HCO_3^- + SO_4^{2-} will be close to the 1:1 line when carbonate dissolution is the dominant reaction in the system. All water samples plot below the theoretical equiline with a pronounced deviation at higher concentrations (Fig. 3.3b). Higher HCO_3^- + SO_4^{2-} content compared to Ca^{2+} + Mg^{2+} indicates a significant contribution from silicate weathering. The deficiency in the sum of alkaline earth metals relative to bicarbonate requires that the excess negative charge of the anions be balanced by Na^+ + K^+ supplied through the weathering of Na–K silicates in the rocks of the study area (Singh et al., 2005).

Rock weathering occurs when rocks are exposed to the atmosphere and hydrosphere. The HCO_3^-/SiO_2 ratio has been used to verify the mode of weathering in the basin. Because a considerable amount of dissolved SiO_2 is released through silicate weathering, waters with HCO_3^-/SiO_2<5 indicate weathering of silicates is the dominant activity while HCO_3^-/SiO_2>10 point to carbonate dissolution (Srinivasamoorthy et al., 2014). All samples revealed that silicate weathering is the principal source of dissolved ions (Table 3.3, Eqn. 3.1). Furthermore, the role of other geochemical processes was investigated using the NO_3^- vs HCO_3^- plot (Fig. 3.3c). An insignificant negative correlation rules out the possibility of nitrate generating processes given that nitrification or oxidation of organic matter will produce an equivalent of NO_3^- by consuming the same equivalent of alkalinity (Kim et al., 2005).

The relationship between Na and Cl is frequently used to determine the source of salinity in natural waters. Besides, the stoichiometry of halite dissolution demands equal concentrations of Na^+ and Cl^- in solution and a corresponding molar ratio of approximately one (Singh et al., 2005). The molar ratio of Na^+/Cl^- in the water samples compared to seawater (0.86) varied from 0.81 to 111.58 (average 23.2) with 98 % of the samples showing Na enrichment. Higher Na^+/Cl^- ratios (>1) reflect contributions from non–halite sources. From

Table 3.3. Stoichiometric relations between dissolved constituents in surface water of the lower Lom Basin.

Ionic ratio	Minimum	Maximum	Mean	Standard Deviation
(Ca + Mg)/TZ*	0.08	0.78	0.56	0.13
(Na + K)/TZ*	0.22	0.92	0.44	0.13
Ca + Mg/HCO_3	0.11	1.2	0.64	0.16
Ca + Mg/HCO_3 + SO_4	0.11	1.2	0.64	0.16
Na/Cl	0.81	111	23.2	26.9
Na/Ca	0.1	6.28	1.02	0.98
HCO_3^-/SiO_2	0.37	3.26	1.22	0.57
CAI 1	-131	-2.49	-31.6	32.9
CAI 2	-0.99	-0.23	-0.44	0.13

The ratios of the dissolved ions are calculated using meq/l concentrations. TZ*, sum of cations; CAI, chloro–alkaline index; CAI 1 = Cl – (Na + K)/Cl; CAI 2 = Cl – (Na + K)/(SO_4 + HCO_3 + NO_3)

the 1:1 plot of Na^+ against Cl^- (Fig. 3.3d), Na^+ increases without a corresponding increase in Cl^- as would be expected if Na^+ is sourced from sea water or aerosol. Thus, the chemical weathering of rock–forming minerals such as albite and the possible exchange of Ca^{2+} for Na^+ at clay surfaces or organic components of the soil are likely processes liberating extra Na^+ resulting in the Na–HCO_3 water type and higher Na^+/Cl^- ratios. Organic matter and clay minerals have negatively charged ions which can adsorb and hold positively charged base cations by electrostatic force. To verify that ion exchange significantly influences the studied water chemistry, the relationship between $(Na^+ - Cl^-)$ vs $(Ca^{2+} + Mg^{2+}) - (HCO_3^- + SO_4^{2-})$ was investigated. A linear relationship with a slope of –1.0 implies that ion exchange is a major controlling factor (Fisher and Mulican, 1997). Fig 3.3e showed that all the examined streams plot along a line with a slope of –1.15 indicating contribution of ions through ion exchange reactions. The type of ion exchange reaction taking place was determined by using the chloro–alkaline index (CAI) proposed by Schoeller (1967) as follows:

$$CAI\ 1 = Cl^- - (Na^+ + K^+)/Cl^- \quad (3.2)$$

$$CAI\ 2 = Cl^- - (Na^+ + K^+)/(SO_4^{2-} + HCO_3^- + NO_3^-) \quad (3.3)$$

where all values are given in meq/l. When Ca^{2+} or Mg^{2+} in water are exchanged for by Na^+ and K^+ in the surrounding rocks (normal exchange or chloro–alkaline disequilibrium), both the indices above will yield negative values and positive values if the reverse happens (Gupta et al., 2009). All the samples had negative CAI 1 and CAI 2 values (Table 3.3) indicating that apart from the chemical dissolution of the different rock–forming minerals, normal ion exchange contributes in modifying the water composition.

3.5.2 Correlation Coefficient

Pearson's correlation matrix (Table 3.4) was computed to determine the inter–element relationship. From the resultant matrix, pH had negative correlations with Cl^-, NO_3^- and SO_4^{2-} suggesting a negligible contribution to the acidity of the streams. EC showed a perfect correlation with TDS indicating its direct relationship to the amount of dissolved salts in water. Similarly, the strong positive r values observed between Si, HCO_3^- and the major cations indicate a common igneous origin. Chloride showed relatively high (0.715) and poor

Table 3.4. Pearson's correlation matrix ($p<0.05$) of measured water quality parameters.

	pH	EC	TDS	Cl^-	NO_3^-	SO_4^{2-}	HCO_3^-	Si	Na^+	K^+	Ca^{2+}	Mg^{2+}
pH	1											
EC	0.586	1										
TDS	0.584	1	1									
Cl^-	-0.137	0.049	0.051	1								
NO_3^-	-0.057	-0.053	-0.050	0.715	1							
SO_4^{2-}	0.133	0.013	0.014	0.015	-0.094	1						
HCO_3^-	0.615	0.991	0.991	-0.053	-0.155	0.026	1					
Si	0.596	0.911	0.911	-0.133	-0.187	0.013	0.932	1				
Na^+	0.493	0.939	0.939	0.222	0.127	-0.052	0.912	0.875	1			
K^+	0.576	0.748	0.748	-0.050	-0.077	0.088	0.750	0.853	0.737	1		
Ca^{2+}	0.688	0.961	0.961	-0.039	-0.092	0.006	0.963	0.866	0.839	0.686	1	
Mg^{2+}	0.511	0.976	0.976	0.025	-0.101	0.036	0.974	0.858	0.895	0.666	0.929	1

(0.015) correlations with NO_3^- and SO_4^{2-}, respectively. The good correlation between Cl^- and NO_3^- points to an anthropogenic source as discussed below. A very weak correlation (0.133) was observed between SO_4^{2-} and pH suggesting that the mildly acidic to neutral water (pH, 5–7.3) does not enhance high sulphide oxidation. It is generally accepted that at conditions of pH above 4.5 in natural waters, oxidation of sulphides such as pyrite (FeS) and arsenopyrite (FeAsS) occurs at a slow rate with little or no acidity (Lewis, 2010). Also, the acid generated during this process might have been consumed through reactions with silicate minerals, thus providing a long–term buffering capacity (Salomons, 1995).

3.5.3 Principal component analysis

The underlying geochemical processes controlling the composition of stream water in the Lom Basin were investigated following principal component analysis (PCA) computation (Table 3.5). Varimax rotation was adopted. In PCA, eigenvalues are commonly used to identify the number of components (PCs) that can be retained for later study (Ouyang et al., 2006). Only PCs with eigenvalues greater than unity were extracted for further analysis. Thus, three PCs were considered which accounted for 87.4 % of the total variance of information of the dataset. Principal component 1 (PC1) comprised EC–TDS–HCO_3^-–Ca^{2+}–Mg^{2+}–Si–Na^+–K^+–pH and explained 63.6 % of the total variance. The strong positive loading (>0.9) observed in this component suggests a common source, essentially the plutono–metamorphic basement, and to some extent cation exchange. Carbonic acid facilitates the breakdown of silicate minerals (Equation 3.1). This reaction is accompanied by the release of base cations, silicic acid and increased alkalinity (Butler, 1981) as observed in the study area. However, the water–rock reaction is expected to be slower under the neutral conditions in the basin accounting for the low cation concentrations. Potassium showed a moderate loading (0.810) suggesting K^+ was removed from solution by clays in the formation of secondary minerals.

PC2 constituted Cl^- and NO_3^- which explained 15.1 % of the total variance. A poor contribution from the other variables was also observed. The combination of these anions indicated their anthropogenic input through human–related activities such as sewage sludge and cattle rearing in the surrounding communities (Ahialey et al., 2015). High concentration of NO_3^- recorded in the vicinity of refugee camps is probably due to open–air defecation. Many

Table 3.5. Varimax rotated component matrix analysis of stream water parameters.

Variable	Component 1	Component 2	Component 3
EC	**0.991**	0.032	-0.020
TDS	**0.990**	0.035	-0.019
HCO_3^-	**0.989**	-0.079	-0.005
Ca^{2+}	**0.958**	-0.050	-0.001
Mg^{2+}	**0.953**	0.000	-0.019
Si	**0.945**	-1.151	-0.002
Na^+	**0.937**	0.227	-0.085
K^+	**0.810**	-0.059	0.125
pH	**0.656**	-0.126	0.264
Cl^-	0.014	**0.935**	0.028
NO_3^-	-0.065	**0.910**	-0.057
SO_4^{2-}	-0.011	-0.013	**0.978**
Eigen values	7.628	1.808	1.053
% Variance	63.564	15.071	8.776
Cumulative %	63.564	78.635	87.411

Bold values are loadings >0.5

authors have identified the presence of pit toilets and subsistence farming as potential sources of NO_3^- in natural waters, in other parts of Cameroon (Fantong et al., 2009; Eneke et al., 2011; Wirmvem et al., 2013; Kamtchueng et al., 2014). The third component composed of SO_4^{2-} and accounted for 8.8 % of the total variance. This single variable probably reflects the presence of sulphide–bearing minerals associated with gold deposits. Hydrothermal gold occurs as quartz veins associated with pyrite, galena, chalcopyrite, sphalerite and iron oxides in the catchment (Omang et al., 2014).

3.6 Regional spatial distribution and sources of enriched geochemistry

The regional geochemical maps for dissolved ions are presented in Fig. 3.4a–i. Relatively high concentrations of NO_3^- and Cl^- (Fig. 3.4a and b) corresponded to high levels of H^+ or low pH (Fig. 3.4c) in the northeastern portion of the study area. Such similar distribution pattern is observed in localities close to the volatile border between Cameroon and the Central African Republic. These localities host more than a hundred thousand refugees (UNICEF, 2014). Hence, the domestic wastewater produced from these municipalities, stock–raising and open–air defecation contribute to NO_3^- and Cl^- concentrations and account for the mild acidity recorded in water. Bicarbonate, Ca^{2+}, Na^+, K^+, and Mg^{2+} showed similar distribution trends (Fig. 3.4d–h) suggesting they are products of deep soil weathering carried by surface water flow. These cations form the common silicate minerals in the Pan–African basement alongside silicon and oxygen. Also, the incongruent dissolution of silicate minerals that react with dissolved CO_2 gas derived directly from the atmosphere, decay of organic matter in the soil or photosynthesis results in the release of the major cations, bicarbonate and dissolved silica (Stum and Morgan, 1981). Comparable findings have been reported in some natural waters of volcanic terrains in Cameroon (Njitchoua and Ngounou, 1997; Ako et al., 2011; Wirmvem et al., 2013, Kamtchueng et al., 2016). These authors attributed the solute composition of natural waters to the hydrolysis of the rock–forming minerals and the incongruent weathering reactions. The spatial distribution of SO_4^{2-} (Fig. 3.4i) suggests the occurrence of sulphide minerals associated with Au mineralization in the area. Sulphidation of the wall rock has been proposed as a possible mechanism of hypogene gold precipitation within the Lom Group (Omang et al., 2014). However, the concentrations are low given the near neutral pH of the streams hinders complete sulphide dissolution in this catchment.

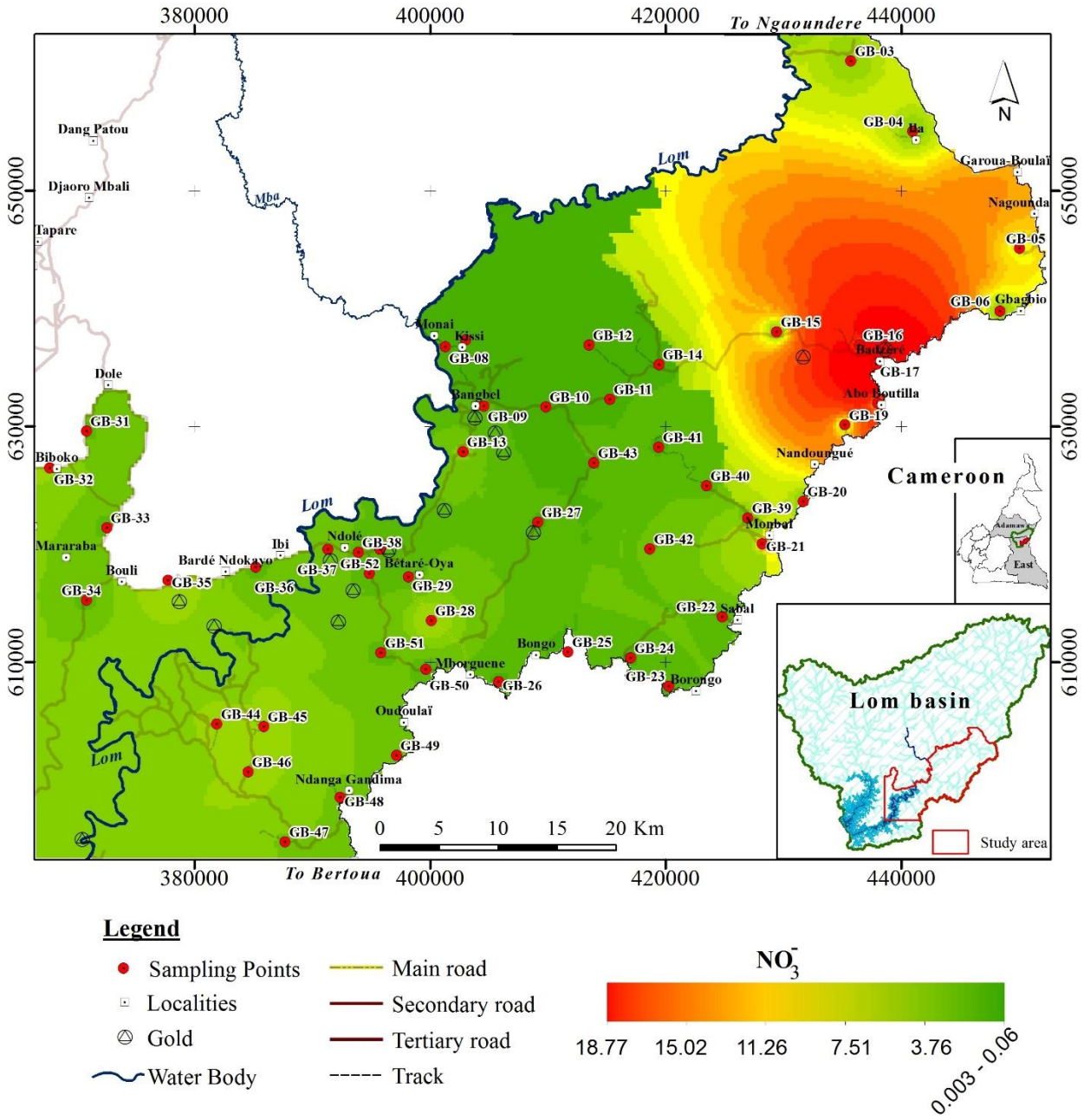

Figure 3.4a. Geochemical background of NO_3^- (mg/l) in surface water of the lower Lom Basin.

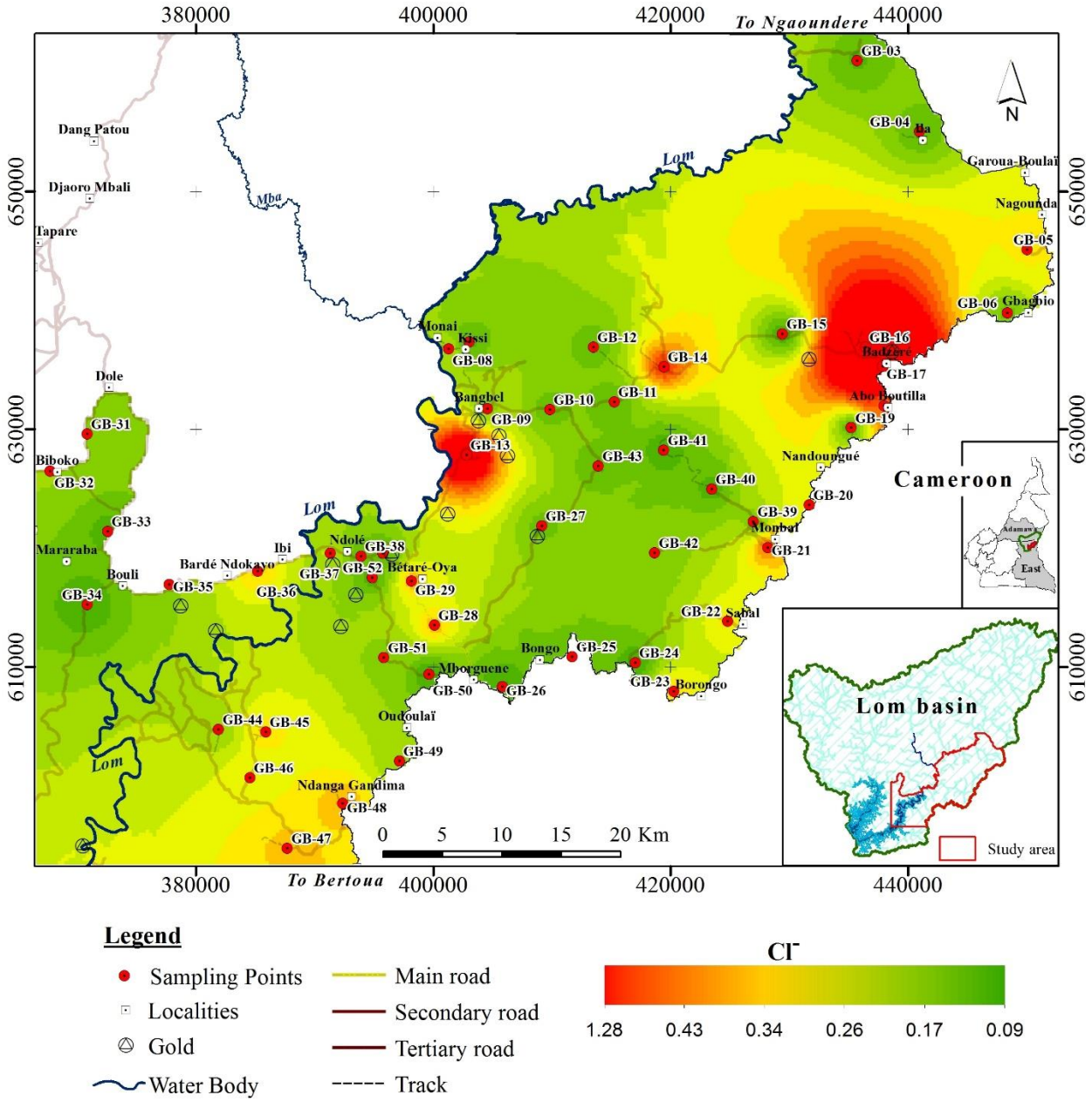

Figure 3.4b. Geochemical background of Cl^- (mg/l) in surface water of the lower Lom Basin.

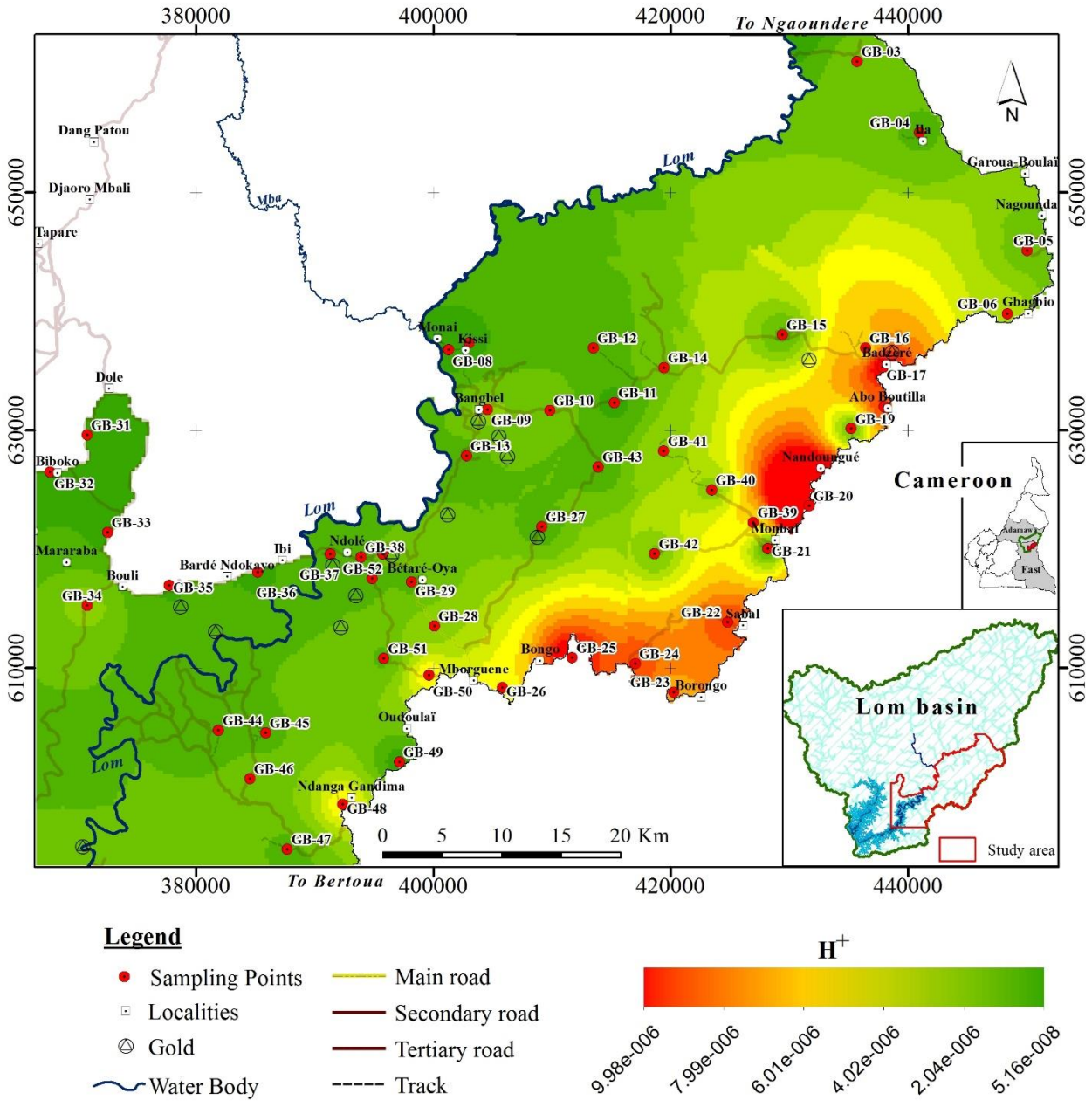

Figure 3.4c. Geochemical background of [H^+] in surface water of the lower Lom Basin.

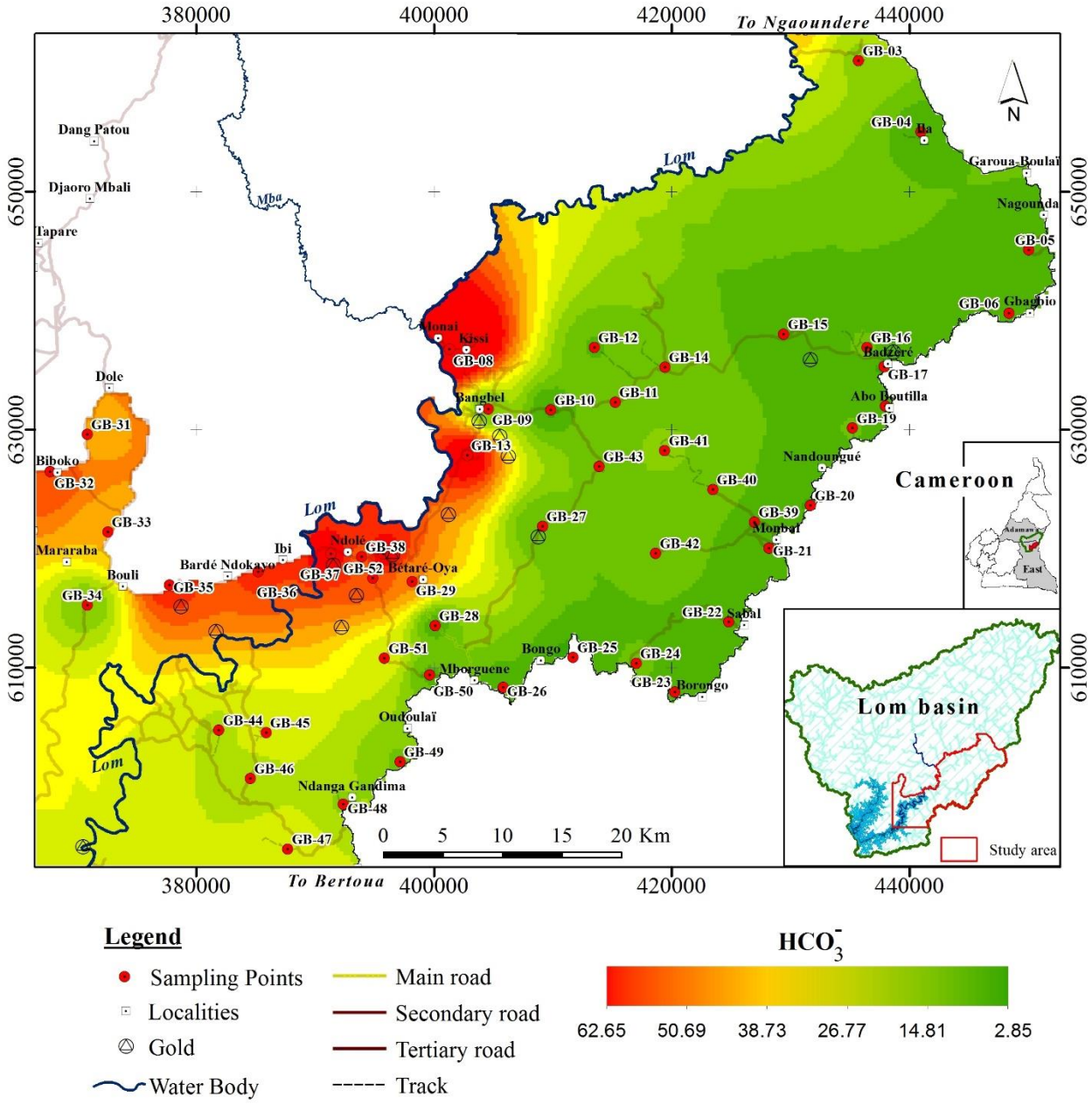

Figure 3.4d. Geochemical background of HCO_3^- (mg/l) in surface water of the lower Lom Basin.

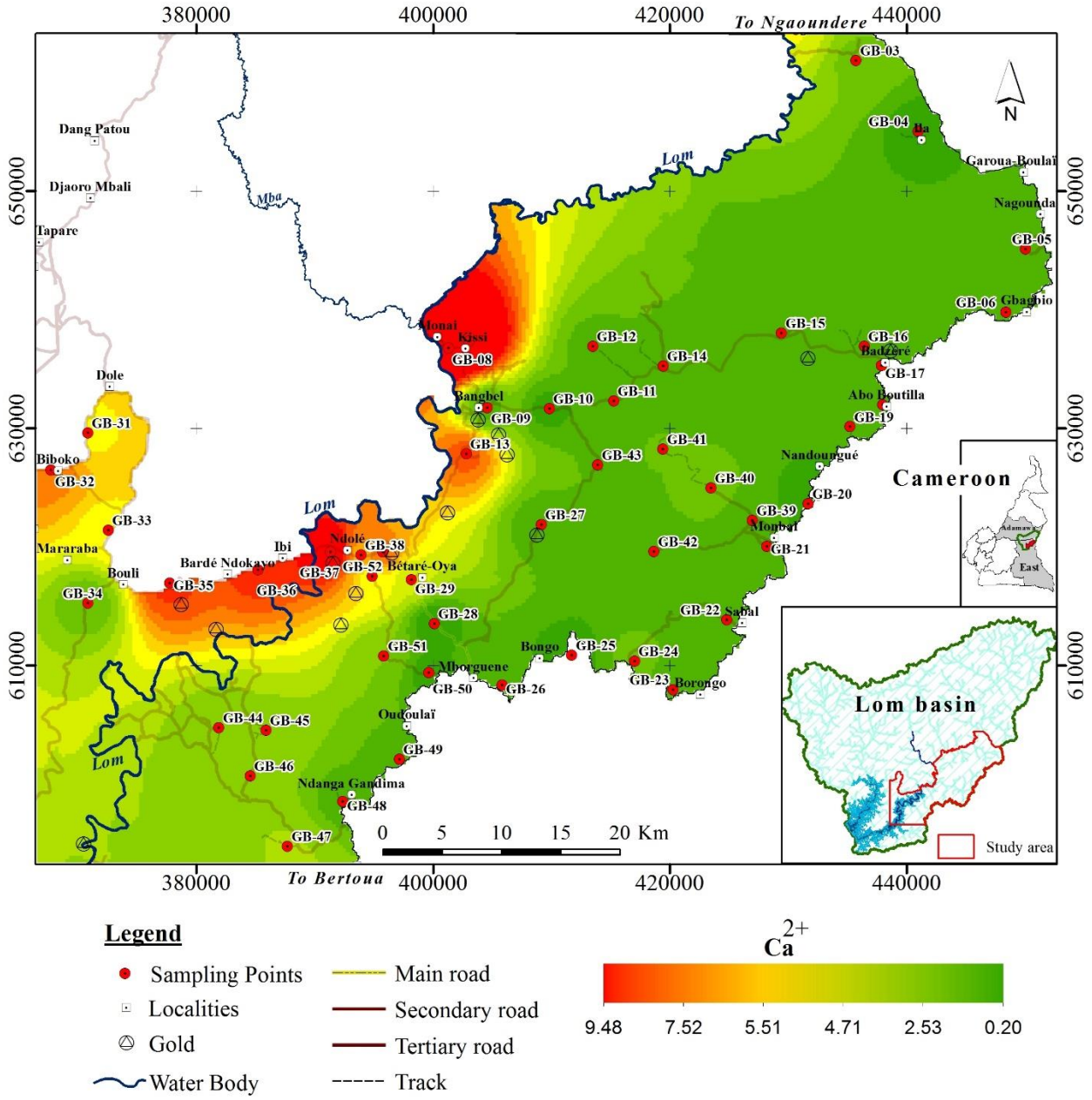

Figure 3.4e. Geochemical background of Ca^{2+} (mg/l) in surface water of the lower Lom Basin.

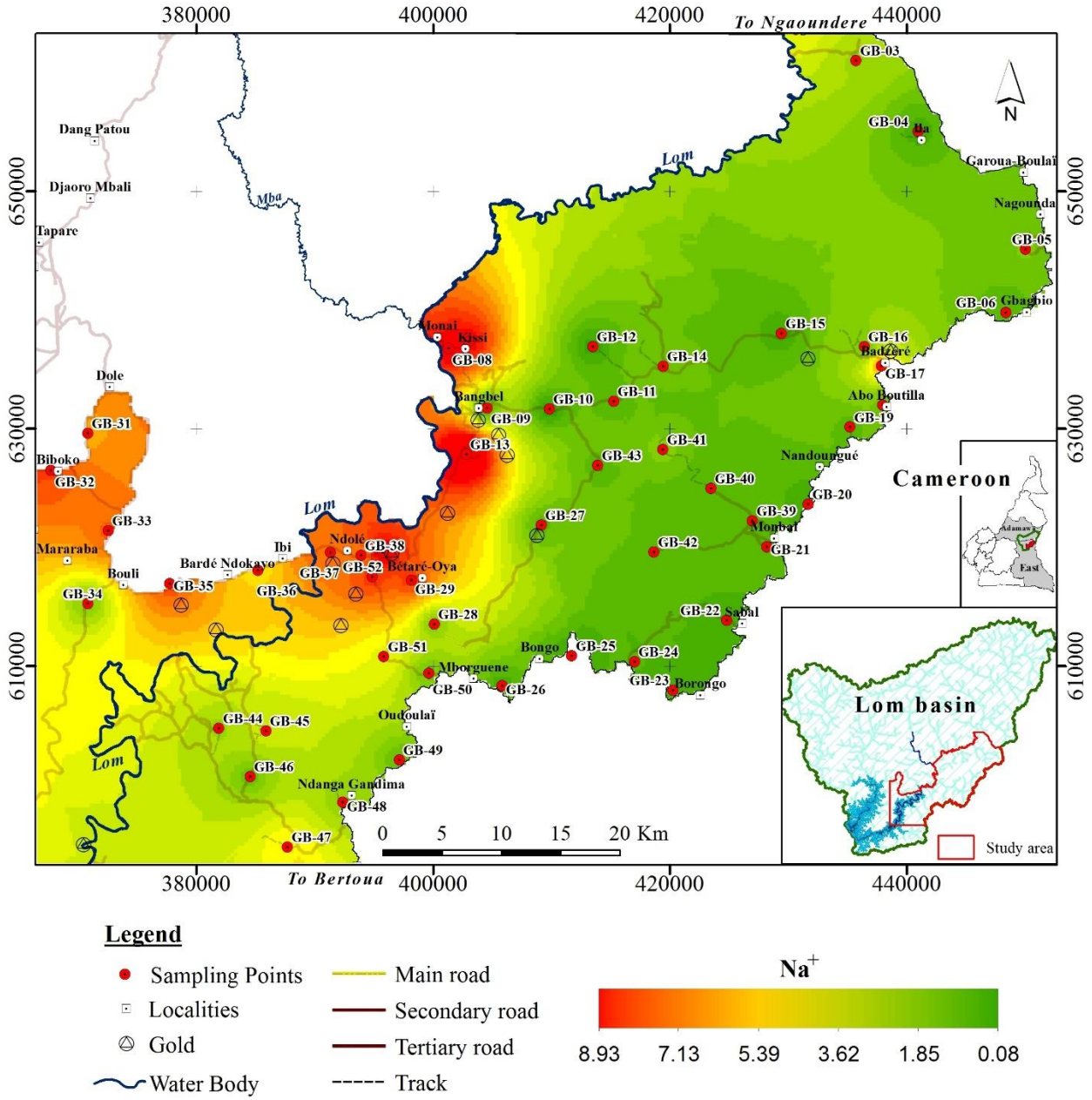

Figure 3.4f. Geochemical background of Na^+ (mg/l) in surface water of the lower Lom Basin.

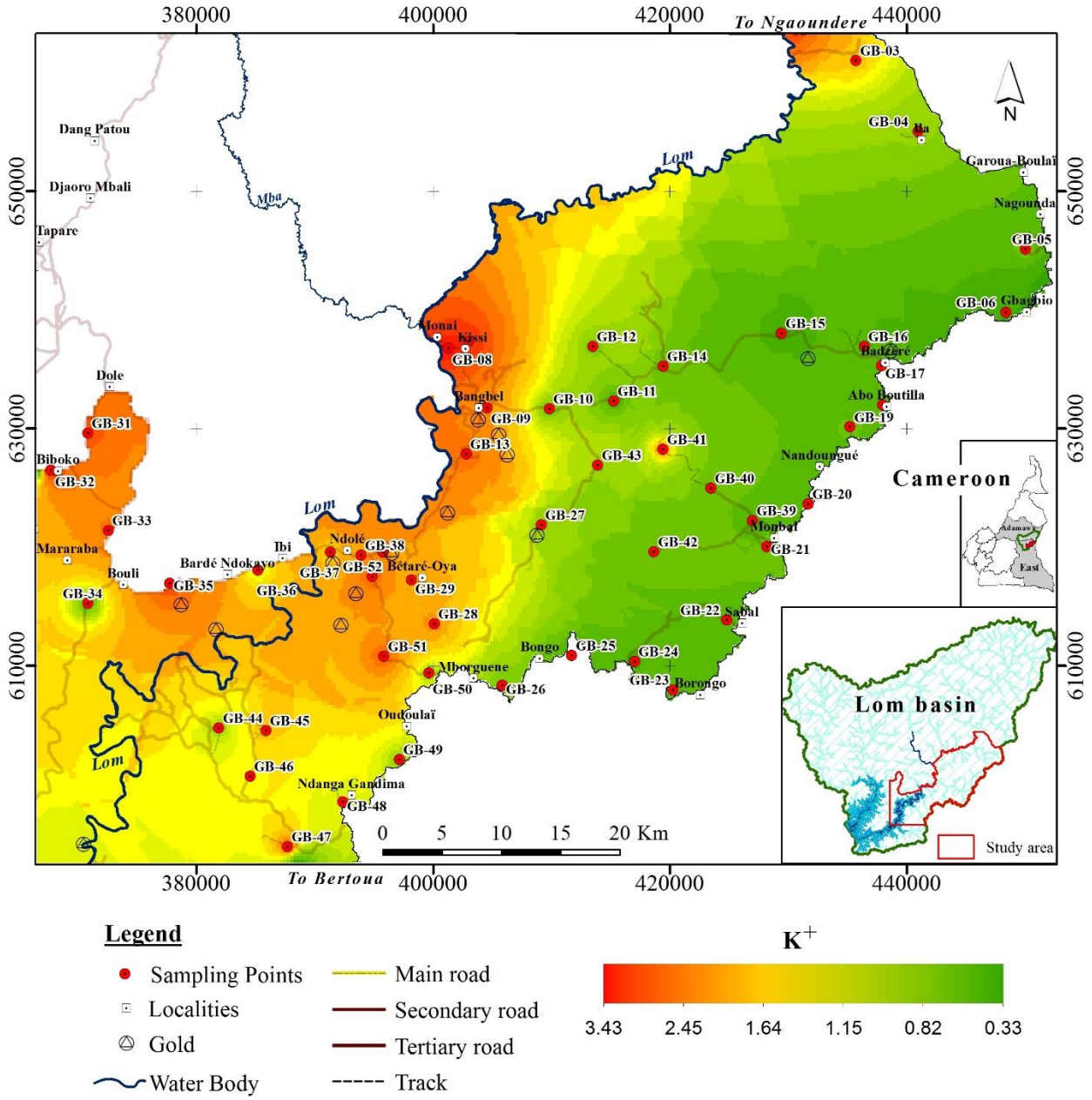

Figure 3.4g. Geochemical background of K^+ (mg/l) in surface water of the lower Lom Basin.

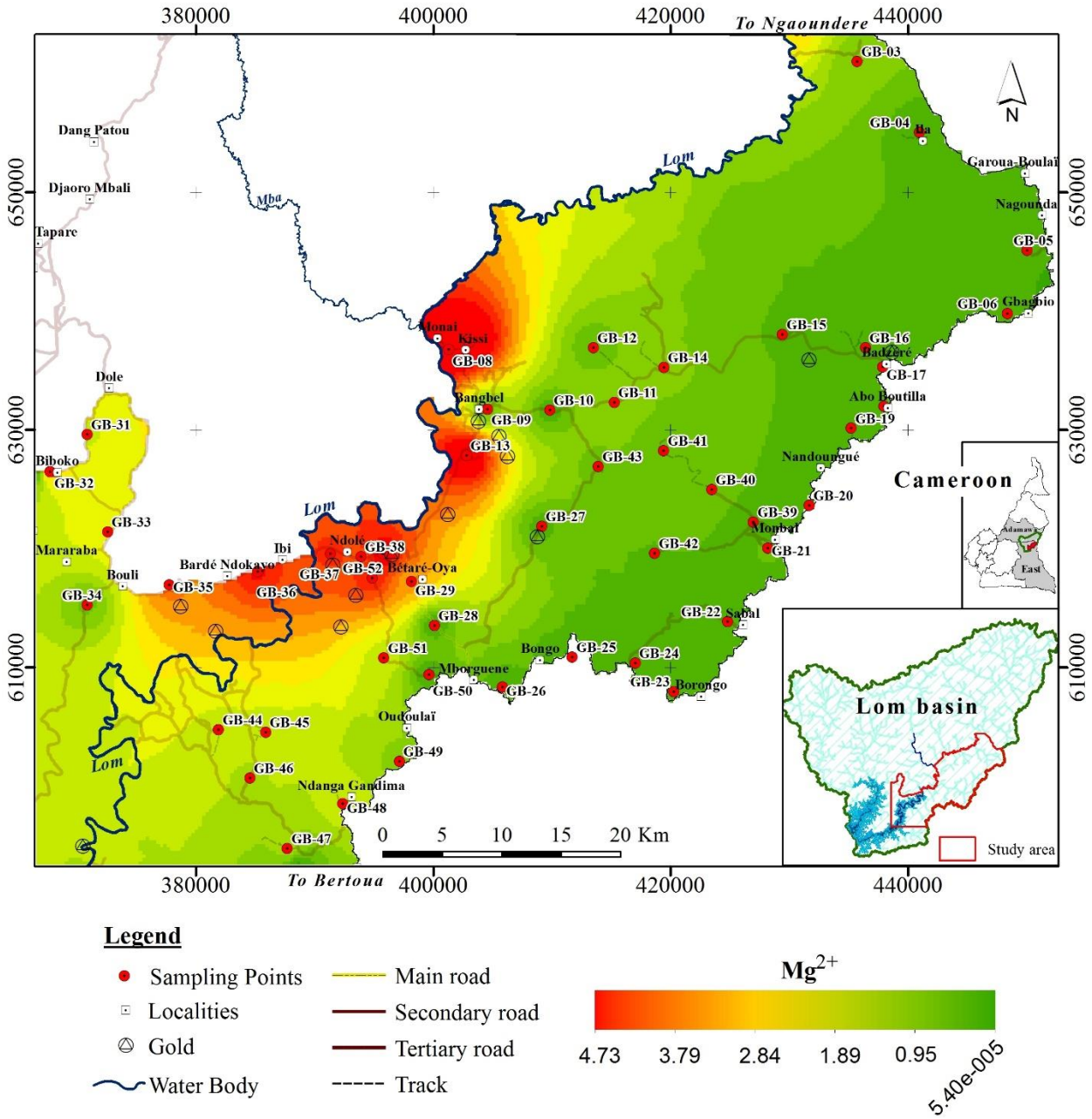

Figure 3.4h. Geochemical background of Mg^{2+} (mg/l) in surface water of the lower Lom Basin.

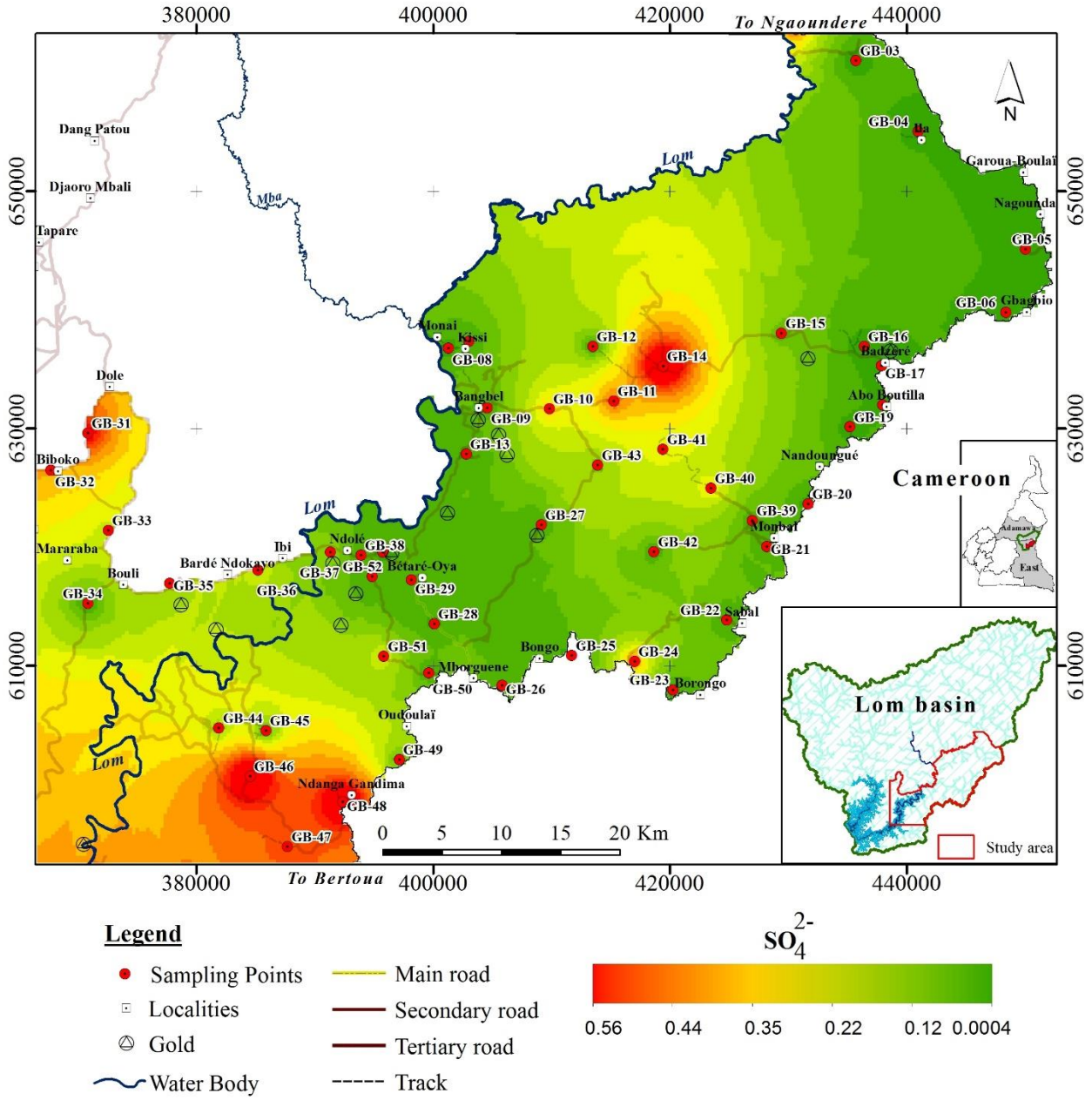

Figure 3.4i. Geochemical background of SO_4^{2-} (mg/l) in surface water of the lower Lom Basin.

3.7 Conclusions

This study assessed the hydrochemistry of surface water in the Lom catchment by determining the physical and chemical characteristics, key processes influencing water chemistry and its suitability for drinking using analytical data of 52 water samples. The physiso–chemical baseline data of surface water generated forms the groundwork for water quality assessment and monitoring ASM activities in the catchment. Most of the studied streams are mildly acidic in nature. Thus, in the event of tap water supply in the area, proper water treatment must be done since acidic water may lead to corrosion and scale formation in pipes. Mean concentrations of EC and TDS are low indicating a less mineralized and fresh water. Generally, the dissolved major ion contents are low and below the desirable limits (WHO) for drinking purposes. Alkali metals (Na + K) slightly exceed alkaline earth metals (Ca + Mg) while weak acids (CO_3 + HCO_3) are significantly higher than strong acids (SO_4 + Cl) in the surface water. The chemical weathering of silicate minerals is the major control on water chemistry as portrayed by the dominance of Ca–HCO_3 (77 %) over Na–HCO_3 (23 %) water type. Although the major ion content is low, the quality of surface water is easily influenced by anthropogenic activities such as the ongoing mining operations in the area. Therefore, the content of potentially hazardous elements in surface water should be determined to assess the impact of such activities. The water quality parameters should also be investigated in the rainy season to estimate the seasonal inputs.

In this research, the interrelationships among dissolved species have been used to determine the roles of different geochemical processes affecting the chemistry of streams draining the Lom basin. Accordingly, the observed chemical composition of the stream water was mostly influenced by the chemical weathering of the surrounding rocks. Ionic exchange of Ca^{2+} in water for Na^+ or K^+ in rocks and anthropogenic inputs of Cl^- and NO_3^- were minor geochemical controls. Also, the provenance of studied elements was distinguished based on geology and land use. Bicarbonate, Na^+, Ca^{2+}, Mg^{2+} and K^+ showed similar distribution trends reflecting the geology. Sulphate distribution correlated with the occurrence of sulphides associated with vein gold deposits in the area. The distribution patterns of NO_3^- and Cl^- reflected pollution from settlements. These dissolved ions were considered to influence the acidity locally.

CHAPTER 4. SEASONAL HYDROLOGICAL INPUTS OF MAJOR IONS AND TRACE METAL COMPOSITION IN STREAMS DRAINING THE MINERALIZED LOM BASIN, EAST CAMEROON: BASIS FOR ENVIRONMENTAL STUDIES[2]

4.1 Introduction

Hydrogeochemical processes help to unravel changes in surface water quality relating to water–rock interaction or anthropogenic impacts (Singh et al., 2005; Kumar et al., 2006; Franz et al., 2014; Kamtchueng et al., 2016). The geochemical properties of surface water also depend on the chemistry of the recharging source as well as the various geochemical processes occurring within the drainage basin. The latter is often responsible for seasonal variations in surface water chemistry (Eneji et al., 2012), hence the chemistry of stream water flowing through a basin can evolve through interaction with weathering products and precipitation. In addition, dissolution and ion exchange reactions as well as anthropogenic actions including artisanal mining activities, which have the potential to damage the environment through water pollution, do play an important role in modifying the chemical composition of stream water along flow paths (Hook, 2005; Ako et al., 2014; Agyarko et al., 2014; Kpan et al., 2014; Simbarashe and Reginald, 2014; Nganje et al., 2015).

The Lom Basin constitutes part of the Precambrian ore deposits in Cameroon (Milesi et al., 2006). Undoubtedly, water is the principal transport route for dissolved solutes derived from both the chemical weathering of the mineralized basement and small–scale mining activities in the area. Stream water and boreholes are the major sources of water supply for domestic and mining activities in this basin. Considering the importance of surface water in the area and the associated environmental problems with artisanal mining, hydrogeochemical baselines were generated to assess the hydrochemistry of surface water and plan water quality monitoring programs. Chapter 3 documents low concentrations of major ions and revealed that silicate weathering was the key factor influencing water

---

[2] *This chapter is an edited version of the article:*
***Mimba, M.E.**, Ohba, T., Nguemhe Fils, S.C., Wirmvem, M.J., Numanami, N., Aka, F.T. **(2017b)**. Seasonal hydrological inputs of major ions and trace metal composition in streams draining the mineralized Lom Basin, East Cameroon: Basis for environmental studies.* Earth Syst Environ, 1:22. *doi 10.1007/s41748-017-0026-6*

chemistry, with ion exchange and anthropogenic inputs as minor controls. However, the increasing population due to the influx of refugees from the neighboring Central African Republic, agro–pastoral activities, increased deforestation, expansion of mine sites and the onset of industrial mining, can influence the seasonal hydrological input and export of dissolved solutes within the catchment. Thus, seasonal estimation of dissolved ions is necessary to understand the contribution of ions and the long–term effects of changes in land use.

Trace metals are common environmental pollutants in mineralized drainage basins and their concentrations in streams can be of natural or anthropogenic origin. Small–scale mining, as well as the weathering of ore deposits, are well known to release elevated concentrations of trace metals into the soil and water systems (Van Straaten, 2000; Nganje et al., 2011; Kusimi and Kusimi, 2012; Edet at al., 2014; Bansah et al., 2016). Moreover, there are growing concerns about the impact of dissolved trace metals on the aquatic ecosystem and human health (Uwah et al., 2013; Dan et al., 2014; Bortey-Sam et al., 2015). No comprehensive survey has been conducted to determine metal levels in stream water of the study area.

Therefore, in this study, an attempt has been made for the first time, to assess the seasonal variation in major ion distribution patterns of stream water. Another major objective is to examine the origin and geochemical behavior of selected trace metals in stream water draining the lower Lom Basin.

4.2 Results and discussion

4.2.1 Seasonal variation of major ions

Seasonal variations of the physico–chemical characteristics of surface water are presented in Table 4.1. All analyzed parameters except pH and Cl^- showed a wide range of values between the sampling periods. This seasonal variability suggests that diverse geological and geochemical conditions probably govern the observed drainage signatures. Concentrations of Cl^-, which is of anthropogenic origin, showed no seasonality throughout the sampling seasons due to the conservative nature and limited potential sources of Cl^- (Grasby et al., 1997; Garizi et al., 2011). Like Cl^-, Na^+ showed only a slight increase during the rainy season. Contrarily,

Table 4.1. Seasonal variation of selected stream water quality parameters in the lower Lom Basin.

	Dry Season			Wet Season		
	Minimum	**Maximum**	**Mean**	**Minimum**	**Maximum**	**Mean**
pH	5.5	6.7	6.12	6	6.7	6.32
EC (μS/cm)	9	107	30.6	20	100	53.9
TDS (mg/l)	5.85	69.6	19.9	13.4	67	36.1
Na^+ (mg/l)	0.06	8.96	2.05	0.41	6.65	2.2
K^+ (mg/l)	0.63	2.53	1.36	0.47	3.65	1.9
Ca^{2+} (mg/l)	0.2	8.52	1.95	0.40	7.69	2
Mg^{2+} (mg/l)	0.01	4.59	0.94	0.06	3.57	0.92
Cl^- (mg/l)	0.07	1.28	0.33	0.08	1.29	0.33
NO_3^- (mg/l)	0.01	20	2.02	0.02	11.3	1.44
SO_4^{2-} (mg/l)	0.01	0.57	0.15	0.13	1.39	0.67
HCO_3^- (mg/l)	0.01	54.1	15.2	4.15	57.6	17.6
Na/(Na+Ca)	0.10	0.88	0.49	0.38	0.80	0.56

EC, electrical conductivity; TDS, total dissolved solids

NO_3^- concentrations within the basin decreased in the wet period owing to dilution by surface runoff during periods of high flow. During rain events, the surface flow waters entering streams have short residence times within the soil and thus, have a low ionic content. Sulphate loadings, like Cl^-, were low for both seasons. Common sources of dissolved SO_4^{2-} in surface water include dissolution of SO_4 minerals, oxidation of pyrite and organic sulphides in natural soil processes, and Sulphur based fertilizers (Hem, 1985; Grasby et al., 1997; Kumar et al., 2006; Nganje et al., 2015). Since agricultural activities are practiced on a fairly small scale in this area, the use of Sulphur based fertilizers is not common. Furthermore, the cluster of points around the near neutral pH field and low SO_4^{2-} content (Fig. 4.1) is typically associated with sulphide gold quartz vein deposits (Ashley, 2002), occurring in the area. Thus, a plausible origin of dissolved SO_4^{2-} is the partial dissolution of sulphide minerals, excluding pyrite as a major source, whose complete oxidation occurs at pH lower than 4.5 (Lewis, 2010). Leaching of soils rich in iron oxides (Freysssinet et al., 1989) by runoff during the wet season accounts for the slight increase in SO_4^{2-} content in the area.

The evolution of stream water chemistry in response to seasonal changes is shown in Figs.4.2 and 4.3. Stream water draining the Lom catchment remained near neutral (5.5 to 6.7) all year round although the pH increased by 0.2 units during the wet season (Table 4.1; Fig. 4.2a). Despite this uniform hydrogen ion activity, EC and HCO_3^- were responsive to seasonal changes (Fig. 4.2b and c). These patterns revealed a shift from very dilute (30.61 µS/cm) solution during the dry season to a solution with increased dissolved solids (53.89 µS/cm) during the months of heavy rainfall. A slight increase in the HCO_3^- content during high–flow conditions of the wet season was also observed, neutralizing the mild acidity recorded during the dry season. There is increased root and microbial respiration during the wet season producing more CO_2 which dissolves to form carbonic acid (H_2CO_3). The dissociation of H_2CO_3 into H^+ and HCO_3^- results in proton consumption via cation exchange reactions on surface soils, liberating cation and HCO_3^- into the water. Hence, besides the supply from the underlying groundwater aquifer, a significant flux of HCO_3^- is generated in the surface soils. In support of the previous report in Chapter 3, the concentrations of Na^+, K^+ and Ca^{2+} slightly increased with increasing flow (Fig. 4.3a–c), exhibiting a similar seasonal pattern as HCO_3^- alkalinity (Fig. 4.3c).

It is well known that stream water cation content usually increases during the dry season. During this period of low stream discharge, high concentrations of major cations derived from silicate weathering are fed into the streams primarily by groundwater. With the advent of

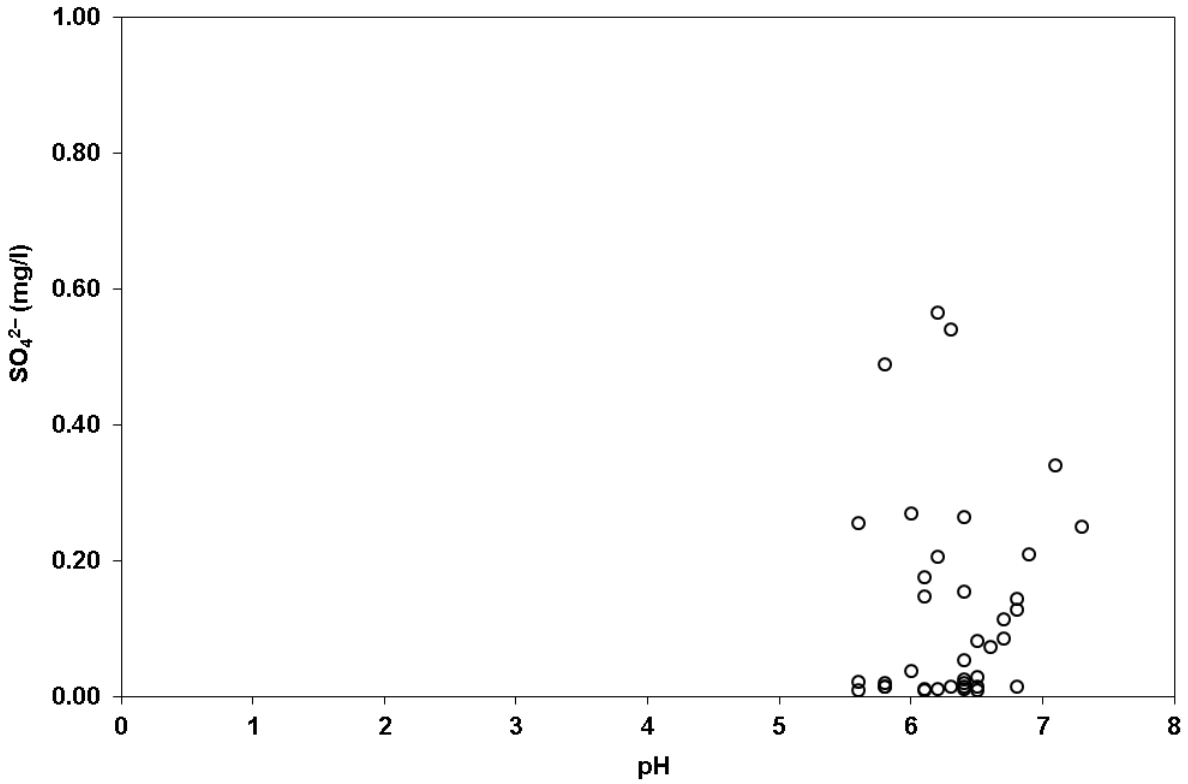

Figure 4.1. Low intensity of acid generation and SO_4^{2-} concentration in surface water of the lower Lom Basin.

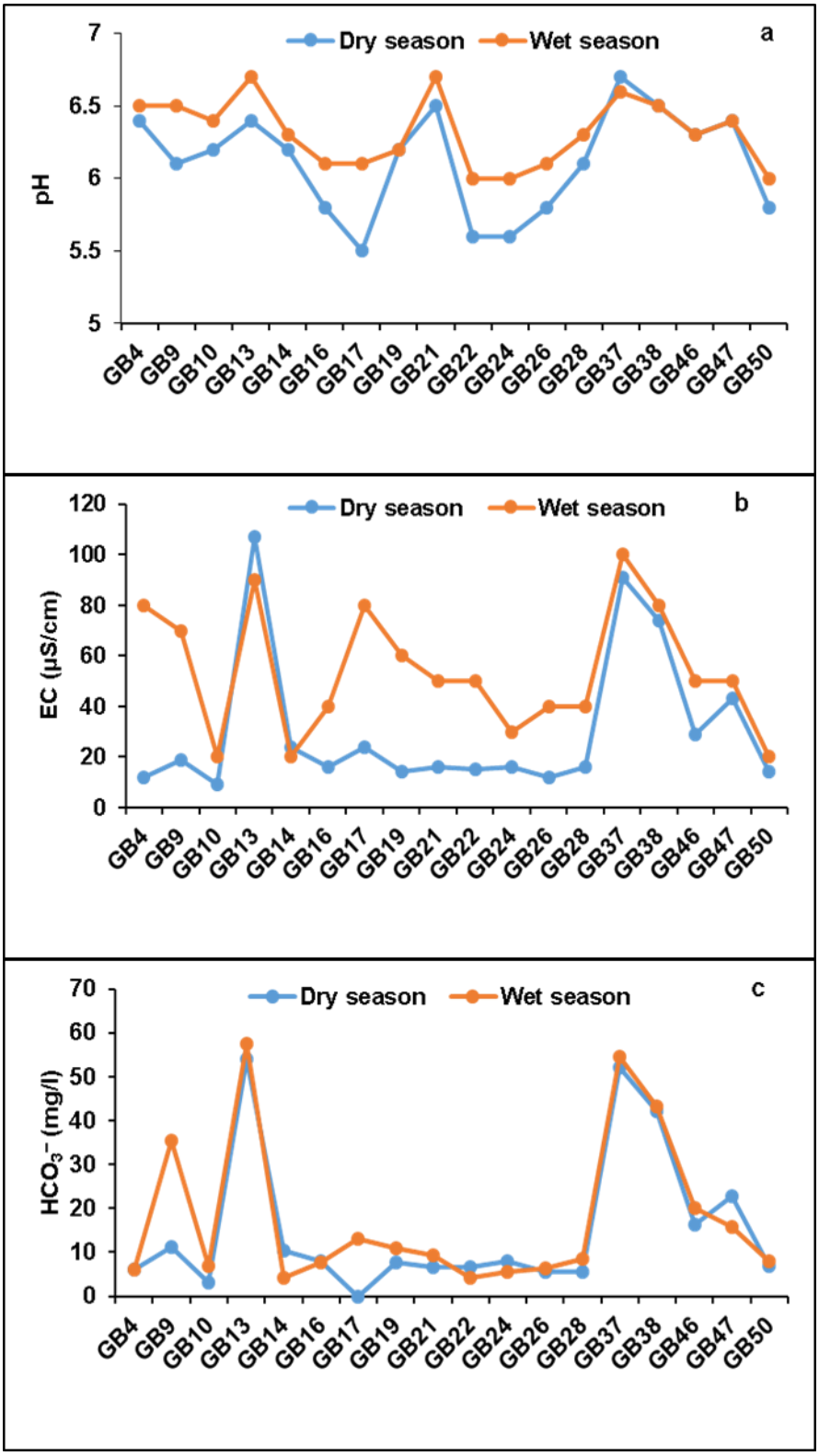

Figure 4.2a–c. Seasonal trend showing an overall increase in pH, EC and alkalinity during the wet season. Dry and wet seasons correspond to periods of base flow and high flow, respectively.

the wet period, stream discharge is expected to increase by surface or lateral flows during precipitation and dilute the streams (Meybeck, 1987; Drever, 1997; Khazheeva et al., 2007; Kelepertzis et al., 2012). Contrarily, a positive correlation was observed between solute concentration and stream discharge similar to observations for streams draining the Amazonian watershed in Brazil (Markewitz et al., 2001) where the high levels of HCO_3^- were attributed to the leaching of cations and HCO_3^- from surface soils to the streams. In such tropical landscapes with highly weathered soils, the ratio of Na/ (Na + Ca) has been used to determine whether the stream water cation content is derived from mineral weathering or rainfall effects. Higher ratios (close to 1) indicate low rates of chemical weathering and vice versa. In the Lom Basin, the majority of samples had Na/ (Na + Ca) ratios approaching one during the rainfall season and dropped during decreased flow (Fig. 4.3d). As expected, inputs from bedrock weathering dissolved in groundwater are predominant during base flow (Fig. 4.3d). In addition, slightly higher concentrations of major cations during the wet season are likely related to precipitation effects as they are flushed from soil surface layers by heavy rainfall. In tropical landscapes, the topsoil layers contain high concentrations of weatherable Na^+, K^+, Ca^{2+} and Mg^{2+} which decrease with depth due to the deep chemical weathering (Markewitz et al., 2001). During rain events, Na^+, K^+ and Ca^{2+} are removed from the cation–exchange complex in soils explaining the increase in their concentrations during the wet season. Therefore, inputs of Na^+, K^+ and Ca^{2+} for the two sampling periods are derived from both the chemical weathering of primary minerals and their leaching from the cation–exchange complexes in surface soils.

The increase in cations during the rainy season may also indicate the biogeochemical influence of surface soil processes on the stream water. Deforestation due to mining activities has been observed in much of the studied watershed (Kouankap Nono et al., 2017). Replacing these forests by mining sites leads to the export of carbon and plant nutrients such as cations, from the ecosystem as wood and emission from fires (Markewitz et al., 2001). The forest plant biomass contributes significant amounts of these nutrients as ash to soils during vegetation clearing and burning. Considering biogenic H_2CO_3 is gradually re–acidifying the surface soils with the subsequent release of K^+, Ca^{2+} and HCO_3^- into the stream, then it is safe to say that the observed seasonal peaks are partly the effects of the changes in land use. Also, deforestation increases rain runoff, rates of erosion and siltation. This enhances the transport of soils into surface water resulting in sedimentation and nutrient enrichment.

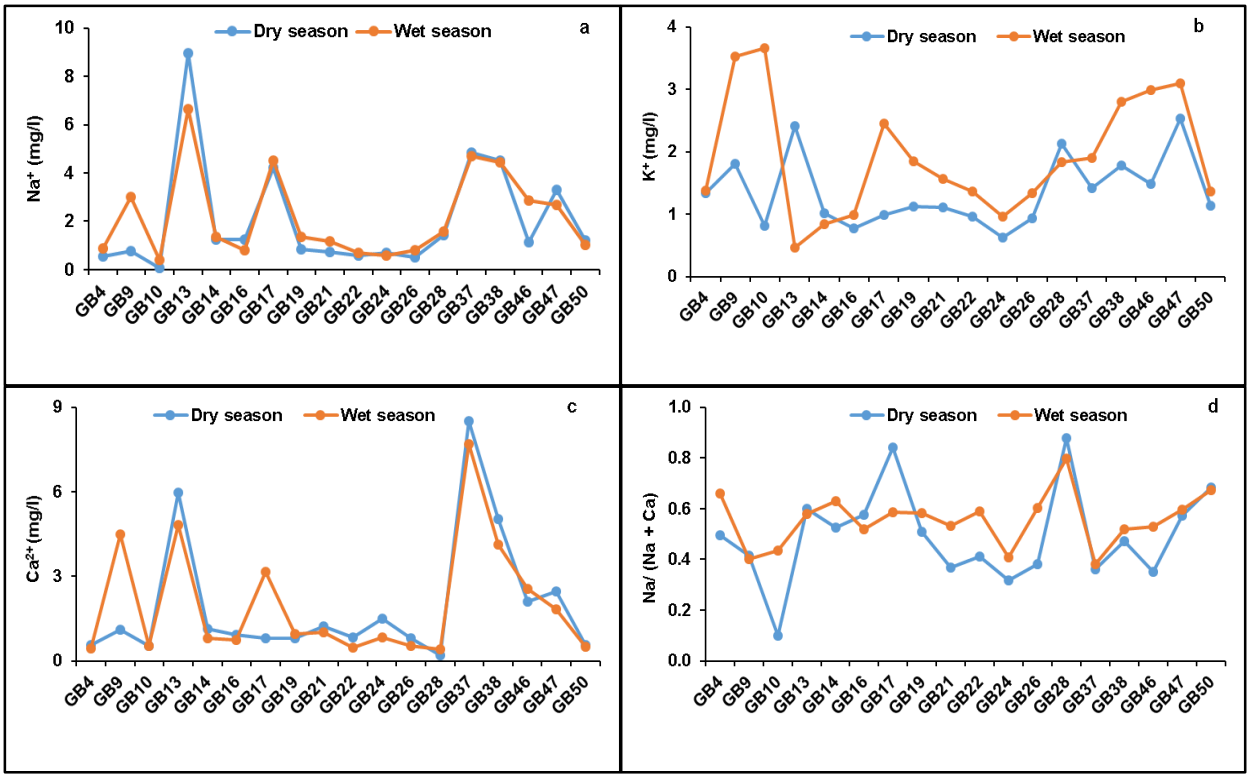

Figure 4.3. Slight increase in Na^{+}, K^{+} and Ca^{2+}concentrations in stream water during the wet season **a–c**; **d**: The mineral weathering index for both seasons: Low Na/ (Na + Ca) ratios indicate mineral weathering while higher ratios signify other sources. GB, Garoua-Boulai–Bétaré-Oya.

4.3 Sources and geochemical behaviour of trace metals in stream water

Trace metal measurements for surface water are presented and a summary of the statistics performed is given in Table 4.2. The elements Cu, Zn and Pb were below the detection limit of the equipment in more than 50 % of the water samples. The most significant metal loadings were those of Fe (20–5011 µg/l) and Mn (0.2–248 µg/l) reflecting metalliferous dissemination within the basin. All water samples were characterized by low concentrations (<1 µg/l) of V, Cr, Co, Cu, Zn, Cd, Pb, and significant concentrations of As (up to 5.45 µg/l), Ni (up to 5.01 µg/l) and Hg (up to 4.98 µg/l). The low levels and mobility of these elements are probably due to the impoverished geological basement and/or very low aqueous solubility of the sulphide minerals in the ore deposits. Besides, these elements could likely be associated with suspended colloids or ferric oxides through adsorption phenomena (Smedley and Kinniburg, 2002). Standard deviation which measures the dispersion of the dataset, varied from 0.0005 (for Zn) to 1.3 (for As) indicating that different factors account for element distribution within the basin.

Trace metal loadings were listed alongside concentrations in Lom River and surface water of the adjacent Batouri gold district (Table 4.3). All analyzed water samples had trace metal concentrations lower than those in the Lom River. When compared to the surface water in the Batouri gold district, only Mn values were higher. Also, Co levels were comparable to those from the neighboring mining area. The low trace metal content in the water can be attributed to the neutral pH (average 6.12) of the streams. In this strongly lateritic environment, the weathering of vein gold mineralization results in sulphide oxidation at the base of the profile. However, a significant portion of the trace metals released in the soils are trapped as lattice components in secondary mineral phases such as ferruginous oxides (Freyssinet et al., 1989) and could be released into the surface water by migration via adsorption, complexation and co–precipitation in a largely acidic environment. Additionally, the overall low concentration of trace metals likely indicates leaching into deep groundwater. This is in agreement with the relatively high levels of trace metals reported for wells within parts of the study area (Rakotondrabe et al., 2017). Given that there are no safe limits for drinking water in Cameroon, the quality of the streams was evaluated by comparing the trace metal concentrations to the desired limits for drinking water according to the World Health Organization (WHO, 2011) (Table 4.3). The maximum concentrations of the selected trace metals in examined samples were used for comparison. Apart from Fe and Mn, all trace metals concentrations were below the WHO threshold values. About 80 % of samples had

Table 4.2. Trace metal composition of surface water (N=52) in the lower Lom Basin.

	Mn	Fe	Sc	V	Cr	Co	Ni	Cu	Zn	As	Cd	Hg	Pb
LOD	0.001	0.01	0.001	0.001	0.001	0.0001	0.001	0.001	0.0001	0.002	0.001	0.001	0.001
	mg/l	mg/l	µg/l	µg/l	µg/l	µg/l	µg/l	µg/l	µg/l	µg/l	µg/l	µg/l	µg/l
GB1	0.003	0.83	0.63	0.6	0.18	0.07	0.19	0.01	0.001	0.97	0.01	4.98	0.01
GB2	0.02	1.25	0.13	0.45	0.09	0.15	0.09	0.11	bdl	0.35	0.01	1.05	0.02
GB3	0.05	0.6	0.07	0.03	bdl	0.62	bdl	bdl	bdl	0.06	0.003	0.62	bdl
GB4	0.01	0.09	0.05	0.02	bdl	0.15	0.1	0.01	0.001	0.05	0.01	0.43	0.01
GB5	0.01	0.07	0.05	0.05	bdl	0.07	bdl	bdl	0.001	0.07	0.001	0.35	bdl
GB6	0.004	0.51	0.05	0.13	0.04	0.07	0.05	bdl	bdl	0.04	0.002	0.28	bdl
GB7	0.09	0.68	0.09	0.47	0.06	0.33	0.61	bdl	bdl	3.28	0.001	0.22	bdl
GB8	0.02	2.68	0.11	1.08	0.08	0.17	0.52	bdl	bdl	3.6	0.002	0.18	0.001
GB9	0.02	0.85	0.06	0.47	0.16	0.18	0.16	bdl	bdl	1.52	0.001	0.16	bdl
GB10	0.01	0.31	0.04	0.15	0.038	0.11	0.06	bdl	0.001	3.97	0.002	0.14	bdl
GB11	0.04	0.68	0.04	0.06	0.0003	0.46	0.44	bdl	bdl	0.004	0.002	0.12	0.001
GB12	0.05	0.61	0.04	0.1	0.05	0.2	0.12	bdl	bdl	1.19	0.001	0.11	bdl
GB13	0.1	1.88	0.08	0.17	0.14	0.68	1.01	bdl	bdl	1.12	0.001	0.12	bdl
GB14	0.07	1.11	0.04	0.08	0.01	0.34	0.89	bdl	bdl	0.46	0.002	0.09	0.01
GB15	0.01	0.16	0.03	0.14	0.03	0.12	0.15	bdl	bdl	0.09	0.001	0.08	bdl
GB16	0.02	0.25	0.04	0.03	bdl	0.32	0.09	bdl	0.001	0.06	0.002	0.09	bdl
GB17	0.003	0.02	0.02	0.02	bdl	0.27	0.59	bdl	0.001	bdl	0.01	0.08	0.01
GB18	0.01	0.49	0.04	0.08	0.02	0.21	0.01	bdl	0.001	bdl	0.004	0.06	bdl
GB19	0.01	0.37	0.05	0.15	0.05	0.11	bdl	bdl	0.001	bdl	0.002	0.05	bdl
GB20	0.004	0.26	0.03	0.04	bdl	0.22	0.13	bdl	0.001	bdl	0.01	0.05	0.01
GB21	0.01	0.82	0.05	0.14	0.07	0.09	0.04	bdl	bdl	bdl	0.01	0.05	0.01
GB22	0.02	1.02	0.05	0.18	0.05	0.33	0.14	bdl	0.001	0.136	0.003	0.05	0.01
GB23	0.01	0.04	0.02	0.01	bdl	0.12	0.01	bdl	0.001	bdl	0.01	0.04	0.01
GB24	0.02	1.56	0.04	0.06	0.06	0.34	0.2	bdl	bdl	bdl	0.01	0.04	bdl
GB25	0.01	4.37	0.03	0.01	bdl	0.11	0.05	bdl	bdl	bdl	0.001	0.03	bdl
GB26	0.01	0.45	0.03	0.02	bdl	0.09	0.02	bdl	0.001	bdl	0.002	0.03	bdl
GB27	0.01	0.68	0.05	0.18	0.07	0.06	0.05	bdl	0.001	bdl	0.003	0.03	0.001
GB28	0.01	0.87	0.07	0.54	0.13	0.08	0.08	bdl	bdl	0.27	0.01	0.05	bdl
GB29	0.166	0.55	0.07	0.17	0.05	1.35	0.32	bdl	0.001	5.447	0.002	0.03	bdl
GB30	0.24	0.51	0.08	0.3	0.14	0.62	0.73	0.13	0.001	5.314	0.01	0.41	0.01
GB31	0.03	1.63	0.08	0.4	0.12	0.2	0.07	bdl	bdl	bdl	0.001	0.03	bdl
GB32	0.06	2.93	0.09	0.9	0.16	0.28	5.01	0.08	bdl	bdl	0.004	0.03	0.01
GB33	0.04	4.72	0.1	0.46	0.24	0.44	0.34	bdl	bdl	bdl	0.001	0.22	bdl
GB34	0.03	1.54	0.05	0.24	0.06	0.29	0.07	bdl	bdl	bdl	0.001	0.04	bdl
GB35	0.07	4.49	0.09	0.49	0.07	0.43	0.35	bdl	bdl	bdl	0.001	0.05	bdl
GB36	0.25	0.1	0.04	0.17	bdl	0.32	0.62	bdl	0.001	1.726	0.003	0.05	bdl
GB37	0.01	1.55	0.07	0.21	0.12	0.1	1.36	bdl	bdl	1.681	0.01	0.02	0.01
GB38	0.09	1.31	0.06	0.1	0.06	0.62	0.8	bdl	bdl	1.14	0.002	0.01	bdl

	Mn	Fe	Sc	V	Cr	Co	Ni	Cu	Zn	As	Cd	Hg	Pb
GB39	0.003	0.31	0.04	0.21	0.05	0.05	bdl	bdl	0.001	bdl	0.001	0.01	bdl
GB40	0.018	0.73	0.04	0.13	0.08	0.13	0.07	bdl	bdl	0.13	0.001	0.01	0.001
GB41	0.01	0.88	0.06	0.13	0.09	0.07	0.002	bdl	bdl	bdl	0.001	0.01	bdl
GB42	0.01	0.89	0.04	0.15	0.18	0.12	0.13	bdl	bdl	bdl	0.002	0.01	bdl
GB43	0.02	0.57	0.05	0.32	0.12	0.16	0.58	bdl	0.001	0.07	0.001	0.01	bdl
GB44	0.01	0.99	0.05	0.31	0.15	0.23	0.54	bdl	bdl	0.22	0.01	0.01	0.01
GB45	0.01	1.5	0.05	0.4	0.15	0.18	0.5	bdl	bdl	0.66	0.002	0.01	bdl
GB46	0.02	1.27	0.04	0.24	0.06	0.15	0.15	bdl	bdl	2.03	0.01	0.01	bdl
GB47	0.02	2.43	0.06	0.37	0.14	0.18	0.25	bdl	bdl	0.03	0.01	0.01	0.01
GB48	0.01	0.33	0.04	0.23	0.13	0.12	0.37	bdl	0.001	0.23	0.01	0.01	0.01
GB49	0.002	0.01	0.03	0.06	bdl	0.009	bdl	bdl	0.001	bdl	0.002	0.04	0.001
GB50	0.01	0.35	0.04	0.07	0.05	0.08	bdl	bdl	0.001	bdl	0.001	0.01	0.001
GB51	0.02	5.01	0.07	0.32	0.12	0.18	0.23	bdl	bdl	1.12	0.01	0.01	bdl
GB52	0.06	1.81	0.07	0.61	0.16	0.57	1.16	0.003	bdl	1.8	0.01	0.004	0.01
Min	0.0002	0.01	0.02	0.004	bdl	0.001	bdl	bdl	bdl	bdl	0.002	0.004	bdl
Max	0.25	5.01	0.63	1.08	0.24	1.35	5.01	0.13	0.001	5.45	0.01	4.98	0.02
Mean	0.04	1.15	0.07	0.24	0.07	0.25	0.37	0.01	0.0004	0.75	0.004	0.2	0.003
SD	0.05	1.22	0.08	0.22	0.06	0.23	0.73	0.03	0.001	1.34	0.003	0.7	0.01

N, number of samples; LOD, limit of detection; GB, Garoua-Boulai–Bétaré-Oya; Min, minimum; Max, maximum; SD, standard deviation

Table 4.3. Comparison of stream water of the lower Lom Basin to concentrations (µg/l) in Lom River, surface water of the Batouri gold district and the WHO standards.

Element	Av. analytical results (µg/l)	Max analytical results (µg/l)	River Lom (µg/l)	Batouri (µg/l)	WHO (µg/l)
Fe	115	5010	2000	400	300
Mn	40	250	100	20	50
V	0.23	1.08	–	4.9	–
Cr	0.07	0.24	20	6.2	50
Co	0.25	1.35	–	0.3	–
Ni	0.37	5.01	–	1.2	70
Cu	0.007	0.13	100	21.5	2000
Zn	0.0004	0.001	100	35.9	3000
As	0.75	5.45	10	36.1	10
Cd	0.003	0.01	50	–	3
Pb	0.003	0.02	100	2.3	10
Hg	0.2	4.98	–	–	6

Av., average; (–), not available; Data for River Lom are adapted from Rakotondrabe et al., (2017) and for Batouri are unpublished data generated by the author.

concentrations of Fe higher than the WHO safe limit and the Mn level in 21 % of samples exceeded the desired limit. While Fe and Mn are known to be essential constituents in human and animal nutrition, excess concentrations can cause undesirable health effects. Excess Fe (> 300 µg/l) stains laundry and plumbing fixtures while high levels of Mn (>50 µg/l) can lead to neurological problems (WHO, 2011).

Principal component analysis (PCA) of metals in stream water conducted produced four factors explaining about 70 % of the total variance (Table 4.4). Factor 1 had strong positive loadings on Fe, V, Cr, pH, Ni and a strong negative loading on Zn. Factor 2 was made up of strong positive loadings on Mn, As and Co while Factor 3 showed strong positive loadings of the elements Pb–Cu–Cd. These factors represent the oxidation and hydrolysis of sulphide minerals associated with gold deposits in the study area. However, in F1, Fe plays a major role in scavenging V, Cr and Ni at near neutral pH but has no co–precipitation effect on Zn as shown by its negative contribution. These metals either adsorb on Fe oxide surfaces or are incorporated in the oxide matrix as impurities during precipitation (Dollar et al., 2001), thereby controlling their uptake and release in water. In contrast, Mn plays a major role in scavenging As in F2 which represents a different phase of mineralization (Omang et al., 2014). Also, Mn is readily soluble at a pH of 7 (Hem, 1963) and Mn hydroxides have been reported to precipitate at high pH (>7) than Fe (pH<5) (Siegel, 2002; Freitas et al., 2013) which implies that Fe and Mn scavenge at different pH of stream water within the Lom Basin. This is because the precipitation of Fe and Mn is pH dependent while that of trace metals depends on their co–precipitation with Fe and Mn. Higher concentrations of dissolved As compared to the chalcophile elements Cu, Zn, and Pb; and its disassociation from this group can be attributed to the weathering of arsenopyrite or the dissolution of metals from stream sediment in near neutral to slightly alkaline waters (Nganje et al., 2011; Kelepertzis et al., 2012). Under such pH conditions as observed in the study area, As becomes more mobile compared to other metals. Although arsenopyrite has been identified as a major sulphide mineralization event within this catchment, the relatively low dissolved concentrations of As can be related to its strong tendency to adsorb on hydrous Mn oxide mineral surfaces (Smedley and Kinniburg, 2002; Cheng et al., 2009). Factor 4 is composed of Hg and pH and could likely be as a result of its adsorption to very fine colloidal particles and dissolved organic matter, which could not be retained by the 0.45–µm membrane filter. Besides, near neutral pH conditions and soil organic material tend to reduce Hg mobility

Table 4.4. Factor analysis (with varimax rotation and Kaiser Normalisation) and total variance explained. N = 52.

Parameter	Factor			
	1	2	3	4
Fe	**0.739**	-0.096	0.077	-0.198
V	**0.735**	0.068	0.371	0.327
Zn	**-0.710**	-0.233	0.258	0.021
pH	**0.636**	0.100	-0.003	**0.516**
Cr	**0.635**	0.000	0.463	0.164
Ni	**0.515**	0.217	0.389	-0.174
Mn	0.111	**0.908**	0.048	-0.013
As	0.073	**0.805**	0.037	0.206
Co	0.005	**0.802**	0.053	-0.208
Pb	0.297	0.160	**0.796**	0.156
Cd	-0.191	-0.130	**0.775**	0.003
Cu	0.425	0.341	**0.652**	0.223
Hg	-0.057	-0.055	0.161	**0.872**
Eigen value	4.254	2.098	1.570	1.130
% Variance	23.001	18.484	17.441	10.698
Cumulative % Variance	23.001	41.486	58.926	69.624

Values in bold represent loadings > 0.5; N, number of samples

(Van Straaten, 2000). Gold amalgamation practiced illegally in the region has been reported as a possible source of Hg (CAPAM, 2016).

The metal composition of the Lom catchment based on the traditional Ficklin diagram (Ficklin et al., 1992) is shown on Fig. 4.4. From this plot, it is obvious that low pH is necessary for significant high metal load to occur through sulphide oxidation. Most trace metals are amphoteric and tend to dissolve forming cations at low pH, or anions at high pH (Salomons, 1995), than at the near neutral pH (5.5 to 6.7) condition of the study area whereby the transport of most suspended and dissolved trace metals is expected to be attenuated (Cravotta, 2000). Thus, the neutral pH of the stream water accounts for the low dissolution of trace metals. Besides, greater dilution and reduced solid to water ratio occurs in wetter climates such as in the tropics. These processes result in the generation of surface water from acid generating deposits such as sulphides with low acidity and trace element content (Plumlee, 1999). Hence, despite the past and active small–scale mining operations within this area, acid generation remains low and this accounts for the low concentrations of dissolved trace metals. On the other hand, there is also a possibility that the acid generated from suphide weathering may have been consumed through reactions with silicate minerals (long–term buffering capacity) occurring in the parent rocks (Salomons, 1995). In summary, the rate of acid generation is usually determined by chemical factors such as pH, temperature, gaseous and aqueous oxygen concentrations, chemical activity of ferric iron and the surface area of exposed metal sulphides as well as biologic parameters.

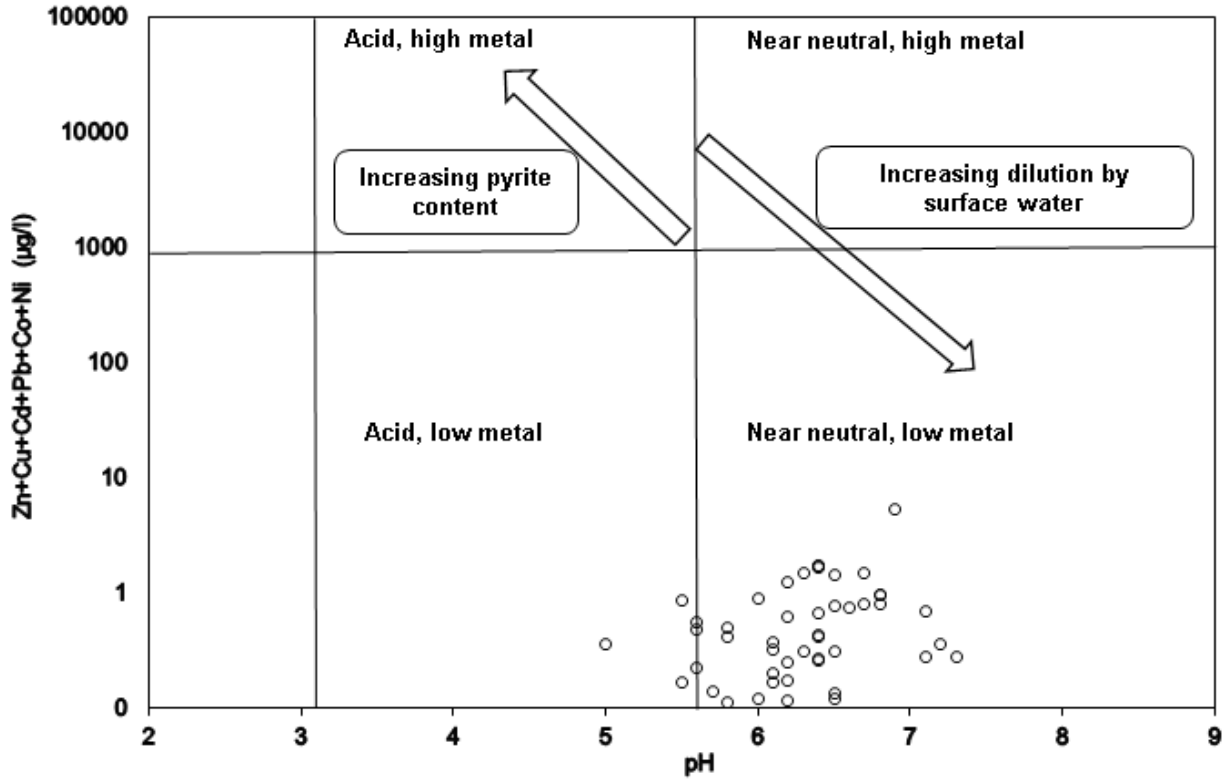

Figure 4.4. Ficklin's diagram of stream water samples from the lower Lom Basin showing low base-metal content.

4.4 Conclusions

For the first time, the seasonal variation of stream water quality parameters and the trace metal composition in streams of the lower Lom Basin have been investigated. Throughout the hydrological year, Cl^- showed no seasonality while Na^+ slightly increased during the wet season. Nitrate, released from anthropogenic practices, decreased during the wet period following dilution by surface runoff. While surface water remained neutral for both seasons, EC and HCO_3^- content increased during periods of high flow. In this tropical basin, silicate weathering is the predominant geochemical process controlling water chemistry. The increase in Na^+, K^+, Ca^{2+} and HCO_3^- during the wet season results from the leaching of surface soils. Also, changes in land use such as vegetation clearing and burning partly contribute to the increased major cation content. Overall, the seasonal pattern of stream water chemistry is controlled by three key processes: a) contribution of major cations and HCO_3^- from chemical weathering supplied by groundwater flow, b) leaching of salts from surface soil layers during rain events and c) dilution by surface runoff during the wet season. Although this study showed only a slight increase in dissolved solutes, identifying the sources and processes governing their contribution is necessary for understanding the effects of future land use changes in the study area.

Trace element geochemistry revealed very low concentrations (<1 µg/l) of V, Cr, Co, Cu, Zn, Cd, Pb and reflect the impoverished parent rocks and leaching into the groundwater. Iron (max 5010 µg/l) and Mn (max 250 µg/l) concentrations in most samples exceeded the WHO (2011) guideline values for drinking water. The dissolution of sulphides associated with quartz vein gold mineralization is the principal source of Cu, Pb, Cd and Zn in the stream water. Arsenic is believed to be leached from a different mineralization source and co-precipitated with Mn owing to its disassociation from the base metals Cu, Zn and Pb.

Drainage signatures of the basin are marked by low acidity, SO_4^{2-} levels and base metal loadings reflecting low sulphide solubility and the likely buffering capacity of silicate minerals. This study showed that despite many decades of past and present small–scale mining activities, the area is currently under no risk of contamination by trace metals. Nonetheless, continuous monitoring of mining activities especially the use of Hg in gold refining in the Lom Basin is highly recommended. Further studies should also include trace metal levels in stream sediments given they are an ultimate sink for trace elements derived from within the catchment.

CHAPTER 5. REGIONAL GEOCHEMICAL BASELINE CONCENTRATION OF POTENTIALLY TOXIC TRACE METALS IN THE MINERALIZED LOM BASIN, EAST CAMEROON: A TOOL FOR CONTAMINATION ASSESSMENT[3]

5.1 Introduction

Stream sediment analysis has been widely used successfully in geochemical mapping investigations because stream sediments provide the composite product of erosion and weathering, representing the geology of the area upstream of the sampling point (Ohta et al., 2004, 2011; Dinelli et al., 2005; Garret et al., 2008; Zumlot et al., 2009; Lapworth et al., 2012; Zhizhong et al., 2014; Zuluaga et al., 2017). This mixture of sediments, rock fragments and soils act not only as an ultimate sink for trace elements derived from within the catchment but are considered as sources of metals based on changes in environmental conditions which could pose pollution problems (Mikoshiba et al., 2006; Smith et al., 2013). Consequently, the geochemical composition of sediments is considered to be a representative of the drainage basin geology and an effective proxy for soil and groundwater (Howarth and Thornton, 1983; Chandrajith et al., 2001). Nevertheless, the spatial distribution pattern of chemical levels in sediments is characterized by a high degree of diversity. Such spatial heterogeneity is a result of many factors including the basin geology, erosion and weathering processes, hydrological features and land use (Plant and Raiswell, 1983). Environmentally, stream sediments act as a reservoir of pollutants. It has been demonstrated that sediment quality is related to other factors such as water quality and aquatic population (Liao et al., 2017). Hence, sediment quality (trace metal composition) will enable the identification of pollution sources and characterize the effects of human activities especially alluvial mining in the watershed. It will also serve as a better guidance to environmental experts. Trace metals in sediments are derived naturally from the weathering of geologic materials. Significant amounts of these metals can also be discharged into the aquatic environment through anthropogenic activities

---

[3] *This chapter is an edited version of the article:*
***Mimba, M.E.**, Ohba, T., Nguemhe Fils, S.C., Nforba, M.T., Numanami, N., Aka, F.T., Suh, C.E. (2018). Regional geochemical baseline concentration of potentially toxic trace metal in the mineralized Lom Basin, East Cameroon: A tool for contamination assessment.* Geochem Trans, 19:11, 1–17.

such as small-scale mining (ASM), where they accumulate on the sediments (Agyarko et al., 2014; Sierra et al., 2017; Taiwo and Awomeso, 2017).

Most stream sediments surveys in Cameroon have focused on mineralization and provenance (e.g Stendal et al., 2006; Etame et al., 2013; Embui et al., 2013; Mimba et al., 2014; Soh et al., 2014; Ngambu et al., 2016). Besides, a national geochemical mapping is yet to be implemented in Cameroon like in many countries since it is logistically demanding and considerably expensive. However, a regional geochemical survey can effectively reveal the geochemical characteristics of the sampled medium. In addition, baseline geochemical mapping of a watershed such as the Lom Basin which includes an important mining site is crucial for future environmental assessment. This region is an important prospective area for gold with extensive research having been carried out on the secondary alluvial gold and primary gold mineralization (Fon et al., 2012; Omang et al., 2015, 2014; Ateh et al., 2017; Mboudou et al., 2017; Vishiti et al., 2017), soil quality (Tehna et al., 2015; Manga et al., 2017) and water quality (Rakotondrabe et al., 2017). On the other hand, there have been no studies on the geochemistry of active bottom sediments for environmental purposes in the area. Thus, the determination of geochemical baseline is fundamental to setting guidelines for environmental management. In fact, geochemical mapping incorporating stream water (Chapters 3 and 4) and stream sediment is a holistic approach to understanding the bulk chemistry and the geochemical processes occurring within this heavily mineralized basin.

This study, therefore, focuses on the mineralogical and geochemical features of stream sediments from the lower Lom Basin. The aim is: (a) to characterize the mineralogical and trace metal composition of streambed sediments, (b) to evaluate the level of trace element contamination in sediments in comparison to local soils and Sub-Saharan Africa soil composition (c) to identify the sources of trace elements based on spatial distribution.

5.2 Materials and methods

5.2.1 Sampling and sample preparation

Stream sediments were sampled from lower order streams draining the southeastern part of the Lom Basin, at a density of one sample every 5 to 10 km (Fig. 5.1). Sampling was done

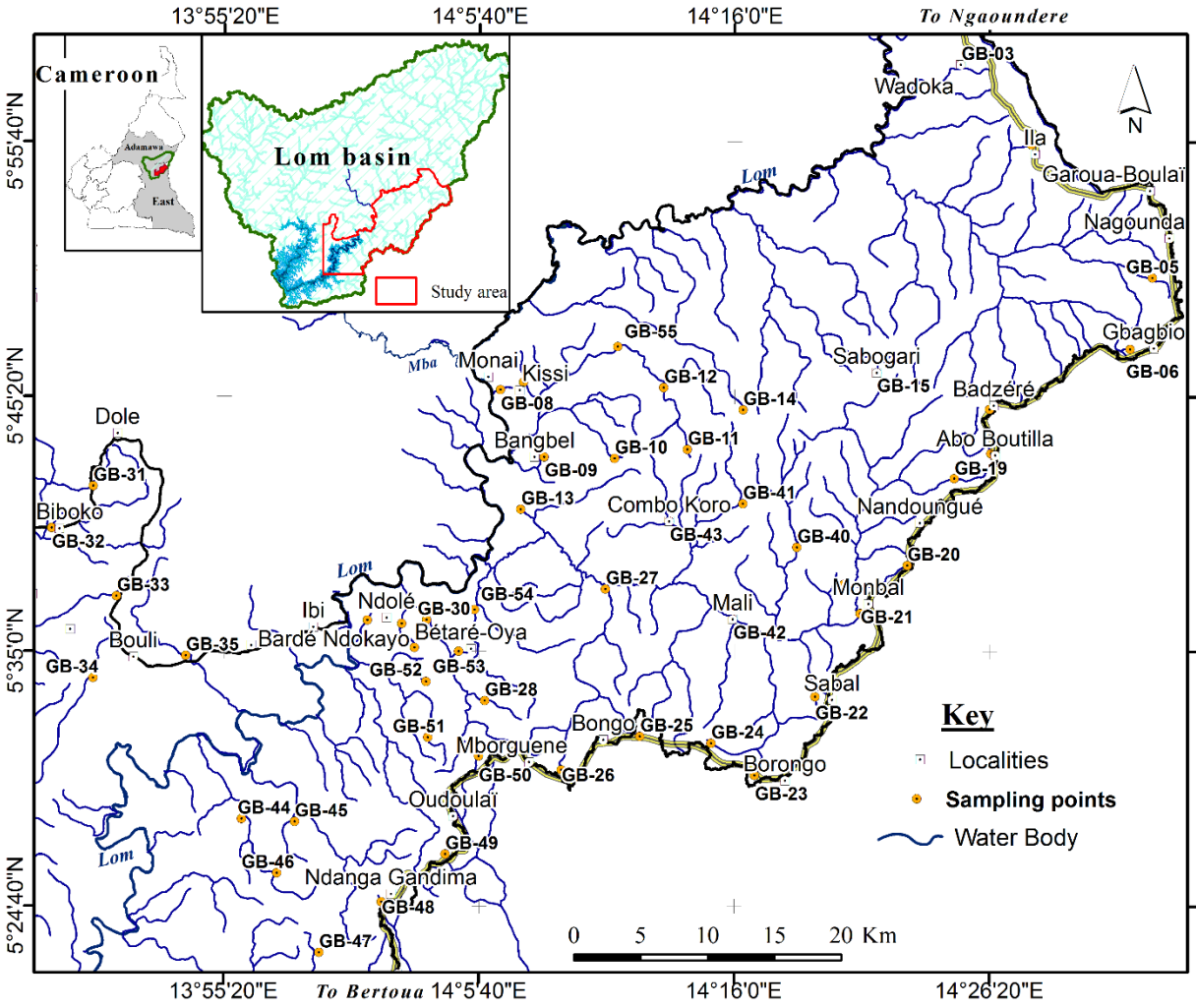

Figure 5.1. Map of study area showing the location and areas of stream sediment sample collection. Samples were collected every 5 to 10 km.

preferably near stream confluences in order to cover the whole drainage network within the area. During sampling, care was taken to avoid areas of site–specific influences. Nonetheless, field observations such as potential sources of contamination, land use, and upstream geology were recorded. A total of 55 active stream sediment samples were collected based on the procedures from Salminen et al. (1998). About 3 kg (to ensure that sufficient fine–grained material would be available for analysis) of the upper layer (0–10 cm) of the stream sediment was collected using a hand trowel. The wet sediment was passed through first, a 300–µm, then 150–µm stainless steel sieves set to obtain the <150–µm fraction. This retained portion was left to settle out and excess water carefully decanted. The drained <150–µm fraction of stream sediment was placed in clean pre–labeled polyethylene bags and air dried. Duplicate samples were collected for each site.

5.2.2 Chemical analyses

In the laboratory, stream sediment samples were rinsed with Milli–Q by shaking in an ultrasonic bath for 30 minutes each, to ensure that all aggregates are broken up. They were then air-dried and homogenized. Wet digestion and dissolution protocol (modified from Makishima and Nakamura, 1997) for trace metals in the stream sediment samples was as follows. 0.15 ml of concentrated perchloric acid (60 wt % $HClO_4$) and 0.3 ml of concentrated hydrofluoric acid (60 wt % HF) were added to 0.02 g of the sediment powder in a Teflon plastic bottle. The bottles were tightly capped and agitated in an ultrasonic cleanser for about three hours to enhance the dissolution of samples. After complete decomposition, the bottles were uncorked, loaded on a ceramic hot plate and the samples were step-wise dried at 120 ^{o}C, 170 ^{o}C and 200 ^{o}C, for six hours at each step. Heating was carried out in a closed system. 0.2 ml of concentrated hydrochloric acid (35-37 wt % HCl) was then added and the bottle was agitated for 2 hours to dissolve the degraded sample completely. Finally, the samples were dried at a temperature of 120 ^{o}C for six hours to prevent the formation of iron oxides or hydroxides upon the addition of nitric acid (HNO_3). The samples were dissolved in 25 ml of 0.5M HNO_3 and stored in 50 ml polyethylene bottles prior to trace metal analysis.

Concentrations of Sc, V, Cr, Co, Ni, Cu, Zn, As, Se, Cd, Hg, and Pb were determined using inductively coupled plasma mass spectrometry (ICP-MS) (ThermoScientific), Fe and Mn by atomic absorption spectroscopy (AAS) (contrrAA700) at the Laboratory of Volcanology and Geochemistry in Tokai University, Japan. The geochemical reference samples JA–3, JB–

3 and JG–3 (Geological Survey of Japan) were used as standards. Internal standards and blanks were run at regular intervals in the analysis for quality control.

The pH of the stream sediments was measured following the procedure by the International Soil Reference and Information Center (ISRIC) (2002). A 1:2.5 ratio of solid to liquid was used. About 2 g of sediment powder was mixed with 5 ml of extra pure water in Teflon plastic bottles. The bottles were capped and agitated in an ultrasonic bath for 2 hours. Prior to pH measurement, the mixture was shaken by hand, allowed to settle and the pH of the supernatant was read using a pH meter (LAQUAtwin), previously calibrated with buffer solutions of pH 4 and pH 7.

5.2.3 X-ray diffraction (XRD) analysis

The relative abundances of the main silicate and oxide minerals were determined semi–quantitatively on the bulk powder using a D8 ADVANCE TKK Diffractometer with automated divergence slit and monochromatic Cu–Kα radiation (4 kV and 20 mA) at the Laboratory of Inorganic Chemistry and Material Science in Tokai University, Japan. Six pulverized (< 150 μm) representative bottom sediment sub–samples were mounted with a random orientation on an aluminum sample holder. The powder from each sample was smoothened using a slide to obtain a uniform level suitable for the X–ray beam. It was scanned from 10^{o} to 80^{o} at a diffraction angle 2θ. The resulting diffractograms were matched automatically with a computerized database of common minerals to identify and quantify the different mineral phases present in the stream sediments. Semi–quantitative estimation of the mineral content based on the diffraction patterns were performed using the software BRUKER–binary V4 (.RAW).

5.2.4 Data processing

5.2.4a Statistical analyses

Statistical analyses were performed using Microsoft Excel and SPSS 20.0 for Windows. The statistical parameters minimum, median, mean and maximum measured the central tendency; while median absolute deviation (MAD), standard deviation, variance and coefficient of variance examined the statistical dispersion. Also, the dataset was tested for asymmetry using skewness. Univariate summary statistics showed that all measured elements were positively skewed. The geochemical data were then log–transformed to obtain

a log–normal distribution. In addition, the data set was checked for outliers using Tukey boxplots (Reimann et al., 2005) and the resultant data subset was used in threshold calculation as follows:

$$Threshold = median + 2MAD \quad (5.1).$$

Multivariate statistical analyses (correlation matrix and factor analysis) were then applied to explore and investigate the data structure, decipher trends and relationship between variables; and infer the underlying factors influencing the stream sediment geochemistry.

5.2.4b Map production

Colored geochemical maps of the data subset were drawn using the ESRI ArcMap 10.2 software package. For interpolation in a grid format, the Inverse Distance Weight (IDW) technique was employed. A maximum of 15 neighboring samples was used for the estimation of each grid point and a power of 2 was chosen to achieve some degree of smoothing. The geochemical data were then classified based on the percentiles 5, 25, 50, 75, 90 and 98 % and colour–coded according to this range. Highest concentrations were shown in hot colours while the lowest ranges were shown in cold colours. Also, graduated symbol plots of factor scores of the element associations obtained by factor analysis were produced to examine their relationship with the basin geology.

5.3 Results and discussion

5.3.1 Mineralogical composition

The diffraction spectra and estimated phase proportions are presented in Fig. 5.2 and Table 5.1. X–ray diffraction analysis identified the following mineral phases: ubiquitous quartz (39–86 %), moderate amounts of micas (biotite and muscovite), clay minerals (kaolinite and gibbsite) and feldspars (microcline and anorthoclase), and traces of rutile, gismondine, tugarinovite, moschelite and parsonite. This variability in mineralogy reflects the composition of the complex basement geology dominated by migmatitic gneisses, granites, metasedimentary and metavolcanic rocks (Fig. 2.1). The predominance of quartz in the sediments is likely due to the reworking of sediments along flow paths. Litho–stratigraphic

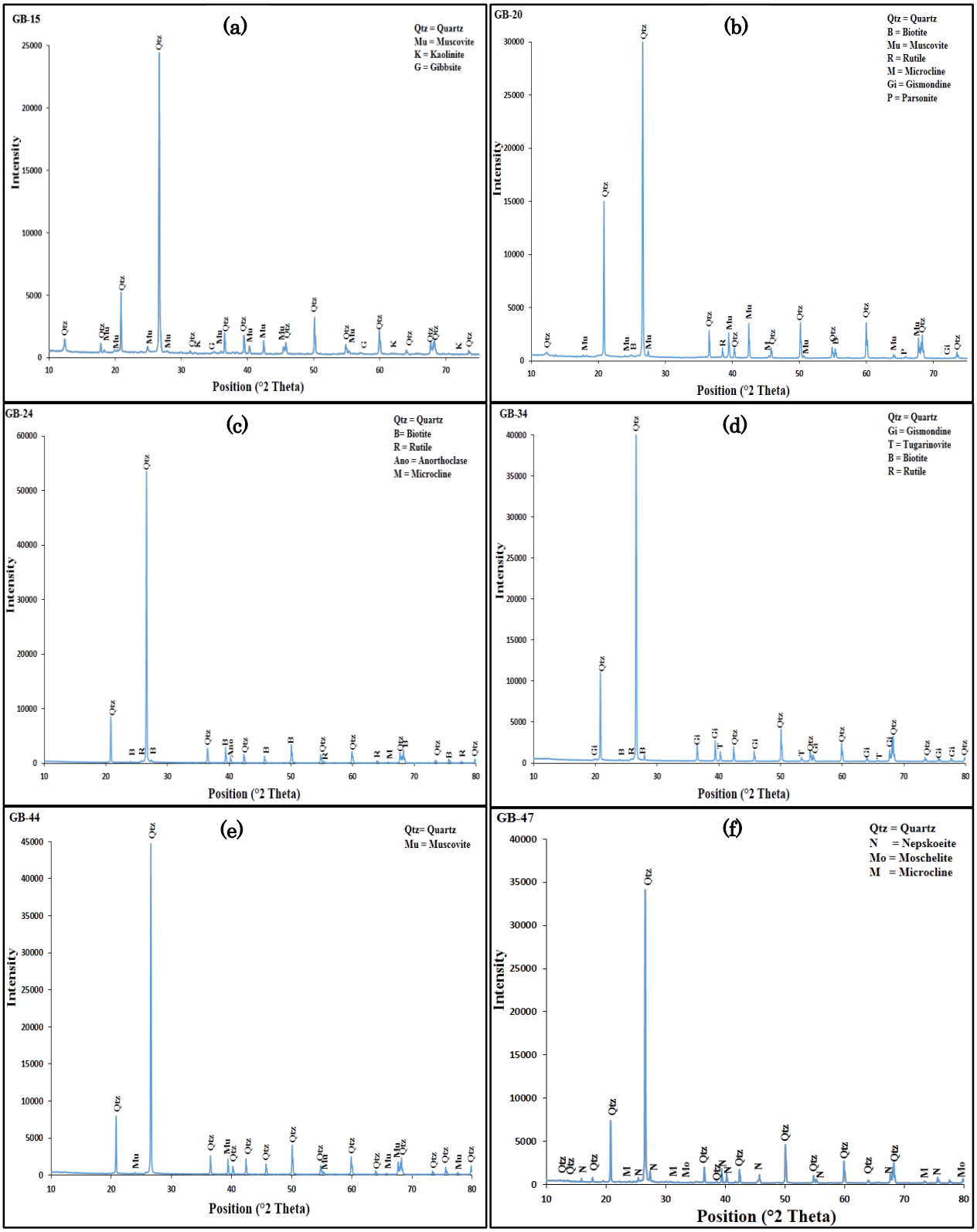

Figure 5.2. X–ray diffraction patterns of 6 pulverized (<150 μm) stream sediments (**a–f**) from the lower Lom Basin.

Table 5.1. Semi–quantitative mineralogical composition of selected stream sediments and representative rock types of the lower Lom Basin.

	GB15	GB20	GB24	GB34	GB44	GB47	Range
Quartz	82	39	79	86	82	72	39–86
Phyllosilicates	45	32	17	5	10	0	0–45
Feldspars	0	12	12	0	0	25	0–25
Rutile	0	27	30	0	0	0	0–30
Gismondine	0	25	0	27	0	0	0–27
Tugarinovite	0	0	0	16	0	0	0–16
Moschelite	0	0	0	0	0	22	0–22
Parsonite	0	9	0	0	0	0	0–9
Nepskoeite	0	0	0	0	0	11	0–11
Rock type	Upper Gneiss	Embrechite	Granodiorite	Lower Gneiss	Schists, Quartzite, Conglomerates	Granite	

GB: Garoua-Boulai–Bétaré-Oya

investigations and grain size analysis of sediments from gold exploration pits in the basin by Mboudou et al. (2017) showed that quartz is the dominant mineral in the profile. Streams flowing within the basin, therefore, transport the eroded sediments from adjacent slopes into the stream channels. In a typical tropical basin like the study area, the high intensity of chemical weathering may also contribute to the modification of the sediment composition (Cadaxo Sobrinho et al., 2014). Additionally, hydraulic energy and sorting are also known to influence the mineral composition of sediments (Silva et al., 2016). The samples GB15, GB20 and GB44 were collected in streams where the water flux was very low. Thus, this accounts for the moderate phyllosilicates content in the bottom sediments.

5.3.2 Trace metal content and sediment quality assessment

Pronounced deviations between means, medians, standard deviations and MADs were observed (Table 5.2). Also, all the selected metals were positively skewed implying the influence of extreme values, the presence of multiple populations and the effects of analytical precision or limits of detection of the data set (Zhang et al., 2005). The mean value of pH=6.4 indicates near neutral conditions of the catchment. Elemental composition showed a wide variation which is likely generated by the physical and chemical weathering processes operating within the drainage basin (Towett et al., 2015; Darwish, 2017). Cadmium (2.65 µg/kg) had the lowest mean concentration followed by Hg (5.40 µg/kg), Se (48.55 µg/kg), Co (92.85 µg/kg) and As (99.40 µg/kg). These elements are usually present in trace amounts in rocks as reported in the mean background contents in the continental crust (Kabata-Pendias, 2011). Iron and Mn had the highest mean concentrations of 28.325 and 442 mg/kg, respectively. When compared to regional stream sediment surveys in South Cameroon (Mimba et al., 2014) and other Sub-Saharan Africa regions (Lapworth et al., 2012; Zhao et al., 2014), the Lom Basin sediments were depleted in all examined trace metals. However, average concentrations of the non-essential trace metals As (99.40 µg/kg), Hg (5.40 µg/kg), V (963.14 µg/kg) and Pb (151.59 µg/kg) were significantly higher than the levels (As=22.3 µg/kg, Hg=<0.01 µg/kg, V= 158.5 µg/kg and Pb=12.3 µg/kg) reported by Taiwo and Awomeso (2017) for sediment from the gold city of Ijeshaland. Also, all the trace metals analyzed showed a similar fingerprint in the stream waters of the study area characterized by low trace metal levels (Chapter 4). Possible reasons for the depletion of these trace metals may be a reflection of the impoverished bedrock and the neutral pH which does not favour the dissolution and mobilization of the trace metals from the sulfide gold–quartz veins (Ashley, 2002).

Table 5.2. Summary characteristics of stream sediment geochemical data and Se:Hg ratios in the lower Lom Basin (N = 55).

Element	Unit	Minimum	Median	Mean	Maximum	MAD	SD	CV (%)	Skewness
Sc	µg/kg	2.11	129	211	1699	4.22	328	155	3.11
V	µg/kg	53.6	85.9	963	12333	5.20	2365	245	3.28
Cr	µg/kg	13.6	39.2	763	10052	1.26	1941.97	254	3.43
Mn	mg/kg	224	319	441	1441	5.86	273.94	62	2.10
Fe	mg/kg	12109	22678	28325	159319	6985	22219	78.4	4.29
Co	µg/kg	0.03	0.47	92.9	1308	0.14	256	275	3.41
Ni	µg/kg	5.59	15.8	239	3125	0.19	607	25.2	3.35
Cu	µg/kg	12.2	211	362	3946	0.04	680	187	3.95
Zn	µg/kg	2.61	315	573	4657	18.4	1008	176	3.11
As	µg/kg	0.35	22.7	99.4	1178	20.1	249	250	3.21
Se	µg/kg	0.10	21	48.6	509	3.82	100	207	3.23
Cd	µg/kg	1.30	2.48	2.65	7.85	5.37	0.98	37.1	3.69
Hg	µg/kg	0.19	2.35	5.40	83.2	18.3	11.9	219	5.55
Pb	µg/kg	7.25	47.6	151	2215	2168	365	241	4.10
pH	–	3.60	6.40	6.38	7.10	–	0.51	7.99	-3.17
Se:Hg	–	0.04	2.70	2.31	7.49	–	–	–	–

N, number of samples; MAD, median absolute deviation; SD, standard deviation; CV, coefficient of variation; (–), not available

Table 5.3 shows the background, mean and threshold values of the trace metals in comparison with analytical results from other studies in order to obtain a preliminary inspection of the level of contamination in the bottom sediments. The median was chosen in this study as the local background because it is representative of the local data and less affected by outliers (Ohta et al., 2005). Threshold values were computed for the geochemical data subset following the elimination of outliers. The statistically derived threshold values are crucial in distinguishing between geogenic and anthropogenic sources of the trace metals (Reimann & Caritat, 2017). These values represent the upper limit of the background concentrations of the potential toxic trace metals in sediments (Rose et al., 1979) and allow for the identification of anomalous concentrations. Because stream sediments are an essential and dynamic component of catchments, they reflect the average chemical composition of the mixture of soils, sediments and rocks (Smith et al., 2013). In this regard, the trace metal contents in this study were presented alongside local background levels in soils (Manga et al., 2017) and mean concentrations in ferralsols of the Sub–Saharan Africa region (Towett et al., 2015). All trace metal concentrations (with corresponding data in soils) in the Lom sediments were lower than the mean levels in local soils. About 18 % of the sediment samples exceeded the concentrations of Fe and Mn in ferralsols. Based on this comparison, the low concentration of trace metals in the sediment is likely due to the interplay of deep weathering, depleted parent rocks and the incorporation of metals in ferruginous clays or organic matter in the lateritic soil cover.

The degree of correlation between pH and trace metals in the bottom sediments is given in Table 5.4. Interestingly, except for Fe and Mn, all trace metals correlated negatively with pH. The poor correlations suggest these metals are relatively immobile at near neutral pH accounting for their low concentrations. Similarly, Fe and Mn correlated poorly with all other elements suggesting a less co–precipitation effect on them in this drainage system. Unlike Fe and Mn, strong positive correlations were observed between Co–Cr–Ni–As–Se–V–Pb and V–Cr–Co–Ni–As and likely indicate that they are sourced from the granitic rocks and partial dissolution of sulphides within the catchment. Indeed, the complete oxidation of metal sulphides is effective under acidic conditions (Lewis, 2010) rather than the near neutral pH (mean = 6.4, Table 5.2) of the sediments.

Table 5.3. Geochemical background and threshold values (µg/kg) of stream sediments from the lower Lom Basin alongside local soil (ppm) and Sub–Saharan ferralsols (mg/kg). Mn and Fe are in mg/kg.

	Sc	V	Cr	Mn	Fe	Co	Ni	Cu	Zn	As	Se	Cd	Hg	Pb
Study background	128	85.9	39.1	319	22627	0.5	15.7	211	314	22.1	15.3	2.5	2.3	47.5
Study mean	105	201	156	406	25899	12.3	58.4	174	248	24.1	19.7	2.4	5.4	56.5
Threshold values	132	96.0	41.4	330	36692	0.7	15.8	211	354	61.2	34.4	7.4	39.0	142
Local soil	–	–	–	–	–	–	–	1	4	0.05	–	1	–	5
Ferralsols	–	30	53	578	34957	–	21	21	41	–	–	–	–	36
Percentage (%) sediment samples exceeding ferrasols	–	0	0	18.2	18.2	–	0	0	0	–	–	–	–	0

Geochemical background, median; Geochemical background threshold, median + 2 (median absolute deviation); (–), not available; metal concentrations in local soil are adapted from Manga et al., (2017) while data for ferralsols are after Towett et al., (2015)

Table 5.4. Correlation matrix of trace metals in stream sediments from the lower Lom basin at $p<0.05$ (N = 55).

	Sc	V	Cr	Mn	Fe	Co	Ni	Cu	Zn	As	Se	Cd	Hg	Pb	pH
Sc	1.00														
V	0.28	1.00													
Cr	0.19	**0.98**	1.00												
Mn	0.12	0.09	0.09	1.00											
Fe	-0.05	-0.02	-0.02	**0.69**	1.00										
Co	0.08	**0.91**	**0.94**	0.06	-0.03	1.00									
Ni	0.20	**0.98**	**0.99**	0.09	-0.02	**0.93**	1.00								
Cu	**0.76**	0.34	0.24	-0.08	-0.18	0.10	0.26	1.00							
Zn	**0.70**	0.32	0.23	-0.05	-0.21	0.08	0.26	**0.96**	1.00						
As	0.33	**0.79**	**0.74**	0.04	-0.07	**0.68**	**0.76**	0.40	0.38	1.00					
Se	0.30	**0.71**	**0.70**	0.22	0.14	**0.65**	**0.70**	0.32	0.32	0.35	1.00				
Cd	**0.52**	0.33	0.27	0.15	-0.05	0.25	0.27	0.38	0.41	0.44	0.16	1.00			
Hg	**0.81**	0.21	0.10	0.21	0.07	0.02	0.13	**0.77**	**0.71**	0.27	0.37	0.42	1.00		
Pb	**0.65**	**0.65**	**0.54**	-0.08	-0.16	0.39	**0.57**	**0.85**	**0.82**	**0.63**	**0.51**	0.47	**0.67**	1.00	
pH	-0.22	-0.46	-0.46	0.08	0.06	-0.41	**-0.50**	-0.31	-0.34	-0.40	-0.48	-0.18	-0.18	-0.42	1.00

N: number of samples

Factor analysis was applied on the log–transformed data to infer the controlling factors behind multi–element associations in relation to catchment geology, mineralization or anthropogenic activities. The spatial distribution of the factor scores of the element associations and their relationship with the geology are shown in Figs. 5.3a–c. Three factors explaining about 79 % of the variance were generated (Table 5.5). Factor 1 accounts for 36.5 % of the total variability. This dipolar factor showed high positive loadings for Ni, Cr, V, Co, As, Se and a negative loading for pH. The F1 association showed high and medium factors scores relating to the metamorphic basement of the catchment (Fig. 5.3a). The high loadings are a function of the catchment lithology. Sediments derived from granitic rocks and other felsic metasedimentary rocks such as quartzites and amphibolitic schists that make up the Lom basement are known to be poor in V, Cr, Ni, Co, and As (Ohta et al., 2005). Besides, Co, V and Ni can easily replace Fe in magnetite (Surour et al., 2003) which is a major oxide in the ferralitic soils of this tropical basin (Freyssinet et al., 1989). The presence of As in this factor is attributable to arsenopyrite dissemination in the parent rocks. Arsenopyrite has been reported as a separate sulphide mineralization event distinct from the main chalcopyrite sulphidation in the study area (Omang et al., 2014). The negative contribution of pH in this factor implies that an acidic environment is required for these metals to be released from their geological materials. A significant proportion of data variability (29.9 %) described by Factor 2 is associated with scores of chalcophiles (Cu–Zn–Hg–Pb–Cd) and Sc. High factor scores (>0) of these elements occur around reported gold indications reflecting the sulphide gold–quartz vein mineralization (Fig. 5.3b). This elemental association indicates the presence of sulphide mineralization. Moreover, studies on the lode–gold quartz veins and weathered overburden have reported the occurrence of chalcopyrite (Cu), sphalerite (Zn) and galena (Pb) in the underlying rocks of the study area (Bafon, 2011; Mboudou et al., 2017; Vishiti et al., 2017). The negative association of As and chalcophile elements is consistent with the claims that two distinct hydrothermal events are related to the epithermal gold mineralization in the study area (Omang et al., 2014). Also, As and Pb have been identified as potential pathfinder elements for gold in the area. The contents and geochemical dispersion haloes of these metals in different lateritic profiles in the area were used to indicate gold mineralization. Arsenic was widely dispersed in soils and considered useful in regional survey while Pb was suited to follow up work (Freyssinet et al., 1989). Scandium is likely associated with organic matter. Its small size and high charge favour the formation of stable organic complexes in soils or adsorption on clay minerals derived from the chemical

Table 5.5. Factor analysis with varimax rotation for 14 trace metals in stream sediments from the lower Lom Basin (N = 55).

Variable	Factor 1	Factor 2	Factor 3	Communality
Ni	**0.983**	0.117	0.018	0.981
Cr	**0.982**	0.091	0.022	0.974
V	**0.965**	0.206	0.021	0.974
Co	**0.958**	-0.041	0.019	0.920
As	**0.749**	0.319	-0.064	0.668
Se	**0.705**	0.269	0.240	0.627
pH	**-0.529**	-0.244	0.138	0.358
Cu	0.154	**0.928**	-0.173	0.914
Zn	0.151	**0.904**	-0.178	0.871
Hg	0.029	**0.897**	0.205	0.846
Sc	0.095	**0.879**	0.080	0.788
Pb	0.487	**0.790**	-0.162	0.888
Cd	0.245	**0.537**	0.092	0.357
Mn	0.060	0.066	**0.919**	0.853
Fe	-0.025	-0.085	**0.892**	0.803
Variance	5.477	4.478	1.868	11.823
% Variance	36.515	29.851	12.451	78.817

Three factors were extracted. The geochemical data were log–transformed prior to factor analysis. (-), Factor loadings ≥ ±0.5 are in bold; N, number of samples

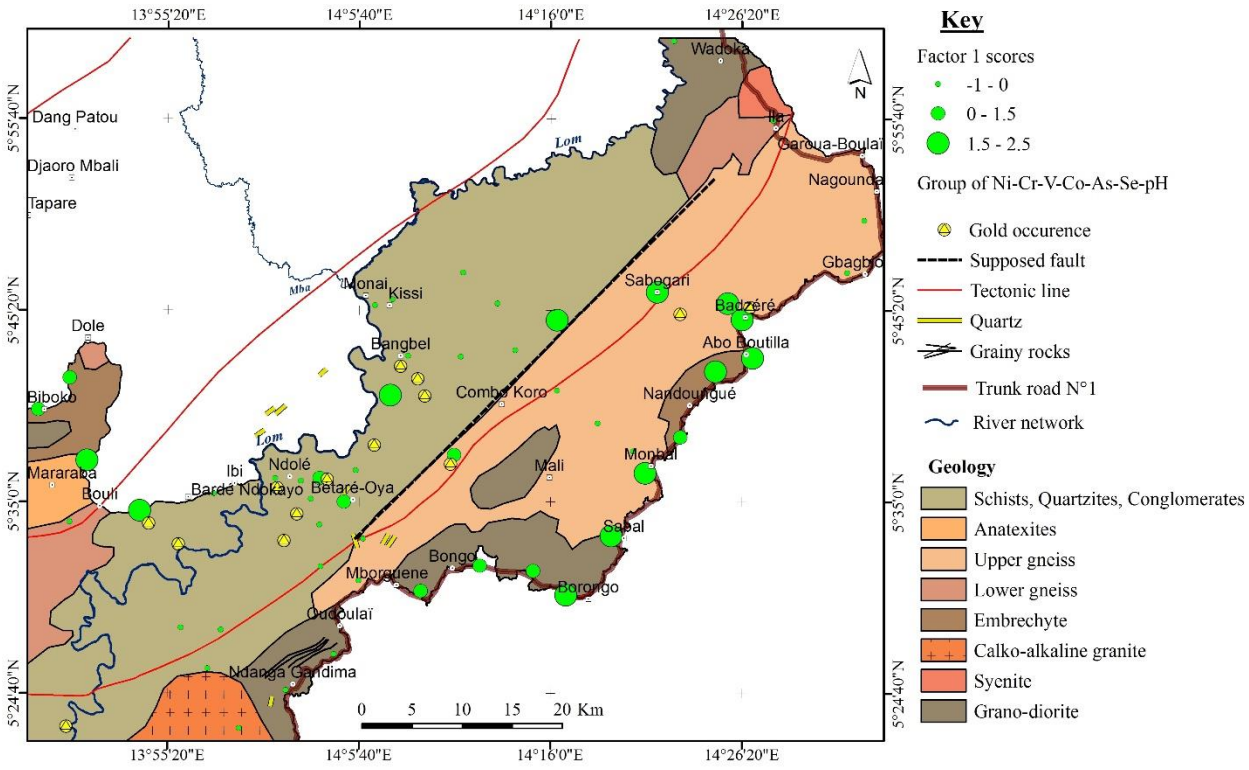

Figure 5.3a. Spatial distribution of factor 1 scores in relation to geology. The elements are ordered in decreasing loading.

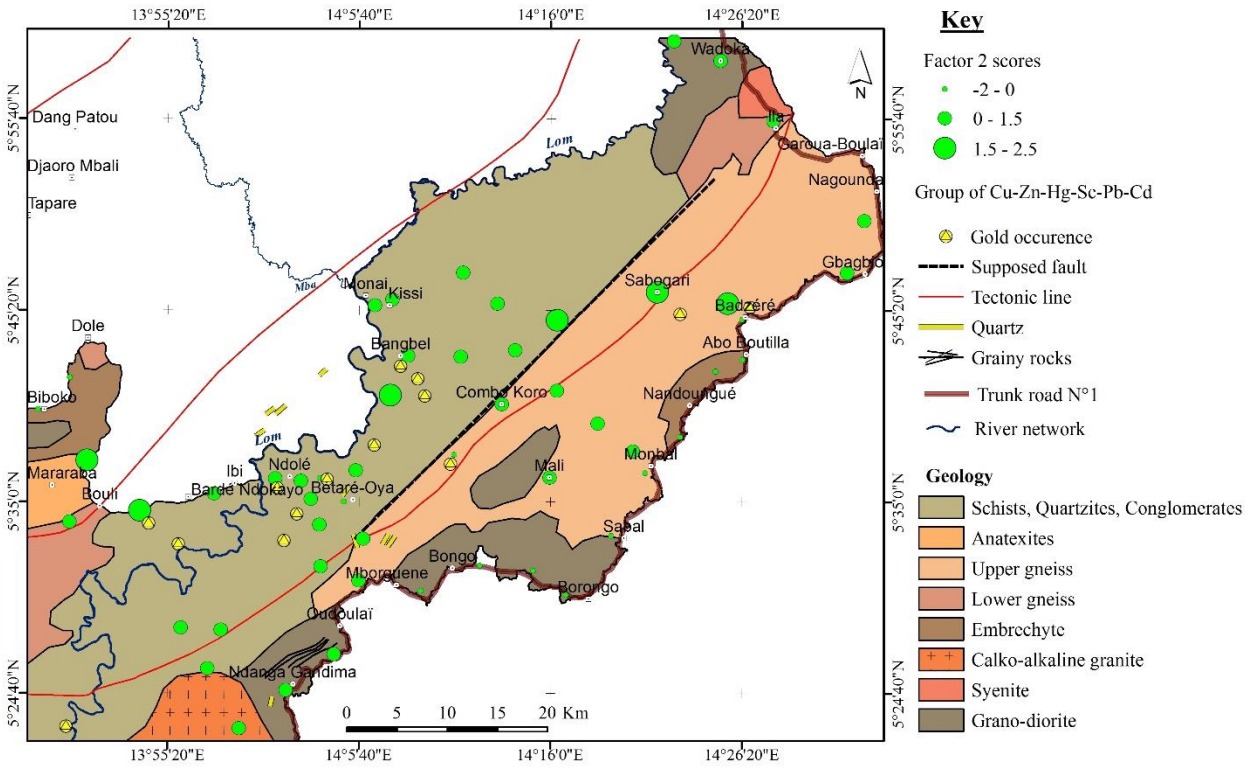

Figure 5.3b. Spatial distribution of factor 2 scores in relation to geology. The elements are ordered in decreasing loading.

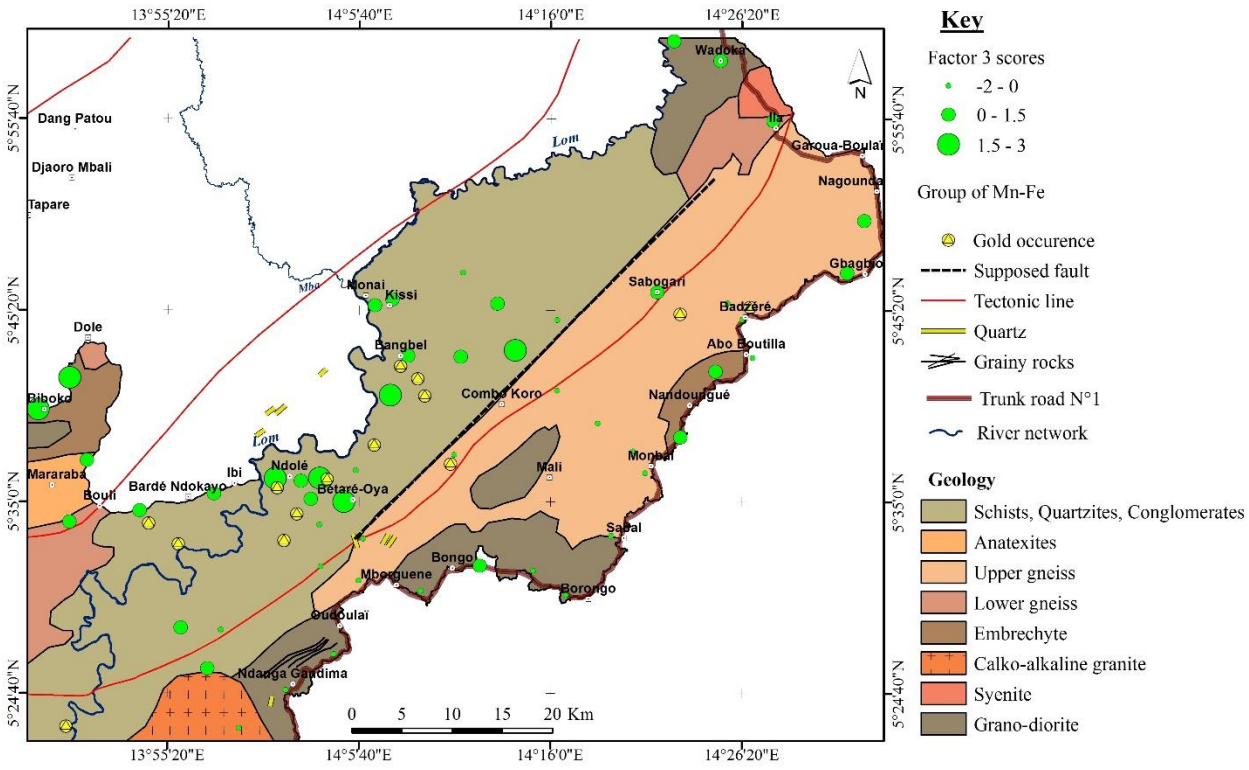

Figure 5.3c. Spatial distribution of factor 3 scores in relation to geology. The elements are ordered in decreasing loading.

weathering of the granitic rocks (Yang et al. 2013). The manganiferous relationship in factor 3 is a clear indication of the presence of Fe–bearing rocks and the co–precipitation effect. Accordingly, the highest F3 factor scores are located in the area underlain by the volcaniclastic schists and the metasedimentary rocks, quartzites and metaconglomerates (Fig. 5.3c). Iron and Mn exist as compensating ions on clay complexes and their precipitation is mainly dependent on the pH of the sediments in the catchment (Nganje et al., 2011). Hence, the poor correlation observed between Fe and Mn and the other trace metals suggests that they do not play a major role in scavenging these elements under near neutral conditions.

5.3.3 Spatial geochemical features

Spatial distributions of high levels of Co, Cr and Ni (Fig. 5.4a–d) cluster in the eastern part and correspond to areas underlain by upper gneisses and granodiorite (Fig. 2.1). Similarly, As and V distributions (Fig. 5.4e) are controlled by the catchment geology even though their concentrations were lower than the calculated thresholds (Table 5.3). Moreover, relatively high concentrations of As coincided with reported gold indications in the area. As previously stated, this observation is in line with the assertion that As is an important pathfinder for gold in this basin (Freyssinet et al., 1989). Arsenic can be introduced into the food chain through its accumulation in plants and natural waters (Parga et al., 2006). Excess As causes cancer and may lead to death due to respiratory and cardiovascular failure.

Contrary to As, the base metals Cu, Zn, Pb, and Sc have very low values around gold deposits (Fig. 5.5a–d). No anomalous sites were observed for these metals and their background concentrations indicate sulphide mineralization related to vein gold deposits. Whole rock geochemistry of the gold–quartz veins by Vishiti et al. (2017) suggest a generally low base metal content resulting from the reaction between the hydrothermal fluid and the granitic rocks in the area. This explains the very low concentration of the base metals in the bottom sediments. The studied quartz veins contain sulphides including galena and chalcopyrite.

Iron and Mn occur naturally in the earth's crust (Cox, 1985) and are dietary requirements for most organisms and humans. Hot spots of Fe and Mn occur in the NW–SW portion of the study area (Fig. 5.6a and b). These elements are important constituents in ferromagnesian silicates and oxides in the underlying metamorphic rocks. In addition to the hypogene and supergene hematite sources, other possible sources of Fe in the sediments are the sulphide minerals pyrite and arsenopyrite associated with the primary gold–bearing

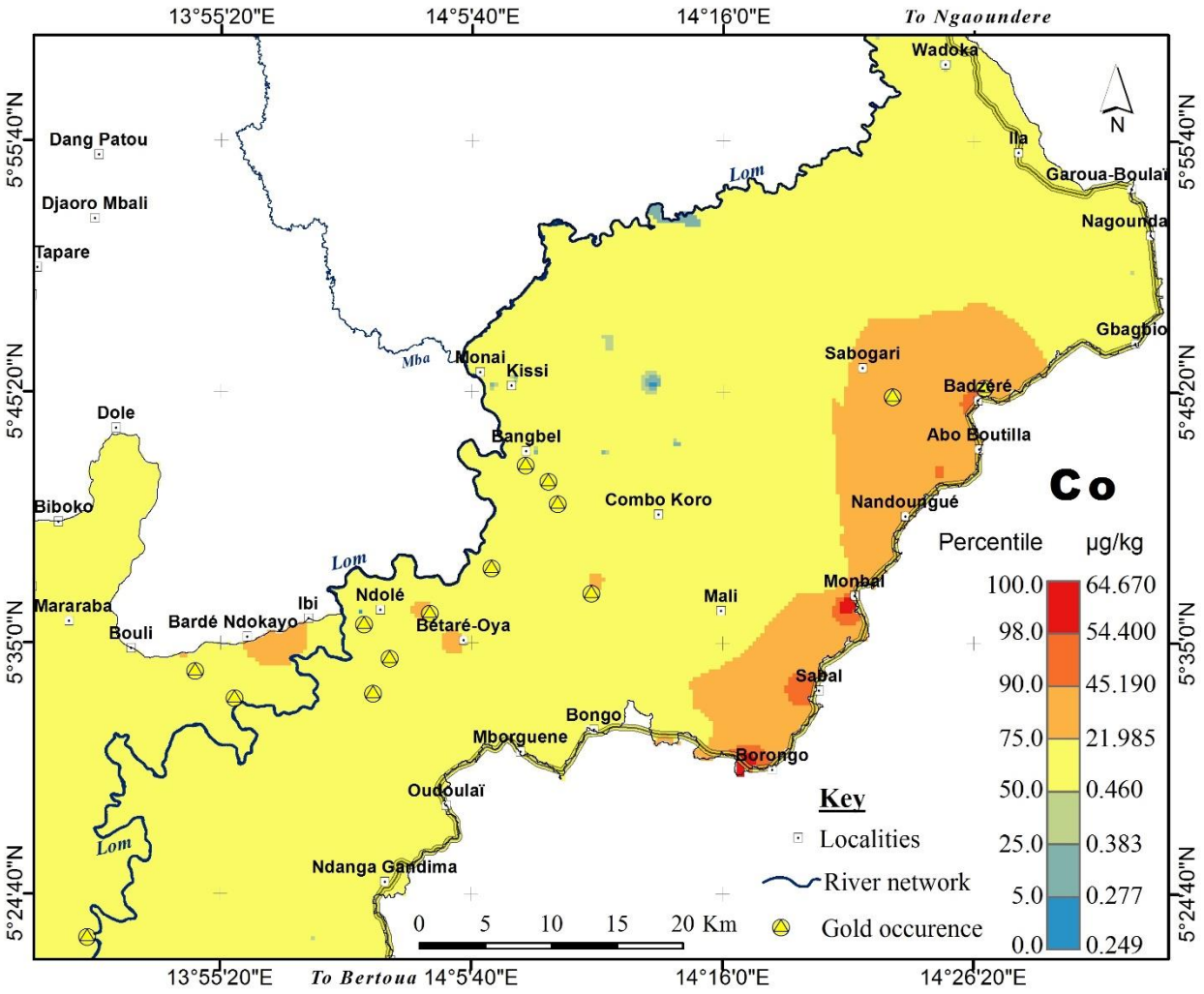

Figure 5.4a. Geochemical background of Co. Enrichment in relation to the threshold (0.7 µg/kg) in the eastern part of the lower Lom Basin.

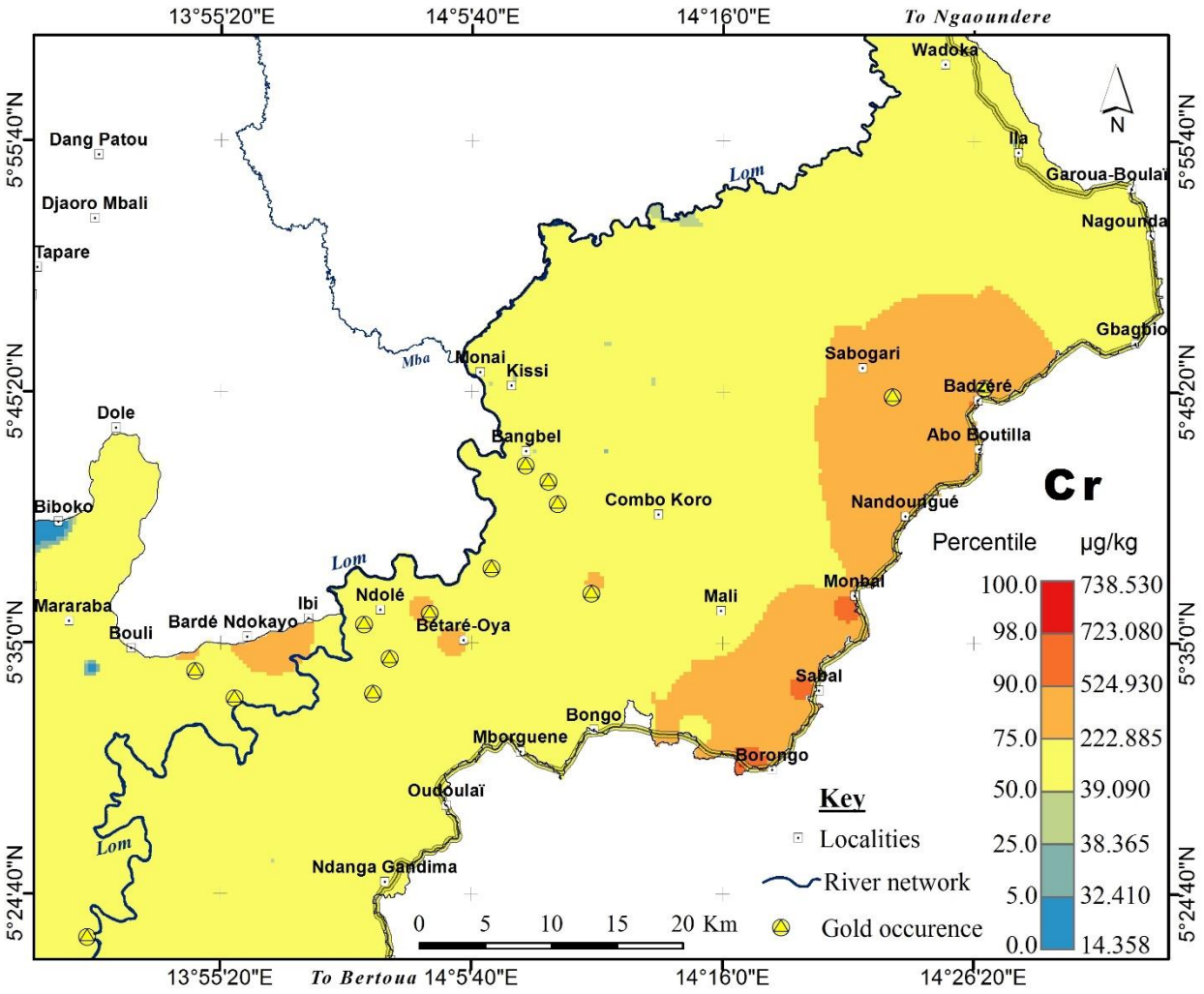

Figure 5.4b. Geochemical background of Cr. Enrichment in relation to the threshold (41 µg/kg) in the eastern part of the lower Lom Basin.

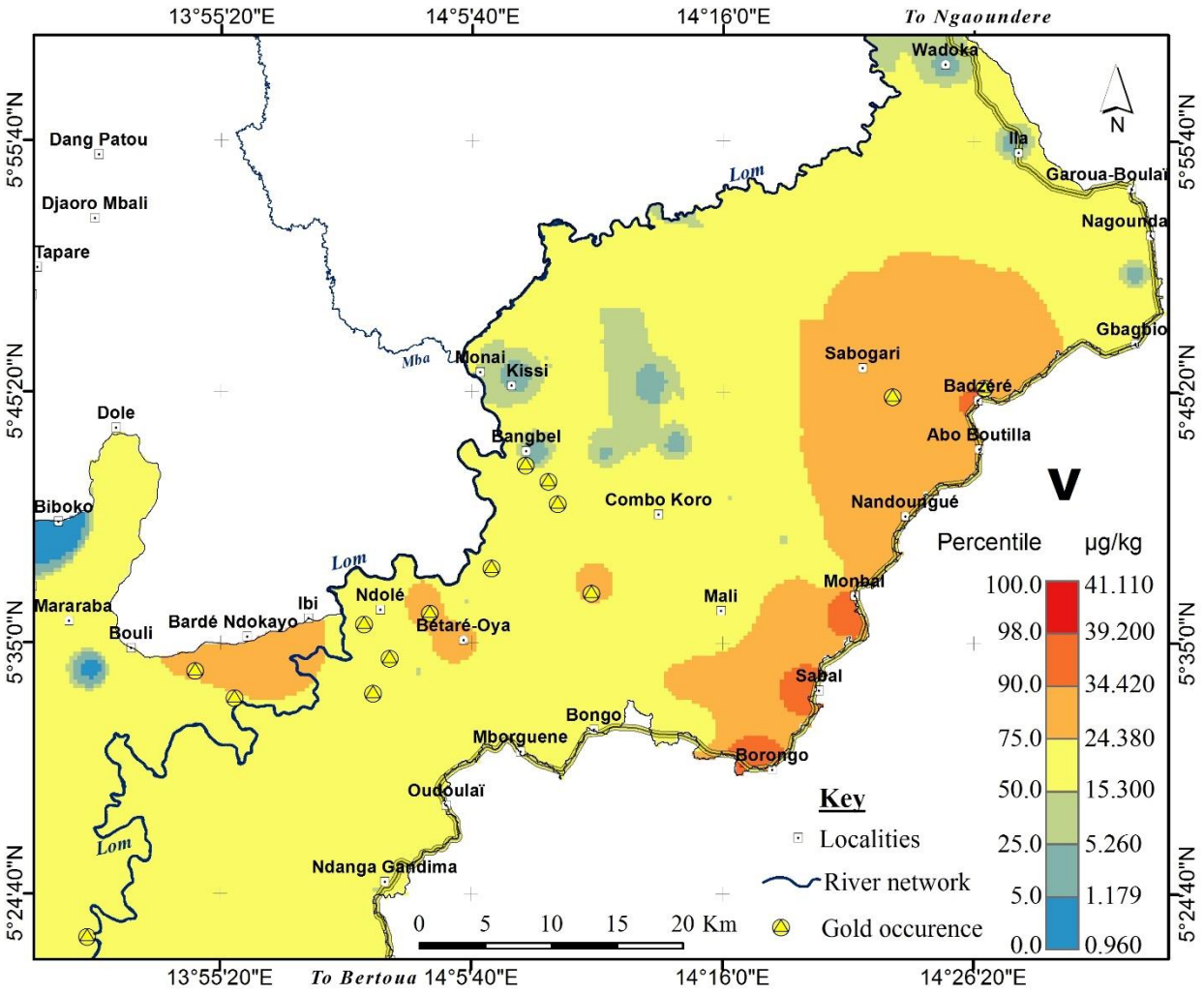

Figure 5.4c. Geochemical background of V.

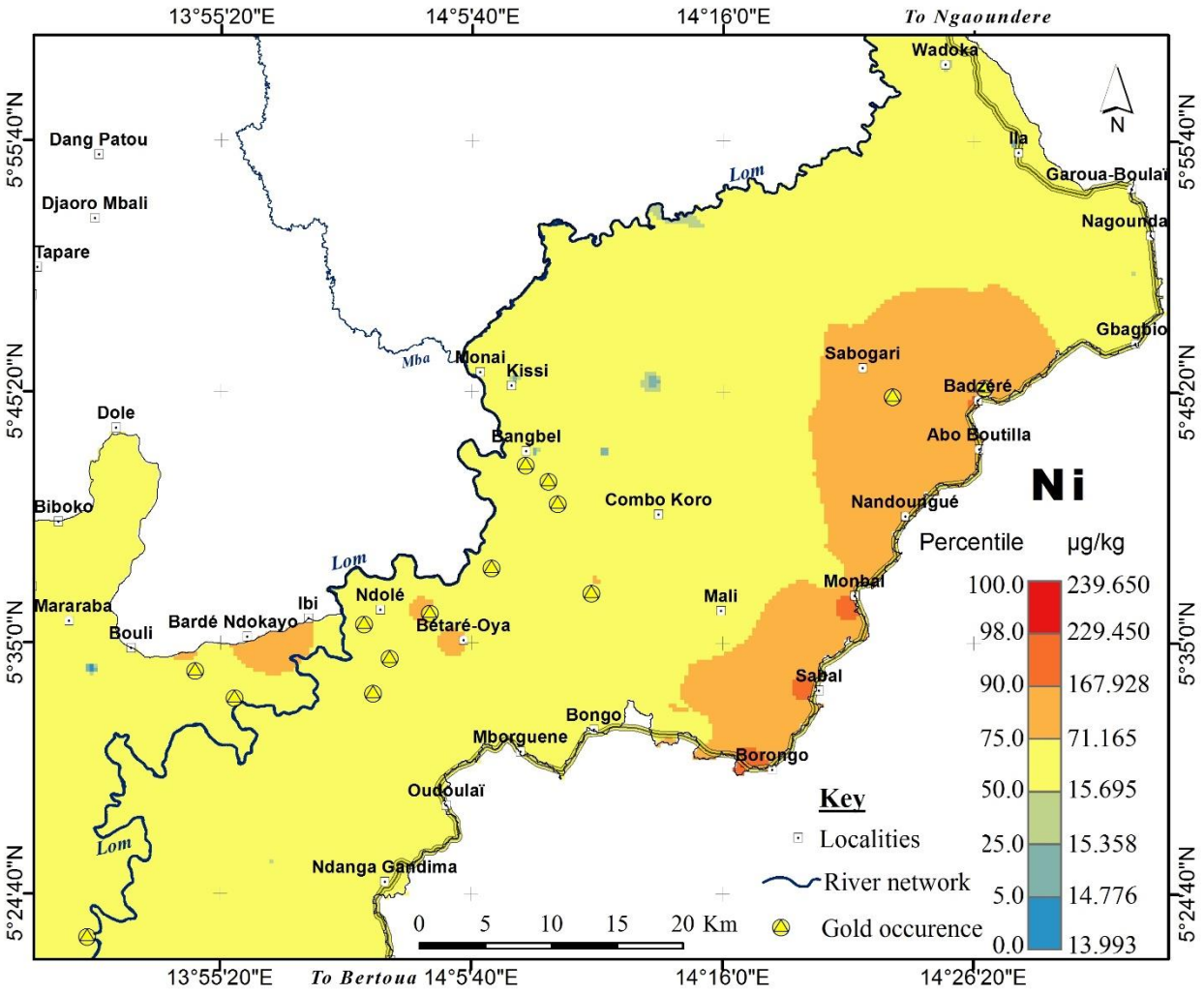

Figure 5.4d. Geochemical background of Ni. Enrichment in relation to the threshold (15.8 µg/kg) in the eastern part of the lower Lom Basin.

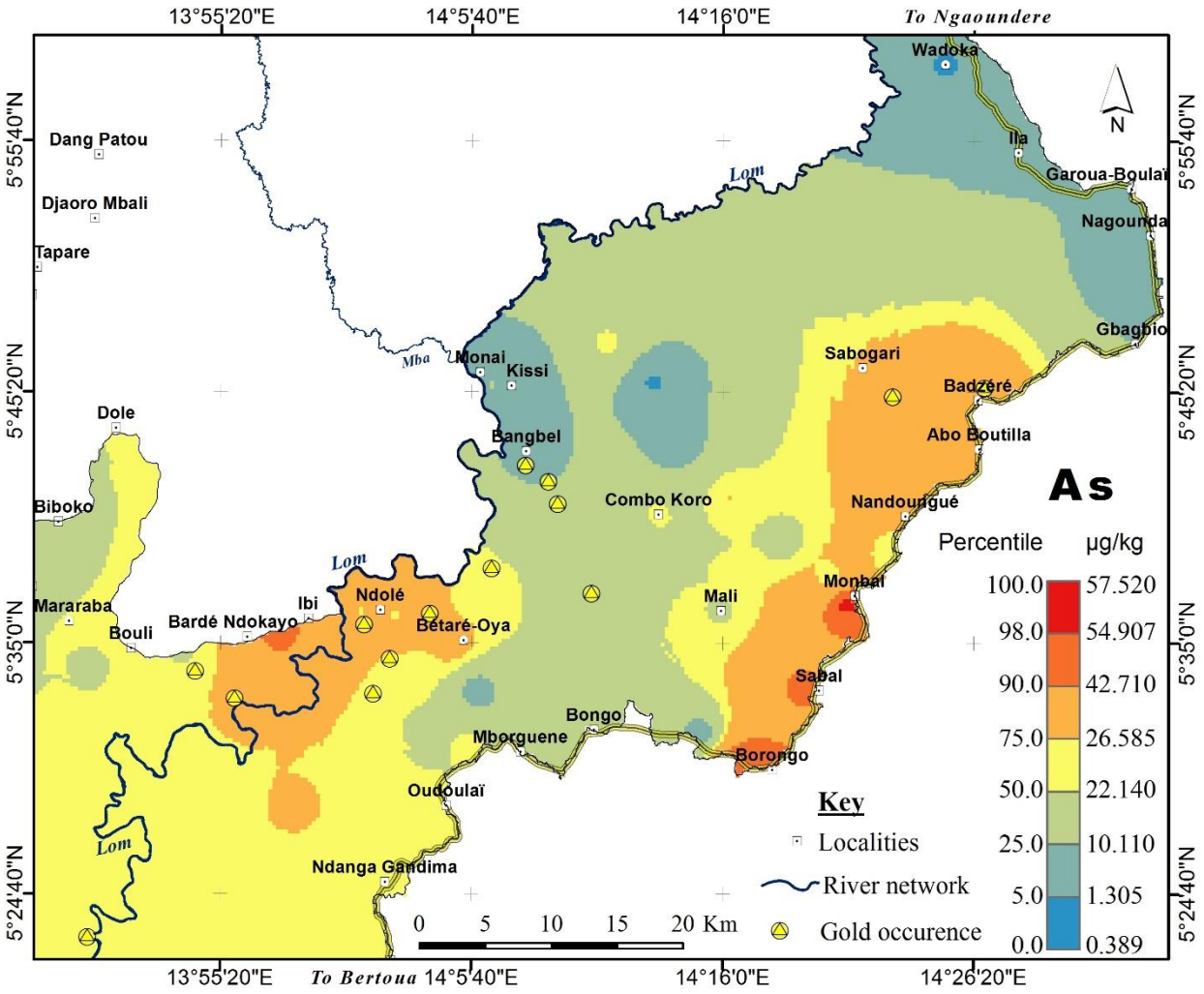

Figure 5.4e. Geochemical background of As. Arsenic distribution shows a coherent relationship with reported gold mineralization in the east and west portions of the lower Lom Basin.

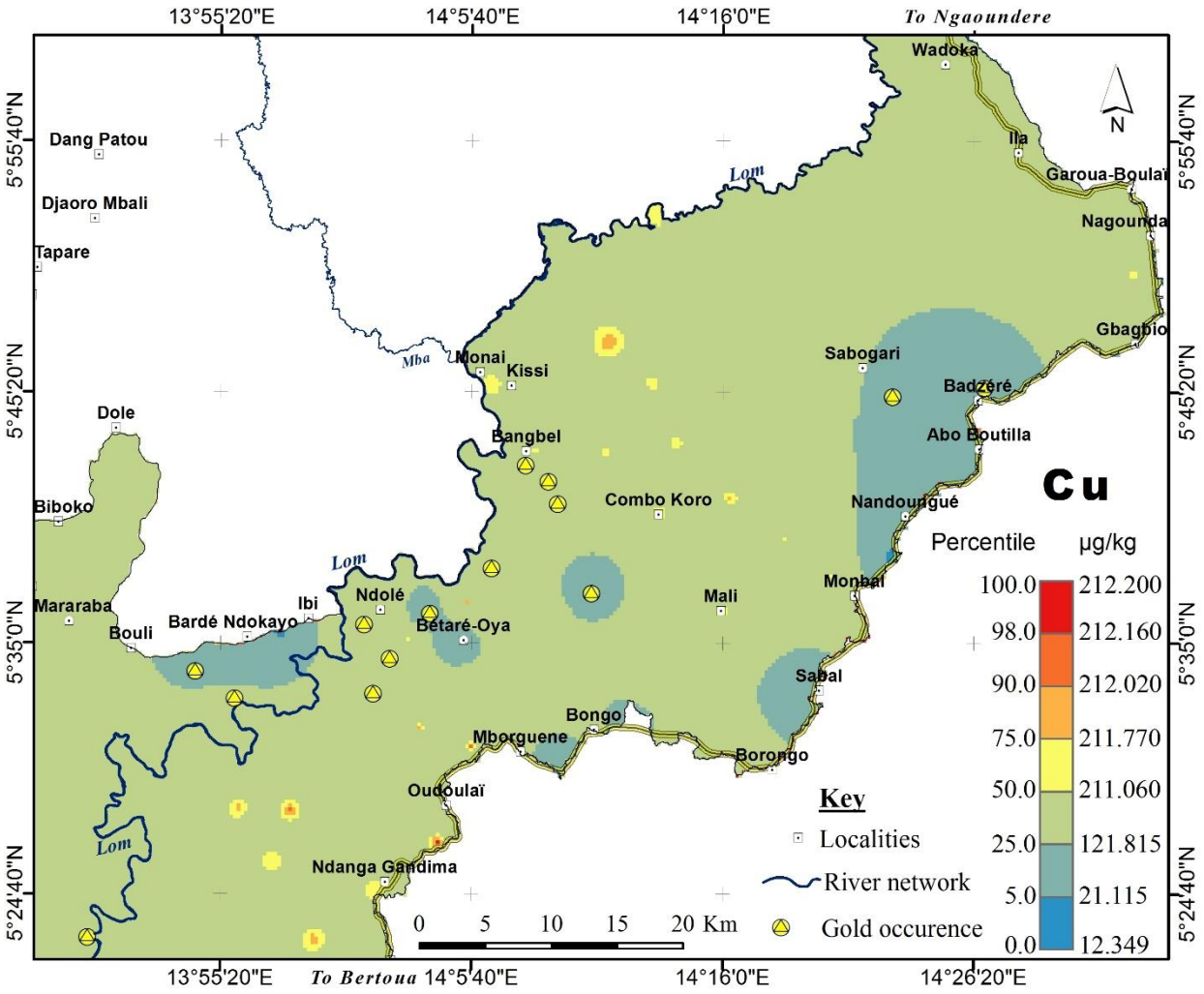

Figure 5.5a. Geochemical background of Cu in the lower Lom Basin.

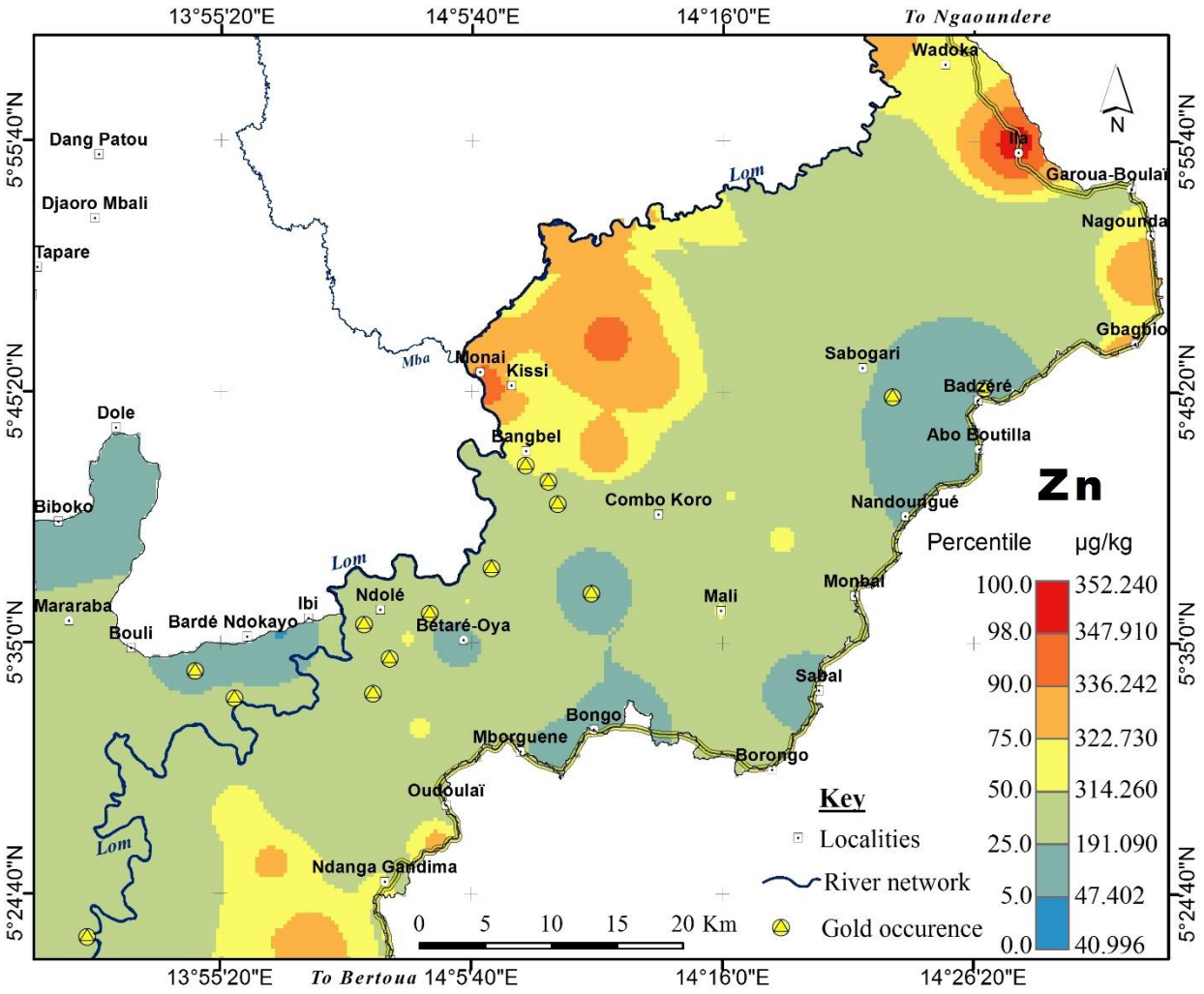

Figure 5.5b. Geochemical background of Zn in the lower Lom Basin.

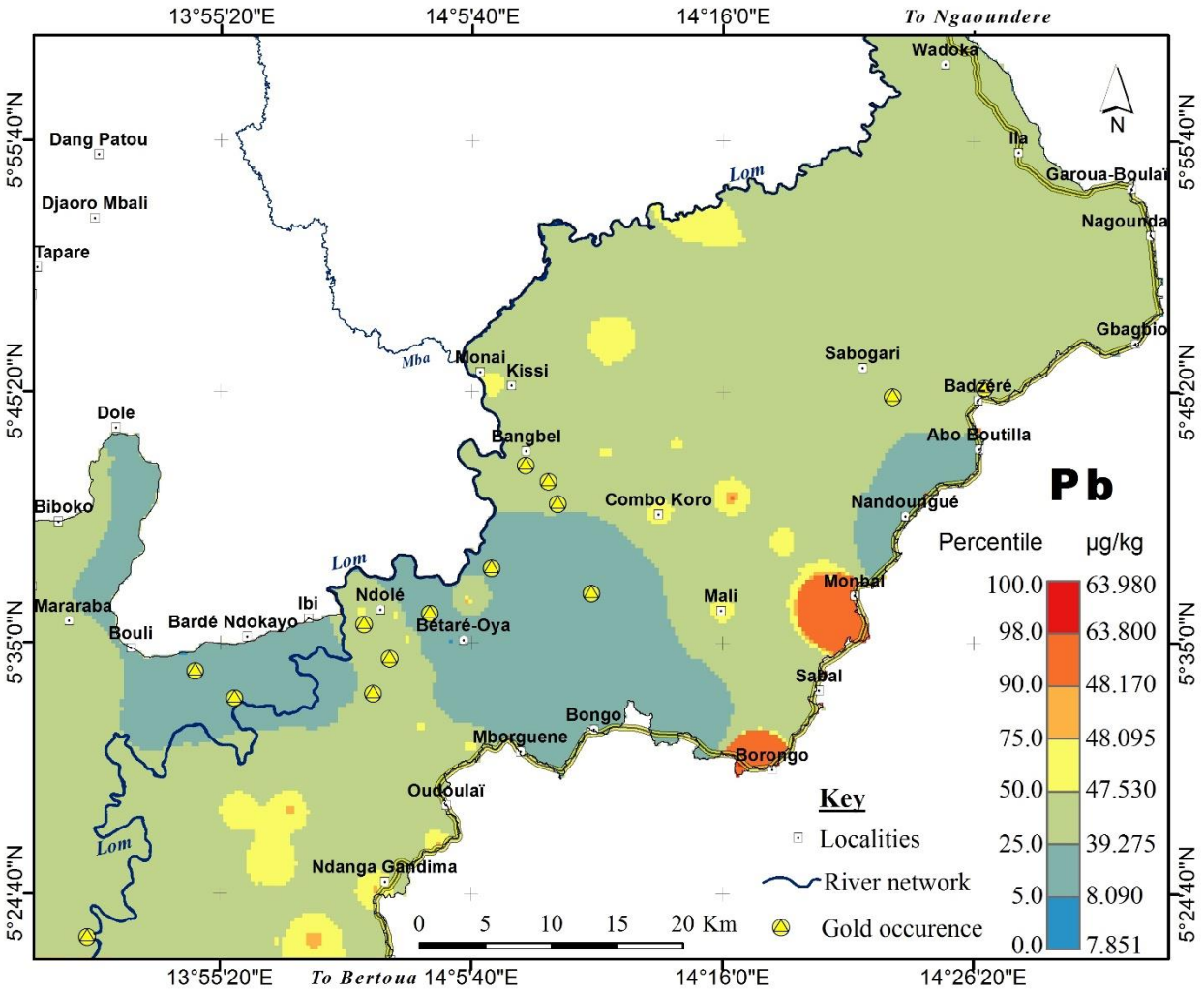

Figure 5.5c. Geochemical background of Pb in the lower Lom Basin.

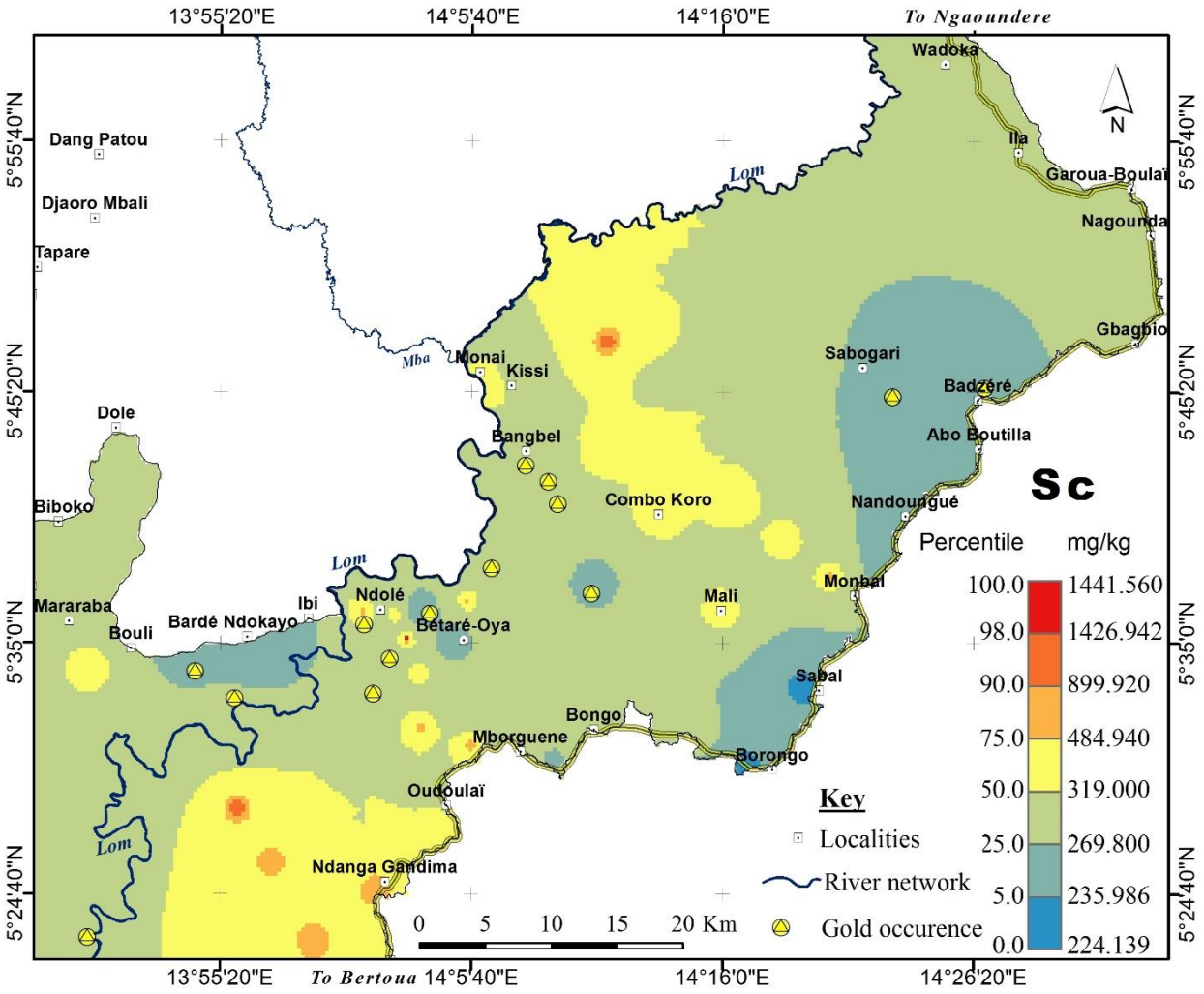

Figure 5.5d. Geochemical background of Sc in the lower Lom Basin.

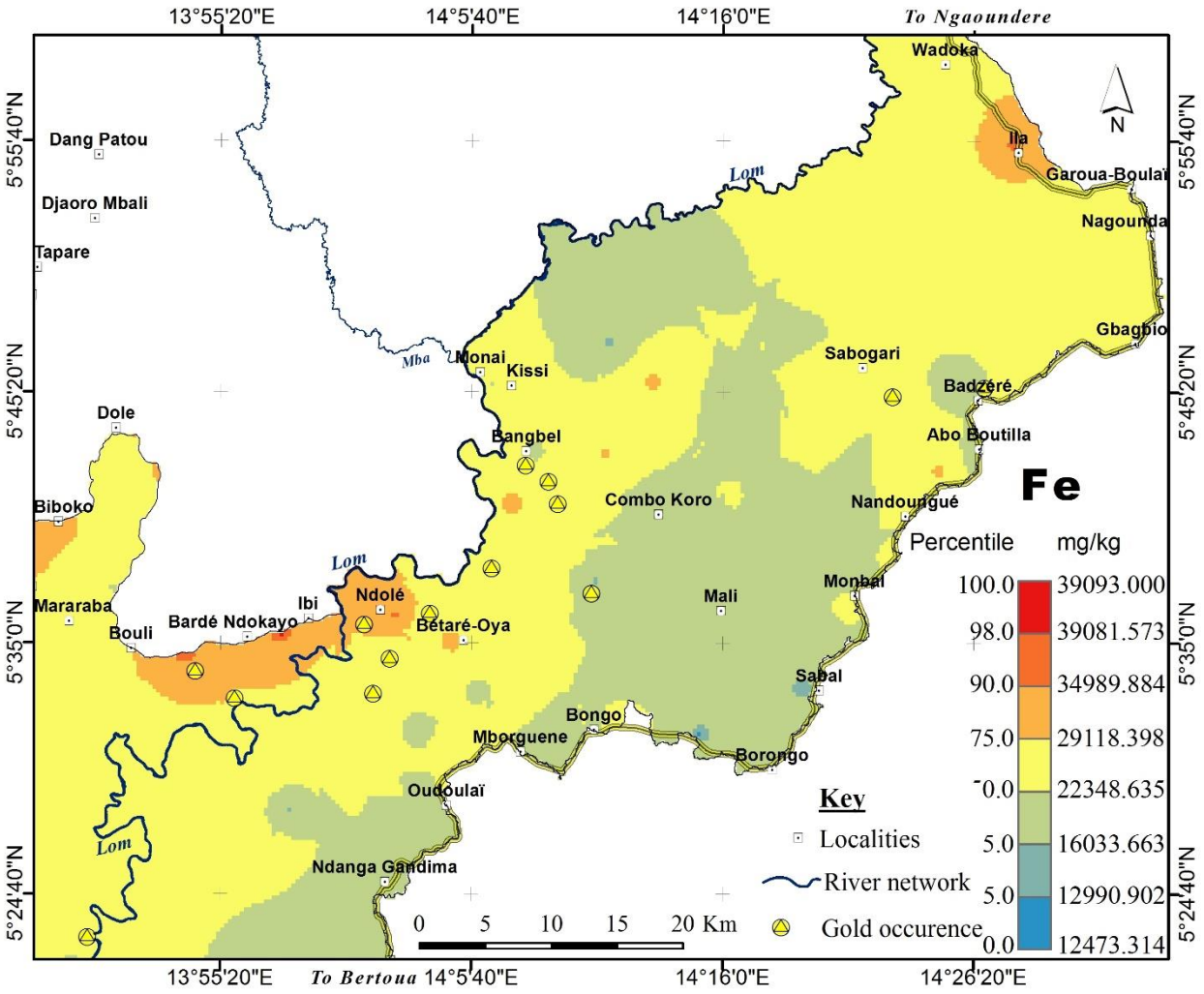

Figure 5.6a. Geochemical background of Fe showing enrichment in relation to the threshold (36692.6 mg/kg) in the western part of the lower Lom Basin.

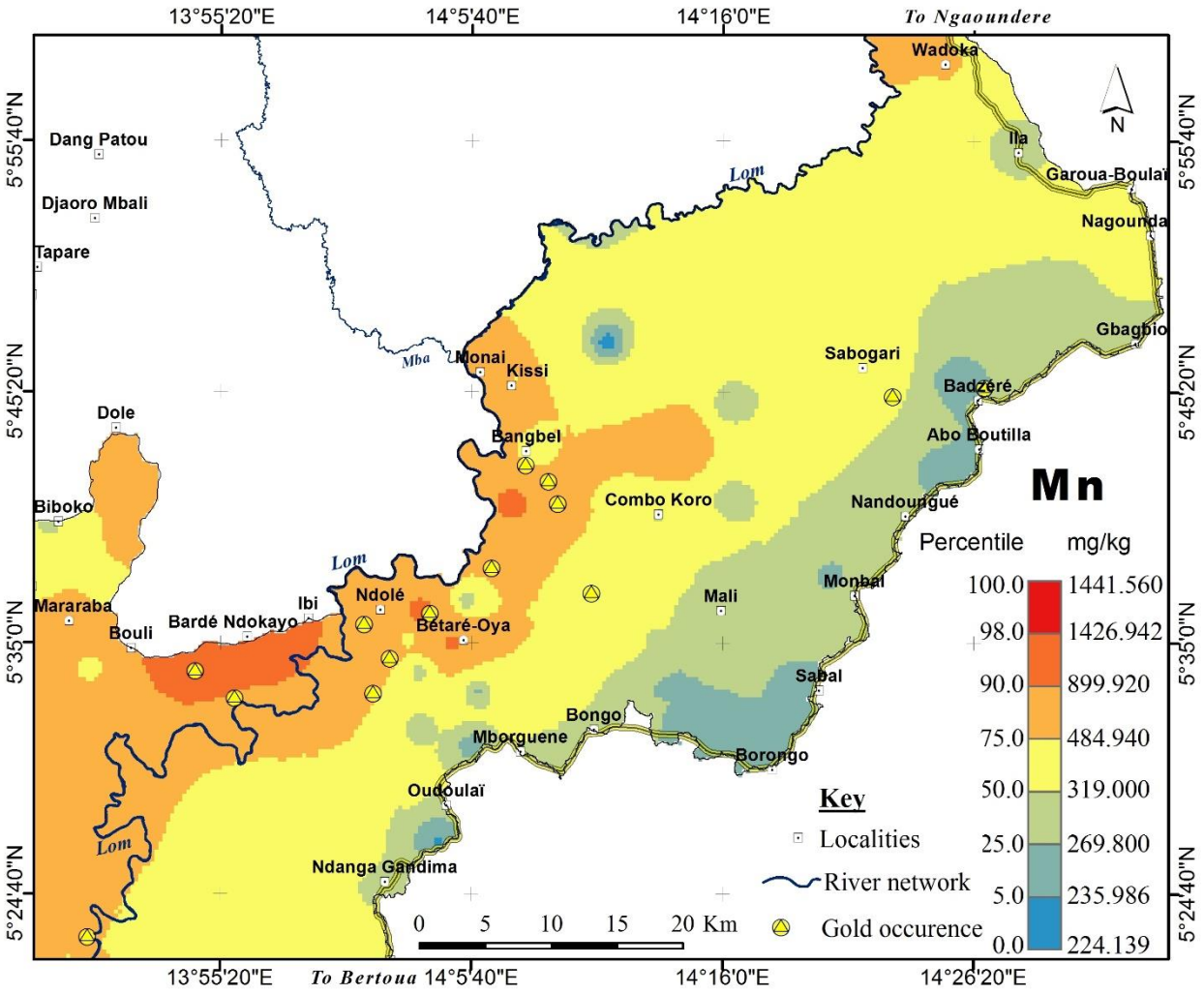

Figure 5.6b. Geochemical background of Mn showing enrichment in relation to the threshold (330.7 mg/kg) in the western part of the lower Lom Basin.

quartz veins (Vishiti et al., 2017). Besides, Cu, As and Pb, Fe is considered as a pathfinder for gold in the area (Mboudou et al., 2017). Hence, deep chemical weathering in this tropical basin results in the enrichment of Fe and Mn in the sediments. In the light of environmental significance, Fe and Mn are environmental scavengers. Heavy metals such as Cu, Zn, As and Pb can form stable complexes with Fe and Mn oxides through adsorption or co-precipitation processes (Gomez et al., 2007). Also, Fe and Mn oxides form thin coatings on minerals and clay particles which serve as natural traps or carriers of the heavy metals discharged into the aquatic system (Galan et al., 2003).

The distribution patterns of Cd, Hg and Se were distinct (Fig. 5.7a–c). Cadmium had lower concentrations (maximum concentration = 3.8 µg/kg) compared to the estimated threshold (13.21 µg/kg) and crustal average (98 ppb) (Taylor and McLennan, 1985). Despite the dissimilar distribution trends for Se and Hg (Fig. 5.7b and c), Se:Hg ratios can be used to check for Hg contamination in sediments (Sakan et al., 2017). The Hg–to–Se molar ratio was first proposed by Ganther et al. (1972) as a reference standard for Hg contamination. Ralston (2008) later suggested that Se:Hg>1 implies Se plays a key role in Hg assimilation processes. Using this approach, the ratios were calculated and presented in Table 5.2. Molar ratios above one imply low Hg content and thus, a protective effect of Hg toxicity. The estimated ratios ranged from 0.04 to 7.49. More than 80 % of the samples had Se:Hg>1 indicating that the sediments had lower Hg and higher Se contents. Thus, the negative effects of Hg are neutralized by a relatively higher Se content through assimilation processes. In the study area, gold amalgamation is practiced (CAPAM, 2016) and therefore, a plausible source of Hg in the sediments. Naturally, Hg occurs in trace amounts in the earth's crust (Cava et al., 2004). Through its use in mining, Hg may be discharged into water, deposited in sediments or released into the atmosphere. Mercury is a toxic substance which affects the reproductive and nervous system (Frumkin et al., 2001). It is therefore important to monitor the use of the hazardous element in mining within the catchment. The distribution of Cd, Se and Hg needs further investigation.

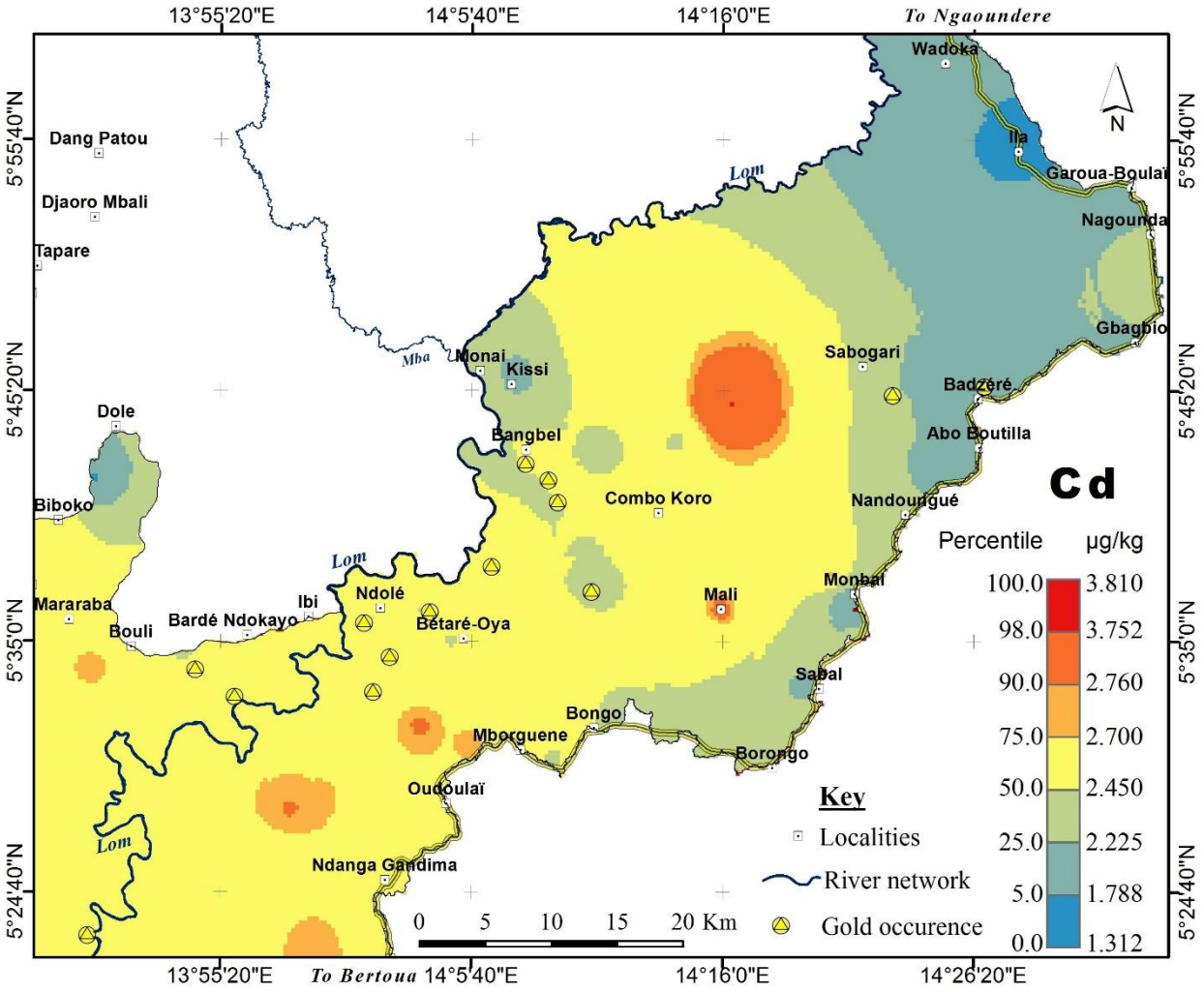

Figure 5.7a. Geochemical background of Cd in the lower Lom Basin.

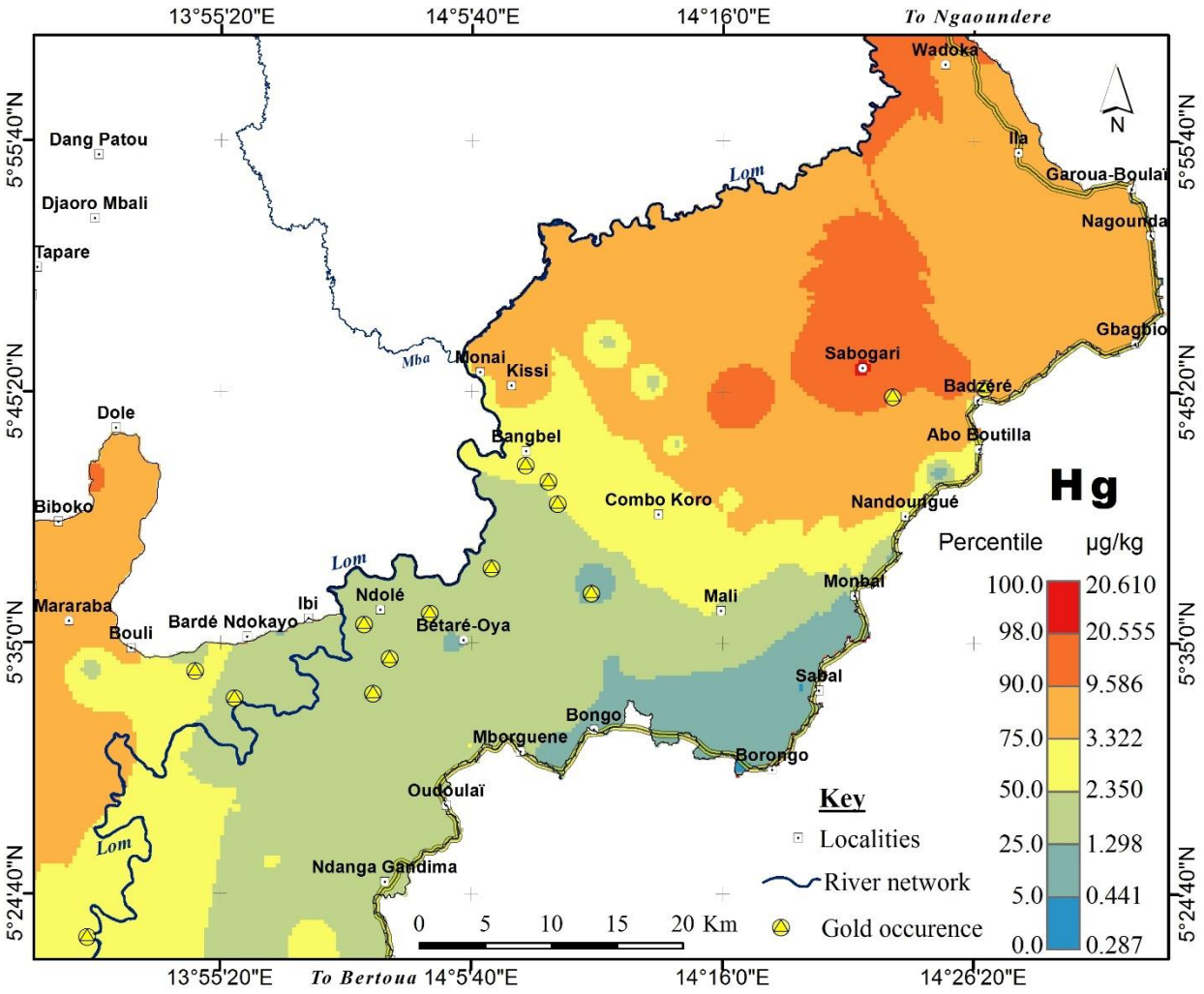

Figure 5.7b. Geochemical background of Hg in the lower Lom Basin.

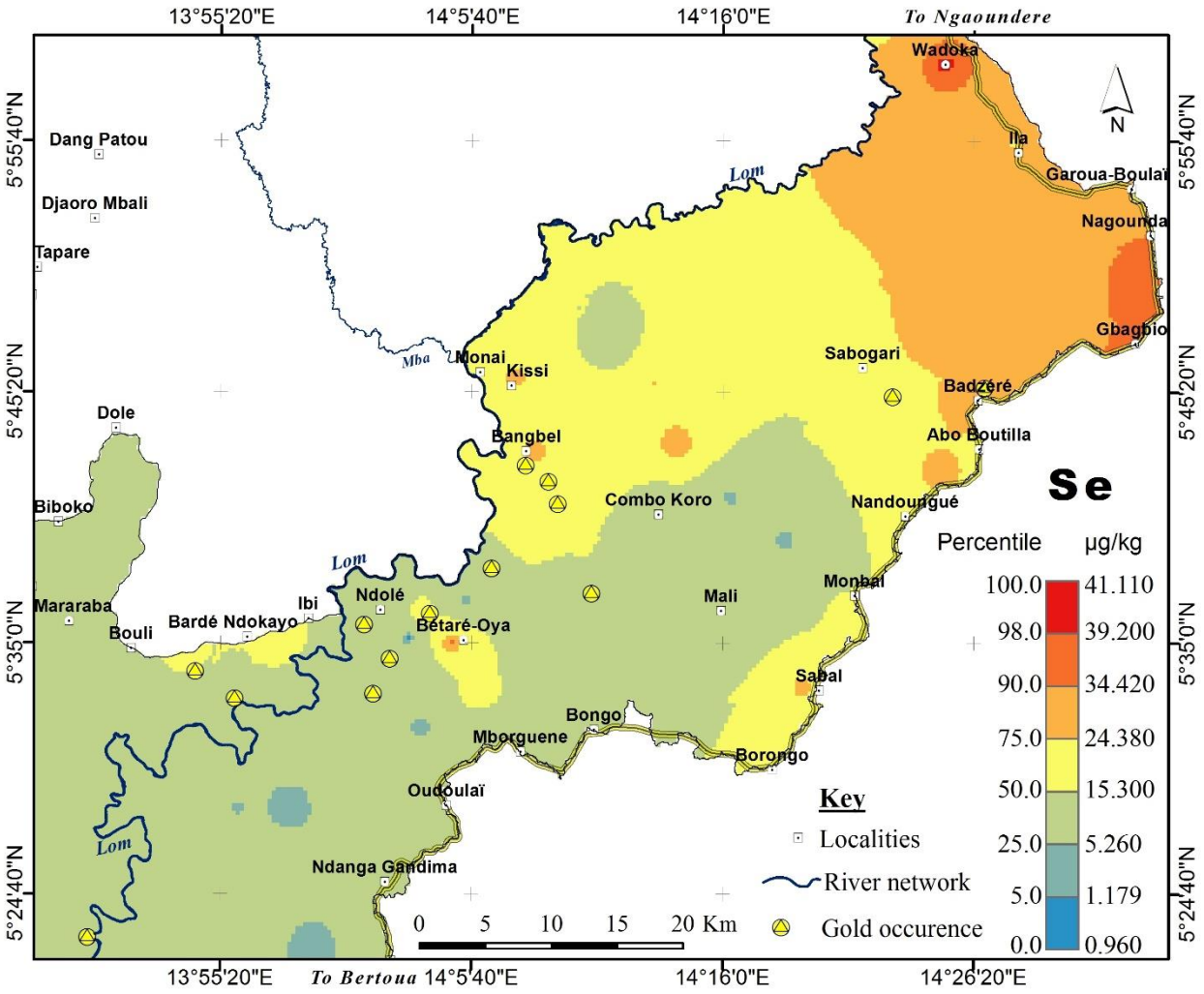

Figure 5.7c. Geochemical background of Se in the lower Lom Basin.

5.4 Conclusions

The mineral composition, background values, threshold values and baseline environmental geochemical assessment of stream sediments from the lower Lom Basin have been provided for the first time. Mineralogically, quartz, phyllosilicates (biotite + muscovite + kaolinite + gibbsite) and feldspars constitute the dominant mineral phases in the sediments. These minerals are derived primarily from the weathering of the complex plutono-metamorphic basement. Also, the mineralogical composition of stream sediments is influenced by hydraulic energy and sorting. In terms of trace metals, concentrations of V, Cu, Zn, As, Se, Cd, Hg and Pb were low while Sc, Cr, Co and Ni were slightly enriched compared to their calculated threshold values. Iron and Mn were the predominant metals reflecting the presence of ferromagnesian minerals in the bedrock. Overall, the low trace metal content of stream sediments is the result of the interaction of the near neutral pH of sediments (which does not favor the dissolution of metal sulphides), impoverished bedrocks and chemical weathering.

Multivariate statistical techniques enabled us to comprehend the basic processes influencing spatial geochemical variability. The spatial distribution of the trace metals Ni, Cr, V, Co and Se is controlled largely by source geology. Arsenic distribution has a coherent relationship to the occurrence of some Au deposits. Mercury, a hazardous environmental pollutant, is released into the basin through its use in gold recovery. Its continued use in refining gold may lead to harmful levels in the sediments.

The results obtained from this study show that the sediments have not been impacted by mining practices. However, given the paucity in fundamental geochemical data in Cameroon, this newly generated stream sediment data will serve as guidelines for future studies (environment, health and agriculture) in the region and other mineralized areas in the country. Future work should include the examination of metal composition in environmental samples from abandoned and active mine sites for comparison and environmental health risk assessment.

CHAPTER 6. CONCLUSIONS AND RECOMMENDATIONS

1. Stream water in the lower Lom catchment is fresh, slightly acidic to near neutral and comprises the Ca–HCO_3 and Na–HCO_3 species. The chemical composition of stream water for both the dry and wet seasons is mostly controlled by silicate weathering. This is also revealed in the spatial distribution of HCO_3^- and the major cations. Cation–exchange has a minor influence on the water chemistry. Seasonal variations show no significant effect on the chemical composition of streams.
2. Pollution of the stream water through anthropogenic activities especially alluvial mining is negligible given the very low concentrations of NO_3^-, Cl^- and the potentially harmful elements V, Cr, Co, Cu, Zn, Cd, Pb and Hg in the water. Still, the use of Hg in gold recovery should be greatly monitored.
3. The stream water in the lower Lom has not been chemically degraded given the low major ions and trace metal levels. However, investigations on the physical and bacteriological impurities in the water should be conducted to determine its suitability for drinking.
4. Stream sediment mineralogy consists of essentially quartz, micas, clay minerals and feldspars derived from the weathering of the Pan–African basement, and influenced by hydraulic energy and sorting.
5. The background of trace metals is considered as the range of metal concentrations in sediments in areas with no geochemical anomalies because the basin has been exploited anthropogenically. The levels of Cr, Co, Sc, Ni, Mn and Fe were slightly enriched compared to their threshold values. Spatial distributions of trace metals are controlled by catchment geology and sulphide mineralization associated with auriferous vein deposits. Gold mining practices in the catchment have not affected the sediment quality. Nevertheless, evaluation of sediments from active and abandoned mine sites for environmental health risk assessment is recommended. The provenance, sedimentary sorting and recycling of sediments in the basin should be further investigated by using trace elements and rare earth elements (REE) ratios.

REFERENCES

Agyarko, K., Dartey, E., Kuffour, R.A.W., Sarkodie, P.A. (2014) Assessment of trace elements levels in sediment and water in some artisanal and small–scale mining (ASM) localities in Ghana. Current World Environ. 9(1), 7–16.

Ahialey, E.K., Kortatsi, B.K., Anornu, G.K., Kaka, E.A., Dartey, G. (2015) Hydrogeochemical processes influencing groundwater quality in the Black Volta Basin of Ghana. Res J Appl Sc Enginer Technol. 11, 975–982.

Ako, A.A., Shimada, J., Hosono, T., Ichiyanagi, K., Nkeng, G.E., Fantong, W.Y., Takem, G.E.E., Njila, N.R. (2011) Evaluation of groundwater quality and its suitability for drinking, domestic, and agricultural uses in the Banana Plain (Mbanga, Njombe, Penja) of the Cameroon Volcanic Line. Environ Geochem Health. 33, 559–575.

Ako, A.A., Shimada, J., Hosono, T., Kagabu, M., Ayuk, A.R., Nkeng, G.E., Takem, G.E.E., Takounjou, A.L.F. (2012) Spring water quality and usability in the Mount Cameroon area revealed by hydrogeochemistry. Environ Geochem Health. https://doi.org/10.1007/s10653-012-9453-3

Ako, T.A., Onoduku, U.S., Ok, S.A., Adam, I.A., Ali, S.E., Mamodu, A., Ibrahim, A.T. (2014) Environmental impact of artisanal gold mining in Luku, Minna, Niger State, North Central Nigeria. J Geosciences and Geomatics 2(1), 28–37.

Appelo, C.A.J., Postma, D. Geochemistry, groundwater and pollution. A.A. Balkema Publi. Leiden. 1996, 683 p.

Ashley, R.P. (2002) Geoenvironmental model for low–sulfide gold-quartz vein deposits. In: U.S. Geological Survey, Chapter K. p.20. https://pubs.usgs.gov/of/2002/of02-195/OF02-195K.pdf. Accessed 18 May 2017.

Ateh, K.I., Suh, C.E., Shemang, E.M., Vishiti, A., Tata, E., Chombong, N.N. (2017) New LA–ICP–MS U–Pb ages, Lu–Hf systematics and REE characterization of zircons from a granitic pluton in the Betare Oya gold district, SE Cameroon. J Geosciences and Geomatics 5(6), 267–283.

Bafon, T.G. (2011) Quartz veining, wall rock alteration and mineralization at the Belikobone Prospect, Eastern Cameroon. Master's thesis, University of Buea, Buea, 52.

Bakia, M. (2014) East Cameroon's artisanal and small–scale mining bonanza: how long will it last? The futures of small–scale mining in sub-Saharan Africa. Futures. 62, 40–50. https://doi.org/10.1016/j.futures.2013.10.022

Bansah, K.J., Yalley, A.B., Dumakor-Dupey, N. (2016) The hazardous nature of small–scale underground mining in Ghana. J Sustainable Mining. 15(1), 8–25.

Basseka, C.A., Shandini, Y., and Tadjou, J.M. (2011) Subsurface structural mapping using gravity data of the northern edge of the Congo craton, South Cameroon: Geofizika. 28(2), 229–245.

Birke, M., Rauch, U., Stummeyer, J. (2015) How robust are geochemical patterns? A comparison of low and high sample density geochemical mapping in Germany. J Geochem Explor. 154, 105–128.

Boboye, O.A., Abumere, I.O. (2014) Environmental impact of elemental concentration and distribution in waters, soils and plants along the Lokoja–Abuja pipeline routes of Bida Basin, northwestern Nigeria. J African Earth Sciences. 99, 694–704.

Boeglin, J.L., Ndam, N.J.R., Braun, J.J. (2003) Composition of the different reservoir waters in a tropical humid area: example of the Nsimi catchment (Southern Cameroon). J African Earth Science. 37,103–110. http://dx.doi.org/10.1016/S08995362(03)000411

Bortey-Sam, N., Nakayama, S.M.M., Ikenaka, Y., Akoto, O., Baidoo, E., Mizukawa, H., Ishizuka, M. (2015) Health risk assessment of heavy metals and metalloid in drinking water from communities near gold mines in Tarkwa, Ghana. Environ Monit Assess. 187:397.

Braun, J.J., Ndam Ngoupayou, J.R., Viers, J., Dupre, B., Bedimo Bedimo, J.P., Boeglin, J.L., Robain, H., Nyeck, B., Freydier, R., Sigha Nkamdjou, L., Rouiller, J., Muller, J.P. (2005)

Present weathering rates in a humid tropical watershed: Nsimi site (South Cameroon). Geochim Cosmochim Acta. 69, 357–387.

Butler, J.N. Carbon Dioxide Equilibria. Lewis Publishers, Chelsea, Michigan. 1981, p. 116–118.

Cadaxo Sobrinho, E.S., Ribeiro, J., Neto, C., Sant'Ovaia, H., Rocha, F., Flores, D., Garção de Carvalho, C.E. (2014) Mineralogy and geochemistry of sediments from São Francisco stream (Amazonian River Basin, Brazil). Comunicações Geológicas. 101(1), 57–60.

CAPAM (2016) Mission de suivi environnemental des sites d'exploitations minières artisanales dans les régions de l'Est et de l'Adamaoua. Technical report, 44 pp.

Caritat, Pde, Cooper, M. (2016) A continental–scale geochemical atlas for resource exploration and environmental management: the National Geochemical Survey of Australia. Geochem: Explor Environ Anal. 16, 3–13.

Caritat, Pde, Lech, M.E., McPherson, A.A. (2008) Geochemical mapping 'down under': Selected results from pilot projects and strategy outline for the National Geochemical Survey of Australia. Geochem: Explor Environ Analy. 8, 301–312.

Castaing, C., Feybesse, J.L., Thieblemont, D., Triboulet, C., Chevremont, P. (1994) Palaeogeographical reconstructions of the Pan-African/Brasiliano orogen: closure of an oceanic domain or intracontinental convergence between major blocks? Precambrian Res.67, 327–344.

Cava, M.P., Rodenas, T.E., Morales, R.A., Cervera, M.L., Guardia, M.C. (2004) Vapour atomic fluorescence determination of mercury in milk by slurry sampling using multi commutation. Analytical Clinical acta. 506, 145–153.

Chandrajith, R., Dissanayake, C.B., Tobshall, H.J. (2001) Enrichment of high field strength elements in stream sediments of a granulite terrain in Sri Lanka – evidence for a mineralised belt. Chem Geol. 175, 259–271.

Cheng, H. Hu, Y., Luo, J., Xu, B., Zhao, J. (2009) Geochemical processes controlling fate and transport of arsenic in acid mine drainage (AMD) and natural systems. J Hazardous Materials 165, 13–26.

Chiprés, J.A., Salinas, J.C., Castro–Larragoitia, J., Monroy, M.G. (2008) Geochemical mapping of major and trace elements in soils from the Altiplano Potosino, Mexico: a multiscale comparison. Geochem: Explor Environ Analy. 8, 279–290.

Cobbina, S.J., Myilla, M., Michael, K. (2013) Small scale gold mining and heavy metal pollution: Assessment of drinking water sources in Datuku in the Talensi–Nabdam District. Int J Sci Techno Res. 2, 96.

Cox, P.A. The Elements on Earth: Inorganic Chemistry in the Environment, New York: Oxford University Press, 1995, 287 pp.

Cravotta, C.A.III (2000) Relations among sulfate, metals and stream flow data for a stream draining a coal-mined watershed in east-central Pennsylvania. Proceedings of the International Conference on Acid Rock Drainage (ICARD), Denver, Colorado: Soc Mining Metallur Explor. 1, 401–410.

Dan, S.F., Umoh, U.U., Osabor, V.N. (2014) Seasonal variation of enrichment and contamination of heavy metals in the surface water of Qua Iboe River Estuary and adjoining creeks, South–South Nigeria. J Oceanography and Marine Sc. 5(6), 45–54.

Darwish, M.A.G. (2017) Stream sediment geochemical patterns around an ancient gold mine in the Wadi El Quleib area of the Allaqi region, south Eastern Desert of Egypt: Implications for mineral exploration and environmental studies. J Geochem Explor. 175, 156–175. https://doi.org/10.1016/j.gexplo.2016.10.010

De Wit, M.J., Linol, B. (2015) Precambrian Basement of the Congo Basin and its Flanking Terrains. In: de Wit, MJ. et al. (Eds.), Geology and Resource Potential of the Congo Basin, Regional Geology Reviews. Springer–Verlag, Berlin Heidelberg. 19–37. https://dx.doi.org/10.1007/978-3-642-29482-2_2

Dinelli, E., Cortecci, G., Lucchini, F., Zantedeschi, E. (2005) Sources of major and trace elements in the stream sediments of the Arno river catchment (northern Tuscany, Italy). Geochem J. 39, 531–545.

Dollar, N.L., Souch, C.J., Filippelli, G.M., Mastalerz, M. (2001) Chemical fractionation of metals in wetland sediments: Indiana Dunes National Lakeshore. Environ Sci Technol. 35, 3608-3615.

Drever, J.I. The geochemistry of natural waters; surface and groundwater environments, 3rd edn. Prentice Hall, Upper Saddle River. 1997, pp 138–196.

Edet, A., Ukpong, A., Nganje, T. (2014) Baseline concentration and sources of trace elements in groundwater of Cross River State, Nigeria. Int J Environ Monit Analy. 2(1), 1–13.

Edjah, A.K.M., Akiti, T.T., Osae, S. (2015) Hydrogeochemistry and isotope hydrology of surface water and groundwater systems in the Ellembelle district, Ghana, West Africa. Appl Water Sci. https://doi.org/10.1007/s13201-015-0273-3

Embui, V.F., Omang, B.O., Che, V.B., Nforba, M.T., Suh, E.C. (2013) Gold grade variation and stream sediment geochemistry of the theVaimba–Lidi drainage system, northern Cameroon. Natural Science. 5(2A), 282-290.

Eneji, I.S., Onuche, A.P., Sha'Ato, R. (2012) Spatial and temporal variation in water quality of River Benue, Nigeria. J Environ Protec. 3, 915–921.

Eneke, G.T., Ayonghe, S.N., Chandrasekharam, D., Ntchancho, R., Ako, A.A., Mouncherou, O.F., Thambidurai, P. (2011) Controls on groundwater chemistry in a highly urbanised coastal area. Int J Environ Res. 5, 475–490.

Etame, J., Tchameni Ngouabe, E.G., Ngon Ngon, G.F., Ntamak–Nida, M.J., Suh, C.E., Bilong, M.G.P. (2013) Mineralogy and geochemistry of active stream sediments from the Kelle River drainage system (Pouma, Cameroon). Sciences, Technologies et Développement. 14, 35–47.

Fantong, W.Y., Satake, H., Ayonghe, S.N., Aka, F.T., Asai, K. (2009) Hydrogeochemical controls and usability of groundwater in the semi–arid Mayo Tsanaga River Basin: Far North Province, Cameroon. Environ Geology. 58, 1281–1293. https://doi.org/10.1007/s00254-008-1629-x

Feybesse, J.L., Johan, V., Triboulet, C., Guerrot, C., Mayaga Mikolo, F., Bouchot, V., and Eko N'dong, J. (1998) The West Central African belt: A model of 2.5–2.0 Ga accretion and two–phase orogenic evolution: Precambrian Res. 87, 161–216. https://doi.org/10.1016/S0301-9268(97)00053-3

Ficklin, W.H., Plumlee, G.S., Smith, K.S., McHugh, J.B. (1992) Geochemical classification of mine drainages and natural drainages in mineralised areas. In: Kharaka, Y.K., Maest, A.S. (Eds.) Proceedings of 7th International Symposium, Water Rock Interaction, pp 381–384.

Fisher, R.S., Mullican, F.W. (1997) Hydrochemical evolution of sodium-sulphate and sodium-chloride groundwater beneath the Northern Chihuahuan Desert. Hydrogeol J. 5, 14–16.

Fon, A.N., Che, V.B., Suh, C.E. (2012) Application of electrical resistivity and chargeability data on a GIS platform in delineating auriferous structures in a deeply weathered lateritic terrain, East Cameroon. Int J of Geosciences. 3, 960–971.

Förstner, U., Ahlf, W., Calmano, W., Kersten, M. (1991) Geochemistry of the Arno river sediments 545 Sediment criteria development. Sediments and Environmental Geochemistry (Heling D, Rothe P, Förstner, Stoffers, P. eds.). Springer–Verlag. 312–338.

Franz, C., Abbt-Braun, G., Lorz, C., Rorg, H.L., Makeschin, F. (2014) Assesment and evaluation of metal contents in sediment and water samples within an urban watershed: an analysis of anthropogenic impacts on sediment and water quality in Central Brazil. Environ Earth Sci. 72, 4873–4890.

Freeze, R.A., Cherry, J.A. Groundwater. Prentice-Hall, Englewood Cliffs. 1979, 604 p.

Freitas, M.R., Perilli Thomaz, A.G., Ladeira Ana, C.Q. (2013) Oxidative precipitation of manganese from acid mine drainage by potassium permanganate. J Chemistry. 13. http://dx.doi.org/10.1155/2013/287257

Freyssinet, P.H., Lecompte, P., Edimo, A. (1989) Dispersion of gold base metals in the Mborguene lateritic profile, East Cameroon. J Geochem Explor. 32, 99–116.

Frumkin, H., Letz, R., Williams, P.L., Gerr, F., Pierce, M., Sanders, A., Elon, L., Mannings, C.C., Woods, J.S., Hertzberg, V.S., Mueller, P., Taylor, B.B. (2001) Health effects of long term mercury exposure among chloralkali plants workers. Am J Ind Med. 39, 1–18.

Galan, E., Gomez-Ariza, J.L., Gonzalez, I., Fernandez-Caliani, J.C., Morales, E., Giraldez, I. (2003) Heavy metal portioning in river sediments severely polluted by acid mine drainage in the Iberian Pyrite Belt. Appl Geochem 18, 409–421.

Gałuszka, A. (2007) A review of geochemical background concepts and an example using data from Poland. Environ Geol. 52, 861-870. https://doi.org/ 10.1007/s00254-006-0528-2

Gałuszka, A., Migaszewski, Z.M. (2011) Geochemical background – an environmental perspective. Mineralogia. 42(1), 7–17. https://doi.org/ 10.2478/v10002-011-0002-y

Ganther, H.E., Goudie, C., Wagner, P., Sunde, M.L., Kopecky, M.J., Oh, S.H., Hoekstra, W.G. (1972) Selenium relation to decreased toxicity of methylmercury added to diets containing tuna. Science. 175, 1122–1124.

Garizi, A.Z., Sheikh, V., Sadoddin, A. (2011) Assessment of seasonal variations of chemical characteristics in surface water using multivariate statistical methods. Int J Environ Sci Tech. 8(3), 581–59.

Garret, R.G., Reimann, C., Smith, D.B., Xie, X. (2008) From geochemical prospecting to international geochemical mapping: A historical overview. Geochem: Explor Environ Anal. 8, 205–217.

Gomez, A.A., Valenzuela, J.L.G., Aguayo, S.S., Meza, D.F., Ramirez, J.H., Ochoa, G.O. (2007) Chemical partitioning of sediment contamination by heavy metals in the San Pedro River,

Sonora, Mexico. Chem Spec Bioavail. 19, 25–35.

Grasby, S.E., Hutcheon, I., Krouse, H.R. (1997) Application of the stable isotope composition of SO42- to tracing anomalous TDS in Nose Creek, southern Alberta, Canada. Appl Geochem. 12(5), 56 7–5 75.

Gray, D.J., Noble, R.R.P., Reid, N., Sutton, G.J., Pirlo, M.C. (2016) Regional scale hydrogeochemical mapping of the northern Yilgarn Craton, Western Australia: a new technology for exploration in arid Australia. Geochem: Explor. Environ. Analy. 16, 100–115.

Guillén, M.T., Delgado, J., Albanese, S., Annamaria Lima, J.M.N., De Vivo, B. (2011) Environmental geochemical mapping of Huelva municipality soils (SW Spain) as a tool to determine background and baseline values. J Geochem Explor. 109, 59–69.

Gupta, S., Dandele, P.S., Verma, M.B., Maithani, P.B. (2009) Geochemical assessment of groundwater around Macherla- 524 Page 22 of 24 Environ Monit Assess (2016) 188:524 Karempudi area, Guntur District, Andhara Pradesh. J Geol Soc India. 73, 202–212.

Hawkes, H.E., Webb, J.S. Geochemistry in Mineral Exploration. Harper Collins, New York; 1962.

Hem, J.D. (1963) Chemical equilibria affecting the behavior of manganese in natural water. International Association of Scientific Hydrology. Bulletin, 8:3, 30–37. https://doi.org/10.1080/02626666309493334

Hem, J.D. (1985) Study and interpretation of the chemical characteristics of natural water. United States Geological Survey Water Supply Paper 2254.

Hook, Z. (2005) An assessment of the quality of drinking water in rural districts in Zimbabwe. The case of Gokwe South, Nkayi Lupene and Nwenezi districts. Phys Chem Earth 30, 859–866.

Howarth, R.J., Thornton, I. (1983) Regional geochemical mapping and its application to environmental studies. Appl. Environ. Geochem (Thornton, I., ed.), Academic Press, 14–73.

Ibe, K.K., Akaolisa, C Z. (2010) Hydrogeochemical data as a tool for exploration and mapping: a case study from part of Afikpo Basin southeastern Nigeria. Environ Monit Assess. 160, 393–400.

International Soil Reference and Information Centre (ISRIC). Procedures for soil analysis, Technical Paper 9, sixth edition 2002, 101p.

Jorquera, C.O., Oates, C.J., Plan, J.A., Kyser, K., Ihenfield, C., Vouvoulis, N. (2015) Regional hydrogeochemical mapping in Central Chile: natural and anthropogenic sources of elements and compounds. Geochem: Explor Environ Analy. 15, 72–96.

Kabata-Pendias, A. (2011) Trace elements in soils and plants, 4th ed. Taylor & Francis Group, Boca Raton London New York.

Kamtchueng, B.T., Fantong, W.Y., Ueda, A., Tiodjio, E.R., Anazawa, K., Wirmvem, M.J., Mvondo, J.O., Nkamdjou, S.L., Kusakabe, M., Ohba, T., Tanyileke, G., Hell, J.V. (2014) Assessment of shallow groundwater in Lake Nyos catchment (Cameroon, Central–Africa): implications for hydrogeochemical controls and uses. Environ Earth Sci. 72, 3663–3678. https://doi.org/10.1007/s12665-014-3278-6

Kamtchueng, B.T., Fantong, W.Y., Wirmvem, M.J., Tiodjio, R.E., Takounjou, A.F., Ndam Ngoupayou, J.R., Kusakabe, M., Zhang, J., Ohba, T., Tanyileke, G., Hell, J.V., Ueda, A. (2016) Hydrogeochemistry and quality of surface water and groundwater in the vicinity of Lake Monoun, West Cameroon: approach from multivariate statistical analysis and stable isotopic characterization. Environ Monit Assess. 8:524. https://doi.org/10.1007/s10661-016-5514-x

Kankeu, B., Greiling, R.O., Nzenti, J.P. (2009) PanAfrican strike–slip tectonics in eastern Cameroon - Magnetic fabrics (AMS) and structures in the Lom basin and its gneissic basement. Precambrian Res. 174, 258-272.

Kankeu, B., Greiling, R.O., Nzenti, J.P., Bassahak, J., Hell, J.V. (2012) Strain partitioning along the Neoproterozoic Central Africa shear zone system: structures and magnetic fabrics (AMS) from the Meiganga area, Cameroon. Neues Jahrb Geol. Paläontologie Abh. 265, 27–47.

Kankeu, B., Greiling, R.O., Nzenti, J.P., Ganno, S., Danguene Prince, Y.E., Bassahak, J., Hell, J.V. (2017) Contrasting Pan-African structural styles at the NW margin of the Congo Shield in Cameroon. J African Earth Sciences. 27–47. http://dx.doi.org/10.1016/j.jafrearsci.2017.06.002

Kelepertzis, E., Argyraki, A., Daftsis, E. (2012) Geochemical signature of surface and stream sediments of a mineralized drainage basin at NE Chalkidiki Greece: A pre–mining survey. J Geochem Explor. 114, 70–81.

Khazheeva, Z.I., Tulokhonov, A.K., Dashibalova, L.T. (2007) Seasonal and spatial dynamics of TDS and major ions in the Selenga River. Water Resources 34(4), 444–449.

Kim, K., Rajmohan, N., Kim, H.J., Kim, S.H., Hwang, G.S., Yun, S.T., Gu, B., Cho, M.J., Lee, S.H. (2005) Evaluation of geochemical processes affecting groundwater chemistry based on mass balance approach: A case study in Namwon, Korea. Geochem. J. 39, 357–369.

Kouankap Nono, G.D., Tah Bong, C., Wotchoko, P., Magha, A., Chianebeng Japhet, K., Tene Djoukam, J.F. (2017) Artisanal gold mining in Batouri area, East Cameroon: impacts on the mining population and their environment. J Geol Min Res. 9(1), 1–8. https://doi.org/10.5897/JGMR16.0263

Kpan, D.K., Opoku, A.B., Gloria, A. (2014) Heavy metal pollution in soil and water in some selected towns in Dunkwa-on-Offin District in the Central Region of Ghana as a result of small scale gold mining. J Agricul Chem Environ. 3, 40–47.

Kumar, M., Al Ramanathan, Roa, M.S., Kumar, B. (2006) Identification and evaluation of hydrogeochemical processes in the groundwater environment of Delhi, India. Environ Geol. 50, 1025–1039.

Kusimi, J.M., Kusimi, B.A. (2012) The hydrochemistry of water resources in selected mining communities in Tarkwa. J Geochem Explor. 112, 252–261.

Laplaine, L. (1969) Index and Mineral Resources of Cameroon. Report of mining and geology department.

Lapworth, D.J., Knights, K.V., Key, R.M., Johnson, C.C., Ayoade, E., Adekanmi, M.A., Arisekola, T.M., Okunlola, O.A., Backman, B., Eklund, M., Everett, P.A., Lister, R.T., Ridgway, J., Watts, M.J., Kemp, S.J., Pifield, P.E.J. (2012) Geochemical mapping using stream sediments in west-central Nigeria: Implications for environmental studies and mineral exploration in West Africa. Appl Geochem. 27, 1035–1052.

Laszlo, O., Istvan, H., Ubul, F. (1997) Low density geochemical mapping in Hungaria. J Geochem Explor. 60, 55–66.

Lerouge, C., Cocherie, A., Toteu, S.F., Penaye, J., Milési, J.P., Tchameni, R., Nsifa, E.N., Mark Fanning, C., and Deloule, E. (2006) Shrimp U–Pb zircon age evidence for Paleoproterozoic sedimentation and 2.05 Ga syntectonic plutonism in the Nyong Group, South-Western Cameroon: Consequences for the Eburnean-Transamazonian belt of NE Brazil and Central Africa: J African Earth Sciences. 44, 413–427. https://doi.org/10.1016/j.jafrearsci.2005.11.010

Lewis, A.E. 2010 Review of metal sulphide precipitation. Hydrometallurgy 104:222–234. http://dx.doi.org/10.1016/j.hydromet.2010.06.010

Liao, J., Chen, J., Ru, X., Chen, J., Wu, H., Wei, C. (2017) Heavy metals in river surface sediments affected with multiple pollution sources, South China: Distribution, enrichment and source apportionment. J Geochem Explor. 176, 9–19. http://dx.doi.org/10.1016/j.gexplo.2016.08.013

Makishima, A., Nakamura, E. (1997) Suppression of matrix effects in ICP-MS by high power operation of ICP: Application to precise determination of Rb, Sr, Y, Cs, Ba, REE, Pb, Th, and U at ng g-1 levels in milligram silicate samples. The Journal of Geostandards and Geoanalysis. 21(2), 307–319.

Manga, V.E., Neba, G.N., Suh, C.E. (2017) Environmental geochemistry of mine tailings soils in the artisanal gold mining district of Bétaré-Oya, Cameroon. Environment and Pollution. 6(1), 52-61. https://doi.org/10.5539/ep.v6n1p52

Markewitz, D., Davidson, E.A., Figueiredo, R.O., Victoria, R.L., Krusche, A.V. (2001) Control of cation concentrations in stream waters by surface soil processes in an Amazonian watershed. Nature. 410, 802–805.

Matschullat, J., Ottenstein, R., Reimann, C. (2000) Geochemical background - can we calculate it? Environ Geol. 39, 990-1000. https://doi.org/ 0.1007/s002549900084

Mboudou, G.M.M., Fozao, K.F., Njoh, O.A., Agyingi, C.M. (2017) Characterization of alluvial gold bearing sediments of Betare Oya District-East Cameroon, Implication for gold exploration and recovery. Open Journal of Geology. 7, 1724–1738.

Meybeck, M. (1987). Global chemical weathering of surficial rocks estimated from river dissolved loads. Am J Sci. 287, 401–428.

Mikoshiba, U.M., Imai, N., Terashima, S., Tachibana, Y., Okay, T. (2006) Geochemical mapping in northern Honshu, Japan. Appl Geochem. 21, 492–514.

Milesi, J.P., Toteu, S.F., Deschamps, Y. et al (2006) An overview of the geology and major ore deposits of Central Africa: Explanatory note for the 1:4,000,000 map "Geology and major ore deposits of Central Africa". J African Earth Sciences. 44, 571–595

Mimba, M.E., Nforba, M.T., Suh, C.E. (2014) Geochemical dispersion of gold in stream sediments of the Paleoproterozoic Nyong Series, southern Cameroon. Science Research. 2(6), 155–165. doi: 10.11648/j.sr.20140206.12

Mimba, M.E., Ohba, T., Nguemhe Fils, S.C., Wirmvem, M.J, Bate Tibang, E.E., Nforba, M.T., Aka, F.T. (2017a) Regional hydrogeochemical mapping for environmental studies in the mineralized Lom Basin, East Cameroon: a pre-industrial mining survey. Hydrology. 5(2), 15–31. https://doi.org/10.11648/j.hyd.20170502.11

Mimba, M.E., Ohba, T., Nguemhe Fils, S.C., Wirmvem, M.J., Numanami, N., Aka, F.T. (2017b) Seasonal hydrological inputs of major ions and trace metal composition of streams draining the mineralized Lom Basin, East Cameroon: Basis for environmental studies. Earth Syst Environ. 1:22. https://doi.org/10.1007/s41748-017-0026-6

Mimba, M.E., Ohba, T., Nguemhe Fils, S.C., Nforba, M.T., Numanami, N., Aka, F.T., Suh, C.E. (2018) Regional geochemical baseline concentration of potentially toxic trace metal in the mineralized Lom Basin, East Cameroon: A tool for contamination assessment. Geochem Trans. 19:11, 1–17. https://doi.org/10.1186/s12932-018-0056-5

Ndam Ngoupayou, J.R., Dzana, J.G., Kpoumie, A., Tanwi Ghogomu, R., Fouepe Takounjou, A., Braun, J.J., Ekodeck, G.E. (2016) Present–day sediment dynamics of the Sanaga catchment (Cameroon): from the total suspended sediment (TSS) to erosion balance. Hydrol Sci J. 61 (6), 1080–1093. http://dx.doi.org/10.1080/02626667.2014.968572

Nédélec, A., Nsifa, E.N., and Martin, H. (1990) Major and trace element geochemistry of the Archaean Ntem plutonic complex (south Cameroon): Petrogenesis and crustal evolution: Precambrian Res. 47, 35–50. https://doi.org/10.1016/0301-9268(90)90029-P

Ngako, V., Affaton, P., Njonfang, E. (2008) Pan–African tectonics in northwestern Cameroon: implication for the history of western Gondwana. Gondwana Res. 14, 509–522.

Ngako, V., Affaton, P., Nnange, J.M., Njanko, T.H. (2003) Pan–African tectonic evolution in central and southern Cameroon: transpression and transtension during sinistral shear movements. J African Earth Sciences. 36, 207–221.

Ngambu, A.A., Kouankap Nono, G.D., Kouske, P.A., Wotchoko, P., Takodjou, W.J.D., Agyingyi, C.M., Anzah, A.R., Suh, C.E. (2016) Geochemical investigation of stream sediments from the nlonako area; Littoral, Cameroon: implications for Au, Ag, Cu, Pb and Zn mineralization potentials. Int J Advanced Geosciences. 4(2), 104–112.

Nganje, T.N., Adamu, C.I., Ygbaja, A.N., Ebieme, E., Sikakwe, G. (2011) Environmental contamination of trace elements in the vicinity of Okpara coal mine, Enugu, Southeastern Nigeria. Arab J Geosci. 44, 199–205.

Nganje, T.N., Hursthouse, A.S., Edet, A., Stirling, D., Adamu, C.I. (2015) Hydrochemistry of surface water and groundwater in the shale bedrock, Cross River Basin and Niger Delta Region, Nigeria. Appl Water Sc. https://doi.org/10.1007/s13201–015–0308–9

Njitchoua, R., Ngounou, N.B. (1997) Hydrogeochemistry and environmental isotope investigations of the North Diamare plain, Northern Cameroon. J African Earth Sciences. 25, 307–316.

Nzenti, J.P., Barbey, P., Macaudiere, J., and Soba, D. (1988) Origin and evolution of the Late Precambrian high–grade Yaounde Gneisses (Cameroon): Precambrian Res. 38, 91–109. https://doi.org/10.1016/0301-9268(88)90086-1

Ohta, A., Imai, N., Terashima, S. & Tachibana, Y. (2005) Application of multi–element statistical analysis for regional geochemical mapping in Central Japan. Applied Geochemistry. 20, 1017–1037.

Ohta, A., Imai, N., Terashima, S., Tachibana, Y. (2011) Regional geochemical mapping in eastern Japan including the nation's capital, Tokyo. Geochem: Explor Environ Analy. 11, 211–223.

Ohta, A., Imai, N., Terashima, S., Tachibana, Y., Ikehara, K., Nakajima, T. (2004) Geochemical mapping in Hokuriku, Japan: influence of surface geology, mineral occurrences and mass movement from terrestrial to marine environments. Appl Geochem. 19, 1453–1469.

Omang, B.O., Bih, C.V., Fon, N.N., Suh, C.E. (2014) Regional geochemical stream sediment survey for gold exploration in the upper Lom basin, eastern Cameroon. Int J Geosciences. 5, 1012–1026.

Omang, B.O., Suh, C.E., Lehmann, B., Vishiti, A., Chombong, N.N., Fon, A., Egbe, J.A., Shemang, E.M. (2015) Microchemical signature of alluvial gold from two contrasting terrains in Cameroon. J African Earth Sciences. 112, 1–14.

Ouyang, Y., Nkedi-Kizza, P., Wu, Q.T., Shinde, D., Huang, C.H. (2006) Assessment of seasonal variations in surface water quality. Water Res. 40, 3800–3810.

Parga, J.R., Cocke, D.L., Jesus, L.V., Gomes, J.A., Kesmez, M., George, I., Moreno, H., Weir, M. (2006) Arsenic removal via lector coagulation of heavy metal contaminated ground water in La Comarca Lagurera, Mexico. J Hazardous Materials. 124, 247-254.

Penaye, J., Toteu, S.F., Tchameni, R., Van Schmus, W.R., Tchakounté, J., Ganwa, A., Minyem, D., and Nsifa, E.N. (2004) The 2.1 Ga West Central African Belt in Cameroon: Extension and evolution: J African Earth Sciences. 39, 159–164. https://doi.org/10.1016/j.jafrearsci.2004.07.053

Piper, A.M. (1944) A graphical procedure in the geochemical interpretation of water analysis. Transactions, American Geophysical Union. 25, 914–928.

Plant, J.A., Raiswell, R. (1983) Principles of environmental geochemistry. In: Thonton, I. (Ed.) Applied Environmental Geochemistry. Academic Press. p. 1–40.

Plant, J.A., Smith, D., Smith, B., Williams, L. (2001) Environmental geochemistry at global scale. Appl Geochem. 16, 1291¬–1308.

Plumlee, G.S., Logsdon, M.J. (1999) An earth-system science toolkit for environmentally friendly mineral resource development. In Plumlee, G.S., Logsdon, M.J. (Eds.), The Environmental Geochemistry of Mineral Deposits, Part A. Processes, Techniques, and Health Issues. Soc Econ Geologists, Reviews in Econ Geol 6A, pp. 1–27.

Rakotondrabe, F., Ndam Ngoupayou, J.R., Mfonka, Z., Rasolomanana, E.H., Nyangono Abolo, A.J., Ako Ako, A. (2017) Water quality assessment in the Betare–Oya gold mining area (East Cameroon): multivariate statistical analysis approach. Sci Total Environ. 610–611(2018), 831–844.

Ralston, N.V.C. (2008) Selenium health benefit values as seafood safety criteria. EcoHealth 5, 442–455.

Rapant, S., Raposova, M., Bodisa, D., Marsin, K., Slaninka, I. (1999) Environmental–geochemical mapping program in the Slovak Republic. J Geochem Explor. 66, 151–158.

Reimann, C., Garrett, R.G. (2005) Geochemical background—concept and reality. Sci. Total Environ. 350, 12–27.

Reimann, C., Filmoser, P., Garrett, R.G. (2005) Background and threshold: critical comparison of methods of determination. Sc Total Environ. 346, 1–16.

Reimann, C., Caritat, de P. (2017) Establishing geochemical variation and threshold values for 59 elements in Australian surface soil. Sc Total Environ. 578, 633–648. http://dx.doi.org/10.1016/j.scitotenv.2016.11.010

Rose, (2002) Comparative major ion geochemistry of Piedmont streams in the Atlanta, Georgia region: possible effects of urbanization. Environ Geol. 42, 102–113.

Rose, A.W., Hawkes, H.E., Webb, J.S. (1979) Geochemistry in mineral exploration. Second edition, Academic Press Inc London.

Sakan, S., Sakan, N., Anđelkovićc, I., Trifunovićd, S., Đorđevića, D. (2017) Study of potential harmful elements (arsenic, mercury and selenium) in surface sediments from Serbian rivers and artificial lakes. J Geochem Explor. 180, 24–34. https://dx.doi.org/10.1016/j.gexplo.2017.06.006

Salminen, R., Gregorauskiene, V. (2000) Considerations regarding the definition of a geochemical baseline of elements in the surficial materials in areas differing in basic geology. Appl Geochem. 15 (5), 647–653.

Salminen, R., Tarvainen, T., Demetriades, A., Duris, M., Fordyce, F.M., Gregorauskiene, V., Kahelin, H., Kivisilla, J., Klaver, G., Klein, H., Larson, J.O., Lis, J., Locutura, J., Marsina, K., Mjartanova, H., Mouvet, C., O'Connor, P., Odor, L., Ottonello, G., Paukola, T., Plant, J.A., Reimann, C., Schermann, O., Siewers, U., Steenfelt, A., Van der Sluys, J., deV ivo, B., Williams, L. (1998) FOREGS Geochemical mapping field manual. Geological Survey of Finland, Guide 47, 16–21.

Salomons, W. (1995) Environmental impact of metals derived from mining activities: processes, predictions, prevention. J Geochem Explor. 52, 5–23.

Schoeller, H. (1967) Qualitative evaluation of ground water resources (in methods and techniques of groundwater investigations and development). Water resources series UNESCO. 33, 44–52.

Shang, C., Satir, M., Nsifa, E., Liégeois, J.P., Siebel, W., and Taubald, H. (2007) Archaean high-K granitoids produced by remelting of earlier Tonalite–Trondhjemite–Granodiorite

(TTG) in the Sangmelima region of the Ntem complex of the Congo craton, southern Cameroon: Int J Earth Sciences. 96, 817–841. https://doi.org/10.1007/s00531-006-0141-3

Shang, C.K., Satir, M., Siebel, W., Nsifa, E.N., Taubald, H., Liégeois, J.P., and Tchoua, F.M. (2004) TTG magmatism in the Congo craton; a view from major and trace element geochemistry, Rb–Sr and Sm–Nd systematics: Case of the Sangmelima region, Ntem complex, southern Cameroon: J African Earth Sciences. 40, 61–79. https://doi.org/10.1016/j.jafrearsci.2004.07.005

Siegel, F.R. (2002) Environmental geochemistry of potentially toxic metals. Springer, Berlin. p.218.

Sierra, C., Ruíz-Barzola, O., Menéndez, M., Demey, J.R., Vicente-Villardón, J.L. (2017) Geochemical interactions study in surface river sediments at an artisanal mining area by means of Canonical (MANOVA)–Biplot. J Geochem Explor. 175, 72–81. https://doi.org/10.1016/j.gexplo.2017.01.002

Silva, M.M.V.G., Cabral Pinto, M.M.S., Carvalho, P.C.S. (2016) Major, trace and REE geochemistry of recent sediments from lower Catumbela River (Angola). J African Earth Sciences. 115, 203–217. https://doi.org/10.1016/j.jafrearsci.2015.12.014

Simbarashe, M., Reginald, K. (2014) Environmental monitoring of the effects of conventional and artisanal gold mining on water quality in Ngwabalozi River, southern Zimbabwe. Int J Enginer Appl Sc. 4(10).

Singh A.K., Mondal G.C., Singh, P.K., Singh, T.B., Tewary, B.K. (2005) Hydrochemistry of reservoirs of Damodar River basin, India: weathering processes and water quality assessment. Environ. Geol. 8:1014–1028.

Singh, P.K., Tiwari, A.K., Panigarhy, B.P., Mahato, M.K. (2013) Water quality indices used for water resources vulnerability assessment using GIS technique: a review. Int J Earth Sci Eng. 6(6–1), 1594–1600.

Smedley, P.L., Kinniburgh, D.G. (2002) A review of the source, behaviour and distribution of arsenic in natural waters. Appl Geochem. 17, 517–568.

Smith, D.B., Reimann, C. (2008) Low-density geochemical mapping and the robustness of geochemical patterns. Geochem: Explor Environ Anal. 8, 219–227.

Smith, D.B., Smith, S.M., Horton, J.D. (2013) History and evaluation of national-scale geochemical data set for the United States. Geosci Front. 4, 167–183.

Soba, D., Michard, A., Toteu, S.F., Norman, D.I., Penaye, J., Ngako, V., Nzenti, J.P., Dautel, D. (1991) Donnés géochronologiques nouvelles (Rb–Sr, U–Pb et Sm–Nd) sur la zone mobile pan-africaine de l'Est Cameroun: âge Protérozoïque supérieur de la série du Lom, Comptes Rendus l'Académie Science. 312, 1453–1458.

Soh, T.L., Ganno, S., Kouankap Nono, G.D., Ngnotue, T., Kankeu, B., Nzenti, J.P. (2014) Stream sediment geochemical survey of Gouap–Nkollo prospect, southern Cameroon: Implications for gold and LREE exploration. American J Mining Metallurgy. 2(1), 8–16. http://dx.10.12691/ajmm-2-1-2.

Srinivasamoorthy, K., Chidambaram, S., Prasanna, M.V., Vasanthavigar, M., John Peter, A., Anandhan, P. (2008) Identification of major sources controlling groundwater chemistry from a hard rock terrain–a case study from Mettur Taluk, Salem district, Tamilnadu, India.. J Earth System Sciences. 117(1), 1–10.

Srinivasamoorthy, K., Gopinath, M., Chidambaram, S., Vasanthavigar, M., Sarma, V.S. (2014) Hydrochemical characterization and quality appraisal of groundwater from Pungar sub basin, Tamilnadu, India. J King Saud University–Science. 26, 37–52.

Srivastava, P.K., Mukherjee, S., Gupta, M., Singh, S.K. (2011) Characterizing monsoonal variation on water quality index of River Mahi in India using geographical information system. Water Qual Expo Health. 2, 193–203.

Stendal, H., Toteu, S.F., Frei, R., Penaye, J., Njel, U.O., Bassahak, J., Kankeu, J., Nagko, V., Hell, J.V. (2006) Derivation of detrital rutile in the Yaounde region from the Neoproterozoic Pan–African belt in southern Cameroon (Central Africa). J African Earth Sciences. 44, 443–458.

Stumm, W., Morgan, J.J. Aquatic Chemistry, An Introduction Emphasising Chemical Equilibria in Natural Waters 2nd edition. John Wiley & Sons, Inc, New York. 1981 p.526–538.

Surour, A.A., El–Kammar, A.A., Arafa, E.H., Korany, H.M. (2003) Dahab Stream Sediments southeastern Sinai, Egypt: a potential source of gold, magnetite and zircon. J Geochem Explor. 7(1), 25-43.

Taiwo, A.M., Awomeso, J.A. (2017) Assessment of trace metal concentration and health risk of artisanal gold mining activities in Ijeshaland, Osun State Nigeria— Part 1. J Geochem Explor. 177, 1–10. https://doi.org/10.1016/j.gexplo.2017.01.009

Tamez-Mélendez, C., Hernandez–Antonio, A., Gaona-Zanella, P.C., Ornelas–Soto, N., Mahlknecht, J. (2016) Isotope signatures and hydrochemistry as tools in assessing groundwater occurrence and dynamics in a coastal arid aquifer. Environ. Earth Sci. https://doi.org/10.1007/s12665-016-5617-2

Taylor, S.R., McLennan, S.M. (1985) The Continental Crust: its Composition and Evolution. Blackwell Scientific Publication, Oxford.

Tchameni, R., Mezger, K., Nsifa, N.E., and Pouclet, A. (2001) Crustal origin of Early Proterozoic syenites in the Congo Craton (Ntem Complex), South Cameroon: Lithos, 57, 23–42. https://doi.org/10.1016/S0024-4937(00)00072-4

Tehna, N., Nguene, F.D., Etame, J., Medza Ekodo, J.M., Noa, T.S., Suh, C.E., Bilong, P. (2015) Impending pollution of Betare Oya opencast mining environment (Eastern Cameroon). J Environ Science and Engineering. 4, 37–46.

Tiwari, A.K., Singh, A.K. (2014) Hydrogeochemical investigation and groundwater quality assessment of the Pratapgarh District, Uttar Pradesh. Geol. Soc. India. 83, 329–343.

Toteu, S.F., Penaye, J., Deloule, E., Van Schmus, W.R., Tchameni, R. (2006) Diachronous evolution of volcano–sedimentary basins north of the Congo craton: insights from U–Pb ion microprobe dating of zircons from the Poli, Lom and Yaounde Series (Cameroon). J African Earth Sciences. 44, 428–442.

Toteu, S.F., Penaye, J., Deschamps, Y., Maldan, F., Nyama Atibagoua, B., Bouyo Houketchang, M., Sep Nlomgan, J.P., Mbola Ndzana, S.P. (2008) Géologie et ressources minérales du Cameroun. 33rd International Geological Congress, Oslo, Norway.

Toteu, S.F., Penaye, J., Poudjom, D.Y. (2004) Geodynamic evolution of the Pan–African belt in Central Africa with special reference to Cameroon. Canadian J. Earth Science. 41, 73–85.

Toteu, S.F., Van Schmus, R.W., Penaye, J., Michard, A. (2001) New U–P b and Sm–Nd data from north central Cameroon and its bearing on the pre–pan–African history of Central Africa. Precam. Res. 108, 45–73.

Toteu, S.F., Van Schmus, W.R., Penaye, J., and Nyobé, J.B. (1994) U–Pb and Sm–N evidence for Eburnian and PanAfrican high–grade metamorphism in cratonic rocks of southern Cameroon: Precambrian Res. 67, 321–347. https://doi.org/10.1016/0301-9268(94)90014-0

Towett, E.K., Shepherd, K.D., Tondoh, J.E, Winowiecki, L.A., Lulseged, T., Nyambura, M., Sila, A., Vagen, T.G., Cadisch, G. (2015) Total elemental composition of soils in Sub-Saharan Africa and relationship with soil forming factors. Geoderma Regional. 5, 157–168.

UNICEF Cameroon Humanitarian Situation Report – November 2014. https://reliefweb.int/report/cameroon/unicef-cameroon-humanitarian-situation-report-november-2014. Accessed April 12, 2017.

Uwah, I.E., Dan, S.F., Etiuma, R.A., Umoh, U.U. (2013) Evaluation of status of heavy metals pollution of sediments in Qua–Iboe River Estuary and associated creeks, south–eastern Nigeria. Environ Pollut 2(4), 110–122.

Van Schmus, W.R., Oliveira, E.P., Da Silva Filho, A.F., Toteu, S.F., Penaye, J., Guimaraes, I.P. (2008) Proterozoic links between the Borborema Province, NE Brazil, and the Central African Fold Belt: Geological Society London, Special Publications. 294(1), 69–99. https://doi.org/10.1144/SP294.5

Van Straaten, P. (2000) Mercury contamination associated with small–scale gold mining in Tanzania and Zimbabwe. Sci Total Environ. 259, 105–113.

Vishiti, A., Suh, C.E., Lehmann, B., Shemang, E.M., Ngome, N.L.J., Nshanji, N.J., Chinjo, F.E., Mongwe, O.Y., Egbe, A.J., Petersen, S. (2017) Mineral chemistry, bulk rock geochemistry, and S–isotope signature of lode–gold mineralization in the Bétaré Oya gold district, south–east Cameroon. Geological Journal. 1–18. https://doi.org/10.1002/gj.3093

Webb, J.S., Thornton, I., Thompson, M., Howarth, R.J., Lowenstein, P.L. The Wolfson Geochemical Atlas of England and Wales. Clarendon Press, Oxford; 1978.

Weng, L., Endamana, D., Boedhihartono, A.K., Levang, P., Margules, C.R., Sayer, J.A. (2015) Asian investment at artisanal and small–scale mines in rural Cameroon. Extr Ind Soc. 2, 64–72. http://dx.doi.org/10.1016/j.exis.2014.07.011

Wirmvem, M.J., Ohba, T., Fantong, W.Y., Ayonghe, S.N., Suila, J.Y., Asaah, A.N.E., Tanyileke, G., Hell, J.V. (2013) Hydrogeochemistry of shallow groundwater and surface water in the Ndop plain, North West Cameroon. African J. Environ. Science and Technol. 7(6), 518–530.

World Health Organization (2011) Guidelines for Drinking-Water Quality, Fourth Edition, Geneva, 564 p.

Yang, X.J., Lin, A., Li, X.L., Wu, Y., Zhou, W., Chen, Z. (2013) China's ion–adsorption rare earth resources, mining consequences and preservation. Environmental Development. 8, 131–136. http://dx.doi.org/10.1016/j.envdev.2013.03.006

Zhang, C., Manheim, F.T., Hinde, J., Grossman, J.N. (2005) Statistical characterization of large geochemical database and effect of sample size. Appl Geochem. 20, 1857–1874.

Zhao, G., He, F., Dai, X., Zhang, S., Yu, R. (2014) Ultra–low density geochemical mapping in Zimbabwe. J Geochem Explor. 144, 552–571.

Zhizhong, C., Xuejing, X., Wensheng, Y., Jizhou, F., Qin, Z., Jindong, F. (2014) Multi–element geochemical mapping in Southern China. J Geochem Explor. 139, 183–192.

Zuluaga, M.C., Norin, I.G., Lima, A., Albanese, S., David, C.P., De Vivo, B. (2017) Stream sediment geochemical mapping of the Mount Pinatubo–Dizon Mine area, the Philippines: Implications for mineral exploration and environmental risk. J Geochem Explor. 175, 18–35. https://doi.org/org/10.1016/j.gexplo.2016.12.012

Zumlot, T., Goodell, P., Howari, F. (2009) Geochemical mapping of New Mexico, USA, using stream sediment data. Environ Geol. 58, 1479–1497. https://doi.org/10.1007/s00254-008-1650-0

APPENDICES

Appendix I. Cation (TZ^+) –anion (TZ^-) charge balance error for stream water samples (N = 52) from the lower Lom Basin

Sample	F^-	Cl^-	NO_2^-	Br^-	NO_3^-	PO_4^{3-}	SO_4^{2-}	HCO_3^-	Na^+	K^+	Ca^{2+}	Mg^{2+}	TZ^+	TZ^-	TZ* %
GB1	0.005	0.006	0.001	0	0.007	0	0.005	0.47	0.12	0.07	0.18	0.17	0.54	0.50	4.56
GB2	0.003	0	0	0	0	0.002	0	0.41	0.16	0.05	0.15	0.09	0.46	0.42	4.75
GB3	0.006	0.003	0.001	0	0	0.001	0	0.25	0.08	0.05	0.09	0.06	0.27	0.26	3.04
GB4	0.003	0.003	0.002	0	0.001	0.001	0	0.10	0.02	0.03	0.03	0.01	0.10	0.11	-4.45
GB5	0.001	0.008	0.001	0	0.014	0	0	0.11	0.06	0.03	0.04	0.01	0.15	0.14	1.92
GB6	0.003	0.004	0.001	0	0	0	0	0.10	0.03	0.02	0.04	0.01	0.10	0.11	-4.54
GB7	0.011	0.003	0.001	0	0	0	0	1.00	0.27	0.08	0.47	0.39	1.21	1.01	8.78
GB8	0.011	0.006	0	0	0	0.003	0	1.03	0.28	0.09	0.46	0.36	1.19	1.05	6.54
GB9	0.003	0.005	0.001	0.001	0.001	0.001	0	0.18	0.03	0.05	0.06	0.04	0.18	0.20	-4.97
GB10	0.002	0.003	0	0	0	0	0.004	0.05	0.00	0.02	0.03	0.01	0.06	0.06	0.91
GB11	0.002	0.003	0.001	0.001	0	0.001	0.006	0.16	0.03	0.01	0.04	0.07	0.16	0.17	-3.97
GB12	0.002	0.003	0.001	0	0	0	0	0.12	0.01	0.03	0.06	0.03	0.12	0.13	-1.47
GB13	0.01	0.023	0.002	0	0.006	0	0	0.89	0.39	0.06	0.30	0.38	1.13	0.93	9.75
GB14	0.002	0.013	0.001	0.001	0	0	0.012	0.17	0.05	0.03	0.06	0.07	0.20	0.20	0.19
GB15	0.002	0.002	0.001	0	0	0.002	0.001	0.09	0.02	0.01	0.04	0.03	0.10	0.10	-0.55
GB16	0.001	0.021	0.001	0	0	0	0	0.13	0.05	0.02	0.05	0.03	0.15	0.16	-2.80
GB17	0.003	0.036	0.001	0.001	0.323	0	0	0.05	0.18	0.03	0.04	0.02	0.27	0.41	-21.4
GB18	0.002	0.011	0.001	0	0	0.001	0	0.12	0.05	0.03	0.04	0.01	0.13	0.13	-1.98
GB19	0.002	0.003	0.002	0	0	0	0	0.13	0.04	0.03	0.04	0.02	0.12	0.13	-2.95
GB20	0.002	0.007	0.001	0.001	0	0	0	0.06	0.02	0.02	0.02	0.01	0.07	0.07	0.08
GB21	0.003	0.011	0.001	0	0.029	0.001	0	0.11	0.03	0.03	0.06	0.03	0.15	0.15	0.13
GB22	0.002	0.008	0.003	0	0	0	0	0.11	0.03	0.02	0.04	0.03	0.12	0.12	-0.36
GB23	0.001	0.009	0	0	0	0	0	0.10	0.03	0.02	0.05	0.01	0.11	0.11	-0.29
GB24	0	0.002	0.001	0	0	0.001	0.005	0.13	0.03	0.02	0.07	0.02	0.14	0.14	-0.99
GB25	0.002	0.003	0	0	0	0.001	0	0.04	0.01	0.01	0.03	0.00	0.05	0.05	-0.06
GB26	0.002	0.002	0	0	0	0	0	0.09	0.02	0.02	0.04	0.01	0.10	0.09	2.58

Sample	F^-	Cl^-	NO_2^-	Br^-	NO_3^-	PO_4^{3-}	SO_4^{2-}	HCO_3^-	Na^+	K^+	Ca^{2+}	Mg^{2+}	TZ^+	TZ^-	TZ* %
GB27	0.002	0.004	0	0	0.001	0	0	0.12	0.04	0.03	0.05	0.02	0.14	0.13	2.95
GB28	0.001	0.01	0	0	0.015	0.003	0	0.09	0.06	0.05	0.01	0.00	0.13	0.12	1.79
GB29	0.005	0.01	0	0	0	0.001	0.001	0.59	0.24	0.05	0.15	0.21	0.64	0.61	2.65
GB30	0.008	0.003	0	0	0.001	0	0	0.87	0.30	0.05	0.28	0.34	0.96	0.88	4.65
GB31	0.004	0.004	0	0	0.001	0.001	0.007	0.54	0.17	0.07	0.20	0.12	0.56	0.56	-0.29
GB32	0.005	0.005	0	0	0.006	0	0.004	0.71	0.23	0.09	0.27	0.20	0.79	0.73	3.81
GB33	0.007	0.003	0.001	0	0	0.003	0.003	0.52	0.22	0.05	0.19	0.13	0.59	0.54	4.83
GB34	0.002	0.002	0	0	0.001	0	0	0.20	0.07	0.02	0.07	0.05	0.21	0.20	0.41
GB35	0.006	0.005	0	0.001	0.013	0	0.002	0.76	0.22	0.07	0.32	0.23	0.85	0.78	4.41
GB36	0.006	0.009	0.002	0	0	0.003	0.003	0.73	0.15	0.03	0.33	0.30	0.81	0.75	3.48
GB37	0.005	0.006	0	0	0.004	0.001	0.002	0.84	0.21	0.04	0.42	0.28	0.95	0.86	5.16
GB38	0.006	0.003	0	0.001	0.002	0	0.001	0.69	0.20	0.05	0.25	0.26	0.76	0.70	3.75
GB39	0.003	0.004	0	0	0.001	0.003	0	0.10	0.04	0.02	0.04	0.01	0.11	0.11	1.60
GB40	0.002	0.003	0.001	0.001	0.001	0	0.004	0.16	0.03	0.03	0.08	0.04	0.18	0.17	2.50
GB41	0.002	0.002	0.001	0	0	0.007	0.003	0.21	0.07	0.06	0.07	0.04	0.23	0.22	2.34
GB42	0.002	0.004	0.001	0	0.003	0.005	0	0.14	0.04	0.03	0.06	0.03	0.16	0.16	-0.29
GB43	0.003	0.003	0	0.001	0.001	0	0.002	0.17	0.04	0.03	0.06	0.04	0.18	0.18	-0.81
GB44	0.004	0.005	0	0.001	0.006	0	0.002	0.31	0.08	0.03	0.10	0.12	0.34	0.33	1.20
GB45	0.003	0.009	0.001	0	0.007	0	0	0.36	0.11	0.04	0.12	0.12	0.39	0.38	1.65
GB46	0.003	0.008	0	0	0.007	0	0.011	0.27	0.05	0.04	0.11	0.10	0.29	0.30	-1.13
GB47	0.006	0.009	0	0.001	0.003	0.003	0.006	0.37	0.14	0.06	0.12	0.09	0.42	0.40	2.87
GB48	0.004	0.01	0	0	0.003	0	0.01	0.25	0.07	0.04	0.05	0.12	0.29	0.28	0.98
GB49	0.002	0.005	0	0	0.004	0.002	0.001	0.18	0.04	0.03	0.05	0.07	0.20	0.20	-0.17
GB50	0.001	0.002	0	0	0	0	0	0.12	0.05	0.03	0.03	0.01	0.11	0.12	-1.81
GB51	0.004	0.005	0	0	0	0.001	0.003	0.36	0.13	0.07	0.09	0.11	0.40	0.37	3.80
GB52	0.007	0.002	0	0	0.001	0.001	0	0.70	0.24	0.06	0.19	0.29	0.78	0.71	5.16
Minimum	0	0.002	0	0	0	0	0	0.04	0.002	0.01	0.01	0.001	0.05	0.05	-21.4
Maximum	0.011	0.036	0.003	0.001	0.323	0.007	0.012	1.03	0.39	0.09	0.47	0.39	1.21	1.05	9.75
Mean	0.004	0.006	0.001	0.0002	0.009	0.001	0.002	0.32	0.10	0.04	0.12	0.10	0.36	0.34	0.92

Appendix II. ICP–MS analytical results showing trace metal composition of stream sediments (N = 55) from the lower Lom Basin. Fe and Mn were determined by AAS

Sample	Sc	V	Cr	Mn	Fe	Co	Ni	Cu	Zn	As	Se	Cd	Hg	Pb
LOD (ppb)	0.001	0.001	7.2E-05	–	–	7.1E-05	0.0004	0.001	0.36	0.004	0.03	0.0002	0.001	5.5E-05
GB1	124	82.1	38.2	579	23617	0.35	15.5	211	335	2.96	22	2.11	15	47
GB2	126	82.8	38.2	472	22598	0.32	15.6	211	320	8.54	23.9	2.08	9.66	47.3
GB3	126	80.8	38	489	28682	0.31	15.2	211	315	0.87	41.1	2.17	8.92	47.2
GB4	127	79.7	37.9	300	38522	0.51	15	210	352	8.72	23.9	1.3	8.17	47.2
GB5	126	79.8	38.6	325	28142	0.33	15.4	211	331	3.31	36.3	2.39	5.37	47.5
GB6	129	81.5	38.4	271	29664	0.27	15.3	211	341	9.94	39.2	2.2	3.66	47.6
GB7	126	78.8	38.3	483	27464	0.33	15	210	317	1.74	26.8	1.98	4.22	47.5
GB8	130	82.1	38.3	615	21505	0.33	15.6	212	348	10.3	22	2.33	3.21	47.8
GB9	126	78.7	38.5	424	17848	0.30	14.9	211	321	5.23	27.7	2.51	2.63	47.4
GB10	131	81.2	37.6	497	32771	0.32	15	211	334	11	20.1	2.3	2.68	47.6
GB11	129	79.4	38.9	832	74250	0.21	15.5	211	313	2.61	34.4	2.36	1.92	47.6
GB12	128	80.1	38.7	399	35822	0.23	15	211	330	0.35	24.9	2.45	1.33	47.4
GB13	752	4526	3567	985	35006	948	1425	1089	2802	1178	510	7.85	83.2	816
GB14	692	5362	4369	269	16956	1308	1823	1369	4506	887	306	3.81	20.6	787
GB15	1699	12333	10053	444	26734	837	3126	3947	4658	889	293	4.99	24.8	2216
GB16	1074	7853	7538	255	15839	553	2086	2663	3375	553	190	1.98	17.8	1071
GB17	23	622	537	270	22657	49.7	176	51.3	76.9	39.9	27.7	2.11	0.49	46.4
GB18	33	555	484	254	12617	44.3	158	28.2	39.6	35	22	2.05	0.19	33.5
GB19	31	597	525	259	34842	46.1	167	41.2	64.3	42.7	28.7	2.02	0.2	35.6
GB20	51.3	449	413	288	25282	38.3	127	12.2	2.61	22	17.2	2.45	0.77	15
GB21	2.11	854	723	291	28999	64.7	229	130	197	57.5	21	1.83	0.35	64
GB22	13.3	683	592	257	12675	54.4	192	70.9	127	45.3	27.7	2.14	0.38	44.8
GB23	12	855	739	266	18305	65	240	138	230	54.9	23.9	2.3	0.26	64
GB24	104	132	152	236	12109	14.4	42.1	130	195	4.01	12.4	2.42	0.63	26.8
GB25	89.3	192	191	272	32661	19	53.4	114	148	11.3	14.3	2.3	1.06	17
GB26	86.6	211	197	285	15563	19.3	62.6	104	144	16.2	15.3	2.42	0.99	11.6

Sample	Sc	V	Cr	Mn	Fe	Co	Ni	Cu	Zn	As	Se	Cd	Hg	Pb
GB27	80.8	263	249	323	14085	23.1	74	84.1	105	14.6	12.4	2.3	0.67	9.3
GB28	101	113	121	265	15857	13.1	35.8	140	191	1.74	22	2.67	1.34	22.2
GB29	66	388	361	965	35699	32.6	114	34.6	57.4	33	36.3	2.39	0.81	7.69
GB30	54.3	439	402	1080	159320	34.2	121	24.5	15.9	40.4	22.9	2.42	1.20	8.49
GB31	42.9	534	476	1320	42446	41.6	150	17.8	40.8	47.9	24.9	2.48	1.19	22.6
GB32	75.2	264	253	1442	44664	22.9	79.4	84.3	129	21.3	21	2.39	1.12	7.25
GB33	1018	7261	5799	543	23855	489	1766	2140	2297	756	389	1.71	11.4	817
GB34	127	53.6	13.6	300	33001	7.35	5.59	200	110	18.3	9.56	2.70	8.83	42.9
GB35	1249	5768	3041	425	19620	370	401	567	1707	159	178	5.86	7.76	623
GB36	131	72.1	28.8	471	21846	0.58	13.8	209	299	21.8	9.56	2.76	1.66	47.2
GB37	132	85.1	38.3	857	80412	0.15	15	211	304	26.5	5.74	2.7	2.11	48
GB38	131	85.4	38.8	663	39093	0.44	15.9	212	313	26.3	6.69	2.54	2.29	48.1
GB39	132	85.8	39.1	260	15656	0.46	15.6	212	311	23.7	4.78	2.73	2.42	48.1
GB40	131	82.6	37.5	319	17368	0.26	15.3	211	322	18.7	1.91	2.67	2.42	47.9
GB41	132	85.6	39.1	289	24328	0.46	15.6	212	314	26.7	2.87	2.67	2.55	48.2
GB42	132	85.9	39.3	270	15250	0.45	16.2	212	317	21.4	4.78	2.85	2.45	48.2
GB43	132	86.1	39.1	316	15851	0.47	15.4	212	313	23.2	4.78	2.67	2.46	48.2
GB44	132	85.8	38.9	369	22100	0.47	15.9	212	322	23.4	4.78	2.7	2.38	48.1
GB45	132	86	38.9	346	15325	0.46	15.8	212	314	29.5	0.96	2.79	2.35	48.2
GB46	132	86	38.9	485	26970	0.44	15.6	212	326	22.8	12.4	2.61	2.39	48.1
GB47	132	86	38.9	381	17591	0.39	15.6	212	331	22.7	2.87	2.73	2.51	48.2
GB48	133	85.7	39.2	305	19009	0.44	15.8	212	316	22.7	8.6	2.61	2.35	48.1
GB49	132	85.9	39.2	235	16503	0.47	15.6	212	326	22.7	7.65	2.64	2.17	48.1
GB50	133	86.2	39.3	249	29743	0.42	15.8	212	314	23.9	9.56	2.76	2.38	48.1
GB51	132	86.2	39.2	277	16093	0.44	16	212	323	21.1	0.96	2.82	2.08	48
GB52	133	86.2	39.3	437	29476	0.44	15.3	212	322	27	0.1	2.7	2.08	48
GB53	131	82.3	36	283	20620	0.03	15.1	211	306	22.1	7.65	2.7	1.78	47.3
GB54	132	85.5	38.8	269	22679	0.42	15.6	212	316	24.2	1.91	2.7	1.95	48.2
GB55	133	85.8	38.9	224	12298	0.38	15.9	212	344	23.7	4.78	2.61	1.77	48.1

Appendix I: N, number of samples; TZ^+, total cationic charge; TZ^-, total anionic charge; TZ*, ion balance error ($TZ^+ – TZ^-$). The equivalent concentrations of the major ions were used. 99 % of samples had charge balance errors <±10 %. One sample, GB17, had a charge balance error >±10 % with an anion excess resulting from anthropogenic activities in the area.

Appendix II: LOD, limit of detection; N, number of samples; (–), Not determined; GB, Garoua Boulai–Bétaré Oya; concentrations of Fe and Mn are given in mg/kg.